I. THE MOLECULAR STRUCTURES OF CERTAIN ORGANIC FOUR-MEMBERED RING COMPOUNDS.

II. THE $BaMg_9$ STRUCTURE.

Thesis by

Elihu Goldish

In Partial Fulfillment of the Requirements

For the Degree of

Doctor of Philosophy

California Institute of Technology

Pasadena, California

1956

ACKNOWLEDGMENT

To Professor Verner Schomaker, who patiently guided the electron diffraction work and provided much helpful advice and discussion, go my sincerest thanks. Thanks are also due Dr. Kenneth Hedberg, who shared the work on cyclobutene; Dr. G. Bergman, who helped in the early stages of the crystal structure investigation, and Dr. R.E.Marsh, who saw it through to completion; and Dr. D. E. Applequist, who initiated and aided in the investigation of 3-methylenetrimethylene oxide. I am greatly indebted to the Office of Naval Research and to the E.I. du Pont de Nemours and Co. (Inc.) for financial assistance, and to Local Board 123, Washington County, Ohio, for permitting me to continue my work without interruption.

ABSTRACT

Part I presents the results of electron diffraction investigations of some relatively simple four-membered organic ring compounds: trimethylene oxide, 3-methylenetrimethylene oxide, trimethylene sulfide, and cyclobutene. Discussion is given of the bond lengths in these and other small-ring molecules.

In a supplementary section are the results of an investigation of dimethyl selenide, which indicates a somewhat larger radius for selenium than is usually given, and preliminary results for decaborane.

In Part II the disordered $BaMg_9$ structure is investigated and discussed. It can be described on the basis of a $CaCu_5$-type structure in which about half the barium atoms are replaced by pairs of magnesium atoms.

TABLE OF CONTENTS

PART I

A. The Molecular Structure of Certain Organic Four-Membered Ring Compounds.

B. Some Miscellaneous Electron Diffraction Studies.

THE MOLECULAR STRUCTURES OF CERTAIN ORGANIC FOUR-MEMBERED RING COMPOUNDS

Introduction

As improved techniques for molecular structure determinations have become available, it has become possible to examine with a greater degree of assurance the effect of constitution on bond lengths and angles. Electron diffraction results have become more reliable partly by reason of improved mechanical procedures, partly because of increased facility in examining and treating the experimental data. The increasing number of results obtained by microwave spectroscopy are also enriching the fund of reliable results on which we may draw. Two convenient compilations are found in ref. 1 and ref. 2, for electron diffraction and microwave spectroscopy, respectively.

Sufficient structural data about simple three- and four-membered organic ring compounds have now become available to enable meaningful comparisons to be made and some conclusions drawn regarding the nature and relative magnitudes of the factors affecting bond lengths in these molecules.

In brief, the following aspects of these small strained molecules must be considered and balanced:

a) Shortening of bonds due to "bent-bond" effect. This is important primarily for three-membered rings such as cyclopropane [3], where the bond distance, 1.525 Å, is significantly shorter than normal.

b) Cross-ring repulsions. These have been suggested as a plausible explanation for the longer bond distance (1.56_8 Å) in cyclobutane[4]. Such repulsions do not, of course, exist for three-member rings.

c) Differential bond angle strain. Distortion of a bond angle from its "normal" value produces strains and compressions[5] in bonds which cancel out completely for symmetrical molecules such as cyclobutane and cyclopropane, but are significant for other strained molecules, such as trimethylene oxide, cyclopropene, etc.

d) Miscellaneous lesser influences, including hyperconjugation, unshared electron pairs, ionic and double-bond character, and others. It is generally possible to ignore these factors, except in cases where it should be a priori clear that some effect is to be expected, as, for example, hyperconjugation effects in cyclobutene.

e) Bond angle changes. No attempt will be made here to consider the problem of bond angles except insofar as necessary for discussion of (c).

Most of our discussion will be confined to qualitative examination of these factors. It is possible to set up more quantitative statements, but for the purpose of our discussion only an order of magnitude and its sign (positive or negative) will be considered. A surprisingly good idea of the expected effects or explanation of the observed parameters can be obtained by thinking of a mechanical analog of the molecule, with spring bonds emanating from fixed directions, and with stressed cross-ring

strains.

As concrete examples of the application of these ideas, brief, and necessarily incomplete, discussions of cyclopropene and spiropentane are given. For the most part, the calculations will be concerned only with checking the internal consistency of a set of parameters for a given molecule in the light of the concepts set forth above; in this way the problem of estimating true bending force constants is by-passed, and it is sufficient to know only the relative magnitudes of these constants for a given molecule.

Cyclopropene is reported[6] to have the unusually short double-bond length of $1.28_6 \pm 0.04$ Å, and a single-bond distance of $1.52_5 \pm 0.02$ Å. The bond-angle deformations are equal (to within the estimated error of the determination): $125^{\circ}16'$ - $\angle$ C-C=C = 60.2° and 109.5° - $\angle$ C-C-C = 59.6°; the force required to bend $\angle$ C-C=C from normal by a given amount is, however, about 50 percent greater than the force necessary to bend $\angle$ C-C-C by the same amount from tetrahedral*. This difference leads to a compressive force in the double bond and a stretching force in each single bond of about half the double bond compression. Since the bond-stretching force constant for a double bond is about twice that for a single bond, it is expected that

*The angle changes involved here are so large that it would be unwise to apply potential functions intended for infinitesimal angle changes. But it might be hoped that the ratio of the energies involved for equal angle deformations would remain roughly proportional to the ratio of the energy constants, expressed in erg radian^{-2} ($V=1/2\ k_{\delta}\delta^2$). In propane this constant is about 0.8×10^{-11} and in propene about 1.2×10^{-11} (see ref. 7, 8, 9). It has therefore been assumed that the angle strain energy is about 50 percent greater for $\angle$ C-C=C than for $\angle$ C-C-C, for equal decrements. Although more detailed considerations might lead to a different ratio of energy constants, for the present we only need to be assured that the effective constant for $\angle$ C-C=C is greater than for $\angle$ C-C-C.

the shortening of the double bond would be about the same as the lengthening of the single bond.

As reference values for discussing hyperconjugation, we take 1.330 Å for a double-bond length, and 1.503 Å for the adjacent single-bond length*. The bent-bond shortening for a single bond in cyclopropane is about 1 percent of its "unbent" length (i.e. 1.540 x 0.99 = 1.525); for the double bond, we assume (arbitrarily) a shortening by 1/2 of 1 percent of the original bond length. The net double-bond shortening due to differential angle strain only is thus 1.330 - 0.007 - 1.286 = 0.037 Å, and we calculate the corresponding single-bond length for cyclopropene to be 1.525 - 0.037 + 0.037 = 1.525 Å, in good agreement with experiment. The subtraction of 0.037 Å is intended to be a correction for shortening due to the adjacent double bond (hyperconjugation).

---

*These are the values found in isobutene[10]; parameters for the more comparable cis-isobutene have not yet been refined to a useful stage. The following results are not yet generally available and are reproduced for comparison[10]:

$$H_3C - CH = CH_2 : \quad C\text{-}C = 1.49_2 \pm 0.02 \text{ Å}$$
$$C{=}C = 1.33_3 \pm 0.01_9 \text{ Å}$$
$$\angle C{=}C\text{-}C = 125^\circ \pm 2^\circ$$

$$\begin{matrix} H_3C \\ H_3C \end{matrix}\!\!\diagdown\!\!\diagup C = CH_2 : \quad C\text{-}C = 1.50_3 \pm 0.01_8 \text{ Å}$$
$$C{=}C = 1.33_0 \pm 0.01_5 \text{ Å}$$
$$\angle C{=}C\text{-}C = 123.5^\circ \pm 2^\circ$$

For a C-C single bond we adopt, somewhat arbitrarily, the value 1.540 Å; this is reasonably close to both the electron diffraction and the spectroscopic results for ethane (1.536 Å and 1.543 Å, respectively)[11].

It has been suggested* that a more exact calculation might be expected to modify the above results somewhat. By examining the problem of differential angle strain analytically, it is found that, for cyclopropene, the ratio of the stretching force in each single bond to the compressive force in the double bond is equal to Cos $\angle$ C-C=C; if, as was assumed in the previous paragraph, $\angle$ C=C-C is 60°, then this factor is 1/2. For the 65.1° value of $\angle$ C=C-C in cyclopropene, the cosine is 0.421. On the other hand the ratio of the double-bond stretching force constant to the single-bond constant is not precisely two, but somewhat greater; we may reasonably assume the ratio $\frac{9.6}{4.50} = 2.13$**. The value calculated for the single bond from the double bond distance in cyclopropene is 1.525 - 0.037 + 0.037 x 0.421 x 2.13 = 1.521 Å. The agreement now is not so good as in the preceding cruder calculation, but the more precise calculation merits the greater confidence. Since we have made use of a large number of uncertain data -- including especially the ratio of the effective bending constants, as well as the ratio of stretching force constants, the shortening by hyperconjugation of strained bonds, the reference values for single and double bonds, the estimation of bent-bond shortening for double bonds, and others -- better agreement, except fortuitously, could hardly be expected. (The calculated value is also well within the 0.02 Å estimated limits of error for the experimental determination.)

Spiropentane[12] presents a less clear-cut example. The central

---

* I am indebted to Prof. V. Schomaker for bringing this to my attention.

** See ref. 22, p. 193.

bonds in spiropentane are short (1.48 $\pm$ 0.03 Å), the peripheral bonds somewhat longer (1.51 $\pm$ 0.04 Å). The central angle in each three-membered ring is under greater strain than the other two angles; whereas the strain at a carbon in cyclopropane is partially relieved by the expansion of $\angle$ H-C-H from tetrahedral to 118°[3], this compensation cannot occur at the central atom in spiropentane. This differential angle strain results in a compressive force in the central C-C bonds, and a stretching force twice as great in the peripheral bonds. In addition, the central bonds should be further shortened by more effective bent-bond shortening.

The greater central angle strain in spiropentane might be expected to lead to lengthened peripheral bonds; instead these appear to be shortened by 0.01_5 Å relative to cyclopropane. Two explanations are possible: either more comprehensive and complex examination of the problem would lead to the conclusion that the peripheral bonds really should be short relative to cyclopropane*, or else the electron-diffraction results are in error (although not necessarily by more than the stated limits of error). To remove any uncertainty regarding the structure determination, it is suggested that spiropentane be reexamined**. If the relative bond lengths are correct, however, they are in accord qualitatively with the expected effects of differential angle strain and bent-bond shortening.

---

*In this regard, see ref. 12.

**In the new apparatus recently constructed in these laboratories. In view of the rigidity expected of the strained carbon skeleton, usable data to high scattering angles should be readily obtained. The outer portions of the pattern should be quite sensitive to the slightly differing C-C distances. Uncertainty regarding wave length is also less in the newer apparatus.

Trimethylene Oxide (C_3H_6O)

Several points regarding the previous investigation [13] of trimethylene oxide (TMO) seemed, to the present author, to indicate the desirability of a reinvestigation. Aside from the interest connected with the structural parameters of this four-membered ring molecule, it was felt necessary to have reliable data for comparison with the 3-methylene derivative. The following paragraphs outline what seem to be the principal weaknesses of the previous work.

First: Shand had reduced the problem to one of determining a single parameter by assuming that all three interior ring angles at carbon atoms were equal; with this assumption the shape of the ring is completely fixed by the ratio of the two different bond distances (the scale parameter fixing the absolute size). Although probably not far wrong, this restriction seems arbitrary and unnecessary. (Some models were investigated for $\angle$ C-C-O $\neq$ $\angle$ C-C-C, but for these $\angle$ C-C-C was assumed to be 90°, which again seems to be unnecessary. In addition Shand calculated curves for some non-planar models; this will be discussed later.)

Second: Shand did not interpolate between calculated curves to obtain his final result. Since the calculated models were spaced at 0.03 Å in C-O (for fixed C-C) an error of 0.01 or 0.02 Å may have resulted.

Third: Shand's data went only to about q = 95, whereas the current reinvestigation is based on measurements extending to q = 125 together with qualitative visual observations extending even further. The region

from q = 90 outward is critically sensitive to some of the parameters; given the extended data it is possible to distinguish between curves which are otherwise quite similar up to q = 90.

The present investigation determines two parameters, $\angle$ C-C-C and $\frac{C\text{-}C}{C\text{-}O}$. By calculating curves for fixed C-O and varying C-C at intervals of 0.02 Å, a series of curves is obtained which is more finely graduated than Shand's (because of the smaller amplitude of the C-C term relative to the C-O term). Recent work in these laboratories also benefits from various mechanical improvements, such as increased wave-length stability, and the use of glass plates.

Experimental. The photographs used in this work were taken in conjunction with the photographs of 3-methylenetrimethylene oxide, using without further purification a sample provided by Dr. D. E. Applequist. Kodak 50 plates were used, with an accelerating potential of 40 kv. (corresponding to about 0.06 Å electron wave length) and a 10 cm. camera distance; the sample-bulb temperature was about -30° C. The usual correlation procedure, employing a visually estimated intensity curve, was followed*.

The appearance of the plates matched that of the older photographs used by Shand very well. The visual curve in Fig. 1 is drawn from the measurements and observations of Prof. V. Schomaker; no radial distribution curve was calculated, however, since Shand's visual curve, as far as it went, did not differ appreciably from the present one. The following points were particularly useful in determining a best model

*For a brief description of these procedures, with references, see, for example, ref. 14.

and assigning the limits of error: the nature of the triple feature max. 7, 8, 9 is approximately as shown in the visual curve, and calculated curves differing too greatly were unacceptable; in the triple feature max. 10, 11, 12 it is probable that min. 12 is deeper than min. 11, but curves with the minima equal or even slightly reversed in depth were accepted; the feature marked max. 13 appears to be split, and although the precise nature of the doubling is somewhat uncertain, curves showing a doublet were preferred to those without it.

Theoretical curves were calculated for planar models with these parameters: C-O = 1.46; C-H = 1.09; $\angle$ H-C-H = 113°36'; $1.52 \leqslant$ C-C $\leqslant 1.58$ (0.02); $84.2^\circ \leqslant \angle$ C-C-C $\leqslant 90.2^\circ (2^\circ)$. All terms were included except H···H, and $Z_H^{eff.} = 1.25$ was used. The simplifying assumptions made are discussed in the following paragraphs.

The use of 113°36' for $\angle$ H-C-H is quite arbitrary, but probably a good average value. It is close to the value found in cyclobutane[4], $114^\circ \pm 6^\circ$, and is also very close to the average $\angle$ H-C-H which would be calculated, by minimizing angle strain energy*, from the ring angles found by the current work. In addition the observed moments of inertia[15] lead to $\angle$ H-C-H $_{Av.} = 113.2^\circ$ (assuming C-H = 1.09 Å).

The planes of the two opposed CH_2 groups were taken perpendicular to the plane of the ring and were also assumed to be perpendicular to the

---

*This leads to the approximate formula

$$\angle \text{H-C-H} = 109^\circ 28' + 1/5\,(109^\circ 28' - \alpha)$$

where α is $\angle$ C-C-O or $\angle$ C-C-C; $\angle$ H-C-H $_{Av.}$ calculated in this way for the best TMO model is 113°38'.

C···O axis; this is an approximation, good to a degree or two, to the bisection of ∠ C-C-O by the plane of the methylene group. Even the assumption of angle bisection may be in considerable error, however, since the hydrogens may actually be attracted somewhat toward the side of the oxygen[16]. A curve was therefore calculated for a model which differed from that for curve J by having the plane of each methylene group adjacent to the oxygen tilted toward the oxygen by 12° from the bisector of ∠ C-C-O*. (The cross-ring C···H and O···H temperature factors were also slightly increased; see below.) No appreciable differences between this curve and curve A were noticeable, and it is therefore concluded that this point cannot be decided on the basis of even the excellent electron diffraction data now available.

A microwave investigation has confirmed[15] the planarity of TMO and indicated the existence of a low-frequency anharmonic out-of-plane bending vibration (the energy levels of the first two vibrational states are reported to be about 60 cm^{-1} and 200 cm^{-1}). This is in general accord with the low frequency "flopping" vibration associated with cyclobutane (145 cm^{-1}) [17, 18] and trimethylene sulfide (73 cm^{-1})[19]. A crude test of the observable effects of such a vibration was made by calculating test curves for models like J and F, but with out-of-plane bending simulated by a 0.01 Å mean shortening of the rigid planar cross-ring C···O and C···C distances, temperature-factored slightly ($a_{C\cdots O}$=

*This is no doubt an extreme angle change; its magnitude was suggested by the corresponding change tested for trimethylene sulfide. In neither case was any refinement of this parameter attempted. A smaller change may be preferable; ∠ H-C-H may also have to be altered.

$a_{C\cdots C} = 0.00045)^*$. Some small improvement occurs for max. 7, 8, 9 of curve J, but at the expense of removing the splitting of max. 13; curve F is also changed only slightly. Since good agreement with experiment is given by rigid planar models, especially in the region of max. 13, it was decided to base the determination on the assumption of rigidity. It is recommended, however, that sectored diffraction photographs be obtained, if possible, to see if some decision cannot be reached regarding this point.

The following values were used in the temperature factor, $e^{-a_{ij}s^2}$: $a_{C-O} = a_{C-C} = a_{C\cdots O} = a_{C\cdots C} = 0$ (but see previous paragraph); $a_{C-H} = 0.0017$; $a_{C\cdots H} = a_{O\cdots H} = 0.0036$. This latter value is probably too small for the cross ring $C\cdots H$ and $O\cdots H$ terms, but no appreciable effect was observed by using $a_{C\cdots H} = a_{O\cdots H} = 0.0056$ with these longer distances in a sample calculation.

Fig. 1 shows several of the calculated intensity curves. The best model lies quite close to J, which shows the splitting of max. 13, and is in good agreement with the other observations as well. Curves F and E show minor points of difference with the visual curve, while curve B is a typical curve well outside the limits of acceptability. All the curves calculated look quite similar out to about q = 65.

Fig. 2 is a plot of parameter space: $\angle$ C-C-C vs. C-C. The closed curve encloses the region of models giving acceptable intensity curves. The planar models considered by Shand lie on the two lines: the lower

---

*Also suggested by work on trimethylene sulfide. A crude calculation was carried out for the sulfur compound; the numbers used for the TMO curves seemed reasonable by comparison.

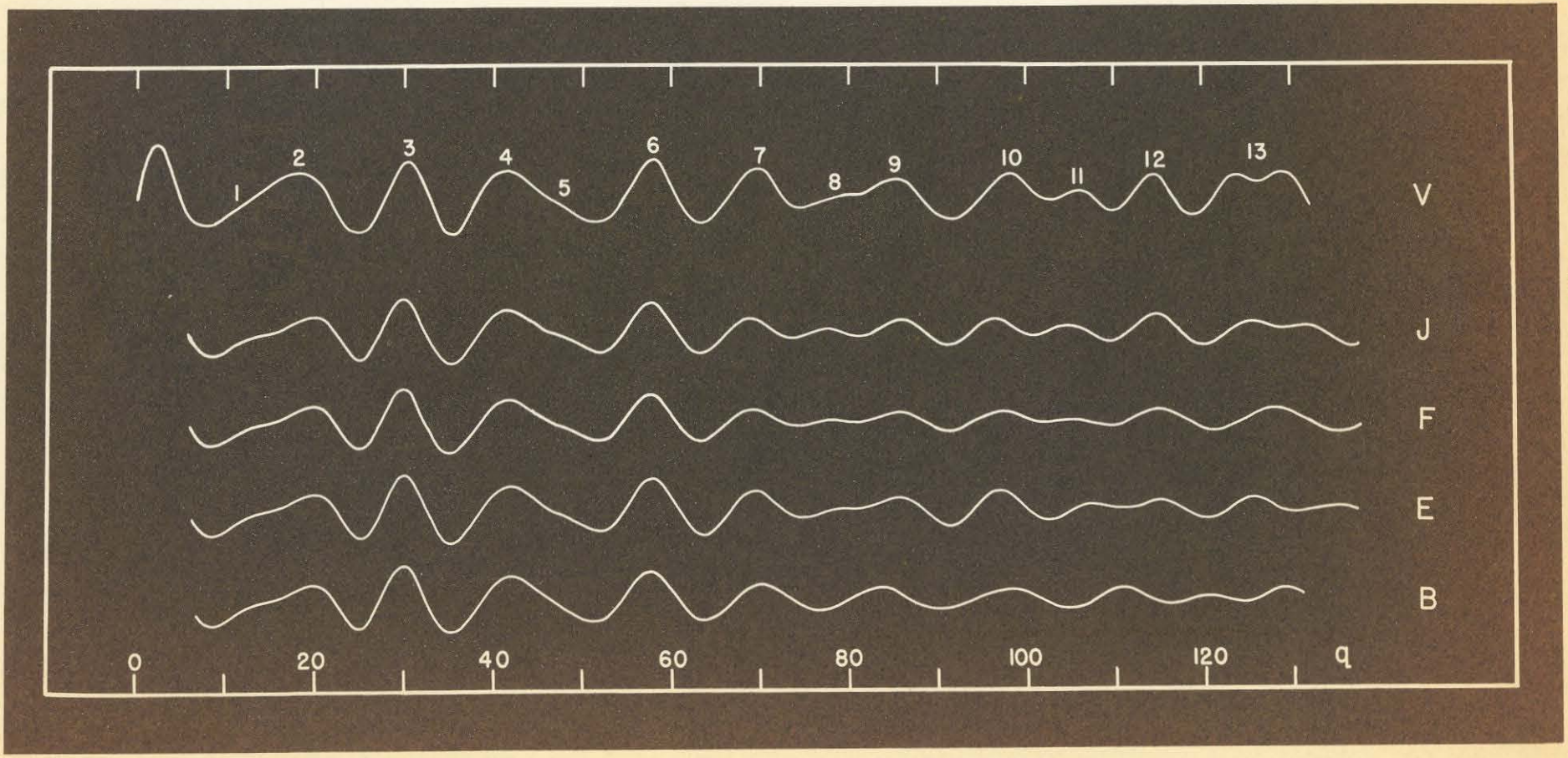

Fig. 1

Fig. 2

Parameter plot for TMO: ∠ C-C-C vs. C-C.

The plain dots are models calculated in this study, the open circles are models calculated by Shand, and the x marks the best model.

(For all models calculated in the current study, C-O = 1.46, C-H = 1.09. See text.)

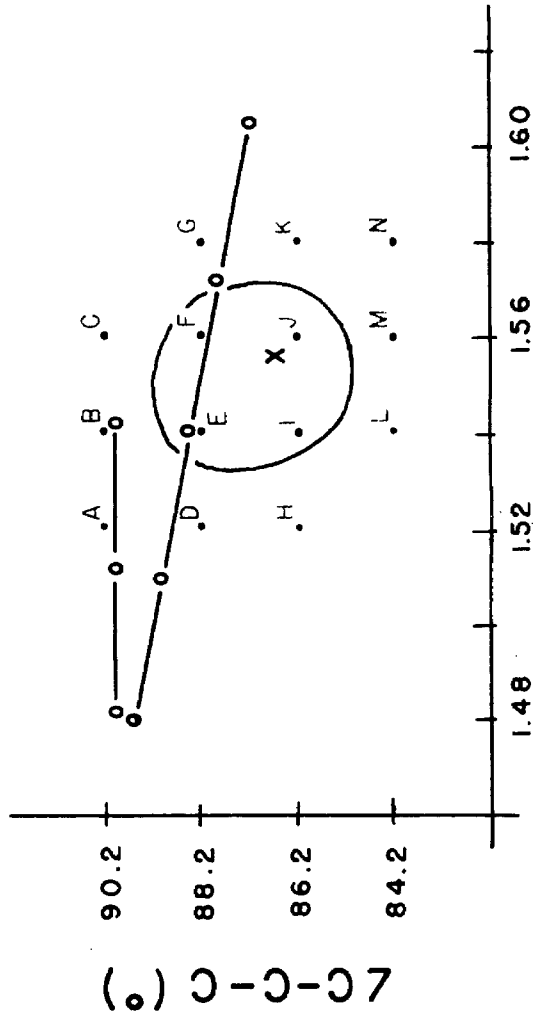

Table I

Min.	Max.	q_E	q_E/q_o	q_F	q_F/q_o	q_I	q_I/q_o	q_J	q_J/q_o
1		8.6	(1.026)	8.4	(1.002)	8.5	(1.014)	8.5	(1.014)
	1	13.3	(1.058)	12.5	(.994)	13.5	(1.074)	13.2	(1.050)
2		16.1	(1.086)	15.4	(1.039)	15.7	(1.059)	15.5	(1.046)
	2	20.0	(1.111)	20.1	(1.117)	20.0	(1.111)	19.9	(1.106)
3		25.1	1.009	24.9	1.001	25.1	1.009	25.0	1.005
	3	30.0	.998	29.8	.991	30.0	.998	29.8	.991
4		35.3	1.002	35.2	.999	35.3	1.002	35.1	.996
	4	41.8	.995	41.7	.993	41.8	.995	41.5	.988
5		46.4	(1.042)	46.3	(1.040)	46.4	1.042	46.2	1.038
	5	48.4	(1.017)	48.5	(1.019)	48.5	1.019	48.5	1.019
6		52.0	1.011	51.8	1.007	52.1	1.013	52.0	1.011
	6	57.9	1.000	57.8	.998	57.8	.998	57.7	.997
7		63.7	1.004	63.3	.998	63.7	1.004	63.3	.998
	7	69.5	.998	69.0	.991	69.3	.996	68.7	.987
8		75.0	1.010	74.0	.996	75.0	1.010	73.6	.991
	8	79.1	1.021	78.2	1.010	78.6	1.015	77.5	1.001
9		80.9	.996	81.1	.998	80.6	.992	81.3	1.001
	9	85.5	1.000	85.9	1.005	85.5	1.000	85.9	1.005
10		91.6	1.001	91.4	.998	91.1	.995	91.3	.997
	10	97.1	.988	97.1	.988	76.7	.984	96.4	.981
11		102.5	1.004	101.8	.998	102.2	1.002	101.0	.990
	11	107.3	1.011	104.9	.988	106.7	1.005	104.9	.988
12		110.8	1.012	109.6	1.001	110.1	1.006	109.5	1.001
	12	115.2	1.009	114.9	1.007	114.7	1.005	114.8	1.006
13		120.2	(1.008)	120.0	(1.006)	119.9	(1.005)	120.2	(1.008)
	13	125.4	(1.004)	128.1	(1.025)	125.1	(1.001)	125.6	(1.005)
Av., 18 features			1.003_8		0.998_2		1.001_6		0.996_3
Av. Dev.			0.006_3		0.004_7		0.006_1		0.006_6

For best model: C-C = $1.556 \times 0.9978 = 1.55_3$ Å

C-O = $1.46 \times 0.9978 = 1.45_7$ Å

line is for models with all the interior ring angles at carbon equal, the upper line for $\angle$ C-C-C = 90°. Shand's best model is very close to E; it is interesting to note that the curves for models E and I are virtually identical, a coincidence which is further evidence of the arbitrary nature of Shand's assumptions.

Table I shows the calculation of q/q_o for several curves. Following are the final parameters and estimated limits of error for TMO:

$$\text{C-O} = 1.45_7 \pm 0.02 \text{ Å}$$

$$\text{C-C} = 1.55_3 \pm 0.03 \text{ Å}$$

$$\angle \text{C-C-C} = 86.8^\circ \pm 2.5^\circ$$

Some additional computed parameters are:

$$\angle \text{C-O-C} = 94.2^\circ \pm 2.5^\circ$$

$$\angle \text{C-C-O} = 89.5^\circ \pm 2.5^\circ$$

$$\frac{\text{C-H}}{\text{C-O}} = \frac{1.09}{1.46} \quad \text{(assumed)}$$

Discussion. A comparison of the results of this investigation and Shand's is presented below (Table II):

Table II

	Shand	Present Work	Change
C-O	1.46	1.45_7	-0.003
C-C	1.54	1.55_3	+0.013
C···O	2.09_5	2.12_1	+0.026
C···C	2.14_7	2.13_4	-0.013
$\angle$ C-C-C	88.5°	86.8°	-1.7°
$\angle$ C-C-O	88.5°	89.5°	+1.0°
$\angle$ C-O-C	94.5°	94.2°	-0.3°
$\frac{8(\text{C-O})+6(\text{C-C})}{14}$	1.49_4	1.49_8	+0.004

The overall size and shape of the TMO molecule, judged by $\angle$ C-O-C and the average bond length, remain almost unchanged by the new investigation. The significant individual changes are the lengthened C-C bond, and the near-equality of the cross-ring distances. The uncertainties of each investigation are sufficiently large so that their results cannot be considered incompatible with each other.

An important check on the current determination is given by comparing the observed[15] with the computed moments of inertia. In computing moments, the electron diffraction results for the bonded distances and ring angles were used, but the H-C-H angles were individually adjusted to minimize strain (by using the formula $\angle$ H-C-H = $109^{\circ}28' + 1/5(109^{\circ}28' - \alpha)$, where α is $\angle$ C-C-O or $\angle$ C-C-C), and the plane of each lateral CH_2 group moved 12° from the C$\cdots$C axis toward the side of the oxygen. In addition, a C-H length of 1.08 Å was assumed. Using this model, results in good agreement with observed moments for the ground vibrational state are obtained:

	Observed	Calculated	Difference
I_A	41.965 amuÅ^2	41.967	0 percent
I_B	43.078	43.293	0.5
I_C	75.101	75.315	0.3

It is reported[15] that work is proceding in an attempt to work out TMO completely by microwave spectroscopy; the results are awaited with interest.

The significance of the new results can be discussed in terms of the

outlined in the introduction. The C-C distance is about 0.01 Å longer than the normal, while the C-O distance is about 0.03 Å longer than the 1.43 Å distance usually associated with this bond*. It is suggested that the two dominant factors here are cross-ring repulsion and angle-deformation strain. The cross-ring repulsion energy for TMO is probably of the same order as for cyclobutane. Since the bond-stretching constants for C-C and C-O** do not differ too greatly, it might be expected that all four bonds of TMO would show lengthenings from normal of perhaps 0.02 - 0.03 Å, in accord with the lengthening of 0.028 Å found for cyclobutane[4]. But although the C-O bonds are lengthened by about this amount, the C-C bonds exceed their normal distance by only about half this quantity.

Looking now at angle-deformation strain, it is noted that $\angle$ C-O-C, 94.2°, is not very far from the 90° angle which would be made by pure p-bonds, whereas each ring angle at carbon is compressed from normal tetrahedral to less than 90°; this unsymmetrical arrangement of strain gives rise to forces which tend to compress the two C-C bonds and stretch the two C-O bonds. Together with the stretching forces due to cross-ring repulsion, angle-deformation strain thus gives rise to the small stretching of the C-C bonds, and the greater

---

*As found, for instance, in the following relatively simple compounds:

(a) $H_3C - OH$[20]: C-O = 1.427 ± 0.007 Å; $\angle$ C-O-H = 108°52' ± 2°

(b) $H_3C - O - CH_3$ [21]: C-O = 1.43 ± 0.03 Å; $\angle$ C-O-C = 111° ± 3°

(c) $H_3C - H_2C - OH$[21]: C-O = 1.43 ± 0.02 Å

** Treating $H_3C - CH_3$ and $H_3C - OH$ as for diatomic molecules, it is calculated that $(k_{C-C} / k_{C-O}) = 0.86$; the stretching frequencies used were: $\nu_{C-C} = 993$ cm^{-1} and $\nu_{C-O} = 1034$ cm^{-1}. Data with references are found in ref. 22, pp. 335, 344.

stretching of the C-O bonds.

Several points should be noted regarding the above argument. It has been assumed that $\angle$ C-O-C is almost strainless because it is forming p-bonds at an angle close to 90°. The true value for the normal angle is probably greater, somewhere between 90° and 109.5° (see ref. 16 and ref. 23, p. 86), perhaps about 103°. The argument remains unaffected however, since the angles at carbon are strained from tetrahedral by at least 12° more than the angle at oxygen is strained from 103°. (The normal angle for a carbon adjacent to an oxygen may also differ somewhat from tetrahedral, but presumably the relative situation remains the same.)

It has also been suggested[15, 18] that the staggered non-planar configuration of cyclobutane arises from torsional strain associated with the preferred staggered orientation of hydrogens on adjacent carbon atoms, and that the substitution of an oxygen for a methylene group relieves a sufficient amount of this torsional strain to enable TMO to be planar. But it seems likely that such strains have little effect on bond lengths [4, 24].

We have taken no account of possible delocalization effects attributable to the presence of the oxygen atom. Some evidence for an effect of this kind is found in diethyl ether [21], which has a C-C distance of only 1.50 ± 0.02 Å; a similar effect is observed, although with less certainty, in 1, 4-dioxane[13] with C-C = 1.51 ± 0.04 Å. This factor may contribute to the lesser stretching of C-C (relative to C-O) in TMO*.

*A similar effect does not seem apparent in diethyl sulfide, ethyl amine, or triethyl amine, nor in ethyl alcohol. Until further examples become available, no attempt will be made to evaluate the significance or magnitude of the shortening.

Finally, ethylene oxide, C_2H_4O, may be mentioned. This substance has the following parameters[25]:

$$C\text{-}C = 1.472$$

$$C\text{-}O = 1.436$$

$$\angle C\text{-}O\text{-}C = 61^\circ 24'$$

$$\angle C\text{-}C\text{-}O = 59^\circ 18'$$

The deformation of the two $\angle$ C-C-O from tetrahedral is $50^\circ 10'$, while $\angle$ C-O-C is reduced by only $28^\circ 36'$ from a right angle (or by $41^\circ 36'$ from 103°). The lesser strain in $\angle$ C-O-C results in a compressive force in C-C, and a stretching force half as large in each C-O. The inner consistency of this explanation can be tested as follows: C-C is shortened from the value for cyclopropane by 0.053 Å; the cyclopprane value in turn is 0.015 Å shorter than the standard C-C distance. The expected C-O distance is then 1.427 - 0.014 + 1/2(0.053)(0.86) = 1.436 Å, in good agreement with the observed value. Here we have made a bent-bond correction for C-O of 0.014 (1 percent of the unbent bond) and have taken account of the slightly greater stiffness of the C-O bond by multiplying by the ratio of the stretching force constants, 0.86. No correction has been made for deviation of the triangular frame from strict equiangularity.

3-Methylenetrimethylene Oxide (C_4H_6O)

This derivative of trimethylene oxide was first prepared by Dr. D. E. Applequist of these laboratories, and reported, together with other compounds, in his thesis[26]. One purpose of the present investigation, which was undertaken cooperatively with Dr. Applequist, is stated in his thesis*:

> "It was considered possible that 3-methylenetrimethylene oxide would provide an example of 1, 3-π - bonding, in the ground state, of the type used to explain the chemical behavior of methylenecyclobutene.. In an effort to demonstrate such bonding by measuring the interatomic distances in the molecule, an electron diffraction investigation was carried out . . ."

A brief preliminary report of the following results was given in an appendix; a full account of the investigation is now presented.

Experimental. Dr. Applequist reports** a boiling point for 3-methylenetrimethylene oxide (MTMO) of 70.0°C. at 745 mm. Electron diffraction photographs were taken on Kodak 50 plates with 40 kv. electrons at 10 cm. camera distance; the sample-bulb temperature was about -35° C. The photographs were interpreted visually in the usual way, and the usual correlation procedure applied***. Data extending to q = 130 were obtained.

Two visual intensity curves are reproduced in Fig. 3. The first, V_G, represents the author's interpretation of the photographs. The second, V_S, is taken from the observations of Prof. V. Schomaker and is substantially the same as the other; it is notable, however, in

---

*Ref. 26, p. 25.
**Ref. 26, p. 66 .
***See, for example, ref. 14.

its attention to fine detail. These details, not noted in curve V_G, are as follows: slight bumps on the inner slopes of max. 1, 5, and 9; a very slight change of slope on the outside slope of max. 1 near the bottom of min. 2; some fine feature on the outer slope of max. 8; and the compound nature of max. 10. Curve 13, which is close to the final best model, is in very good agreement with this detailed visual curve. The radial distribution curve (R of Fig. 3) was calculated from V_G. The vertical lines beneath the peaks are calculated for the best model. (The appearance of a small spurious peak on the outside of each main peak, associated with a minimum on the inside of the main peak, indicates unreliable measurements of q_o.) A number of theoretical curves are included in the figure, the more important cases of disagreement with the visual curve being indicated by critical marks[27].

The present investigation determined three parameters: $\frac{C=C}{C-C}$; $\frac{C-O}{C-C}$; and $\angle$ C-C-C. Fig. 4 represents a three-dimensional view of parameter space and shows the location of models for which curves were calculated. The closed curves demarcate the regions of acceptable theoretical curves; the small cross indicates the best local model for each plane (C=C constant). The best overall model is indicated by the shaded circle.

Curves were calculated for models with the following parameters: C-C = 1.54 ; C-H = 1.09 ; $1.42 \leqslant$ C-O $\leqslant 1.48$; $1.31 \leqslant$ C=C $\leqslant 1.35$; $83^\circ \leqslant \angle C^2\text{-}C^3\text{-}C^4 \leqslant 91^\circ$. As for TMO, it was assumed that $\angle$ H-C^2-H = $\angle$ H-C^4-H = $113^\circ 36'$, and that each of these methylene groups was perpendicular to the ring skeleton and to the straight line C=C$\cdots$O; in

addition $\angle$ H-C^5-H = 120° was used [28]. The skeleton was assumed to be coplanar and rigid. All terms except H···H were included in the calculations, and an effective value for Z_H of 1.25 was used. The same temperature factors were used as for TMO.

Final results, together with estimated limits of error, are:

$$C\text{-}C = 1.53_6 \pm 0.02 \text{ Å}$$

$$C\text{-}O = 1.45_6 \pm 0.03 \text{ Å}$$

$$C{=}C = 1.33_3 \pm 0.02 \text{ Å}$$

$$\angle \text{ C-C-C} = 86.7° \pm 3°$$

Other quantities of interest are:

$$\frac{\text{C-H}}{\text{C-C}} = \frac{1.09}{1.54} \quad \text{(assumed)}$$

$$\angle \text{ C-O-C} = 92.8°$$

$$\angle \text{ C-C-O} = 90.2_5°$$

Ring

$$C\cdots O = 2.12_1$$

$$C\cdots C = 2.10_8$$

Table III shows some typical calculations of q/q_o.

Discussion. Quoting again from Applequist*:

> "It was thought that the bonding interaction between the oxygen and the opposite carbon atom might be sufficiently large to make the intracyclic angle at C^5 substantially larger than 90°, in which case the bonding would have been clearly indicated, but in the absence of suitable data for comparison, the present results cannot be interpreted as evidence for or against 1, 3 - π - bonding."

Table IV lists the corresponding parameters for TMO and MTMO.

---

*Ref. 26, p. 25.

Fig. 4

Three-dimensional representation of parameter space for MTMO. On each plane of constant C = C is plotted $\angle$ C-C-C vs. C-O for fixed C-C (1.54) and C-H (1.09). (See text.) Intersections of volume containing acceptable models with planes of C = C constant are indicated by closed curves; best model for each plane is noted by solid circle, best final model by shaded sphere.

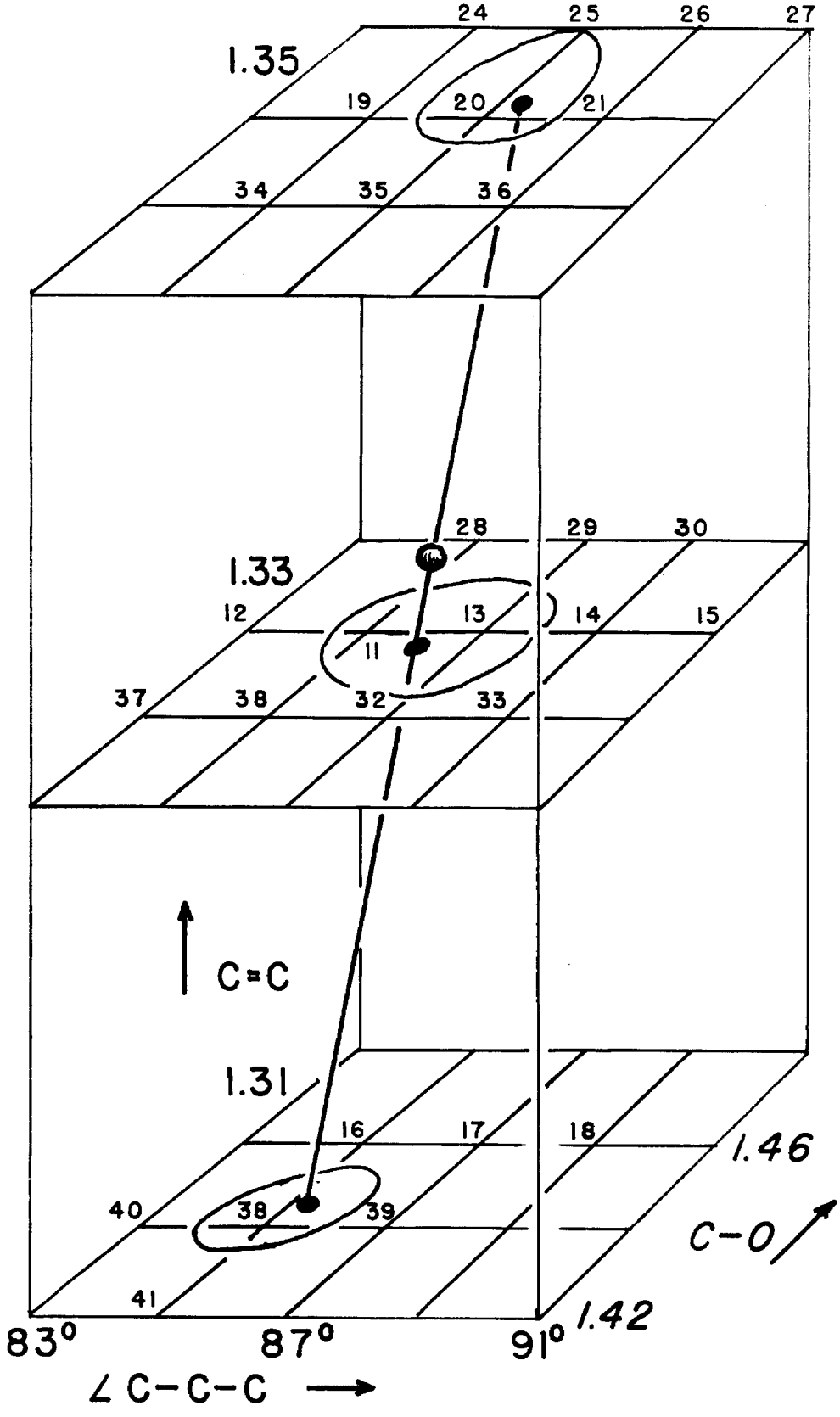
24
25
26
27
1.35
19
20
21
34
35
36
28
29
30
1.33
12
13
14
15
11
37
38
32
33
C=C
1.31
16
17
18
1.46
C-O
40
38
39
41
83°
87°
91°
1.42
∠ C-C-C

Table III

Min.	Max.	q_o	q_{13}	q_{13}/q_o	q_{20}	q_{20}/q_o
1		9.47	10.2	(1.077)	10.0	(1.056)
	1	17.12	19.0	(1.110)	18.8	(1.098)
2		24.38	25.8	(1.058)	25.8	(1.058)
	2	30.46	30.6	1.005	30.4	.998
3		35.28	35.9	1.018	35.8	1.015
	3	41.50	41.1	.990	41.0	.988
4		44.17	44.8	1.014	44.4	1.005
	4	47.54	46.8	.984	46.6	.980
5		51.60	51.3	.994	51.0	.988
	5	58.41	58.9	1.008	58.9	1.008
6		64.10	64.0	.998	64.0	.998
	6	69.70	69.3	.994	69.3	.994
7		74.18	73.7	.994	73.3	.988
	7	78.60	77.2	(.982)	76.9	(.978)
8		81.82	80.6	(.985)	80.3	(.981)
	8	85.46	84.0	(.983)	83.5	(.977)
9		91.36	90.7	(.993)	91.0	(.996)
	9	97.28	97.8	(1.005)	97.7	(1.004)

Av. 10 best features	0.999_9	0.996_2
Av. deviation	0.009_1	0.008_6

Av. for best model: 0.997_7

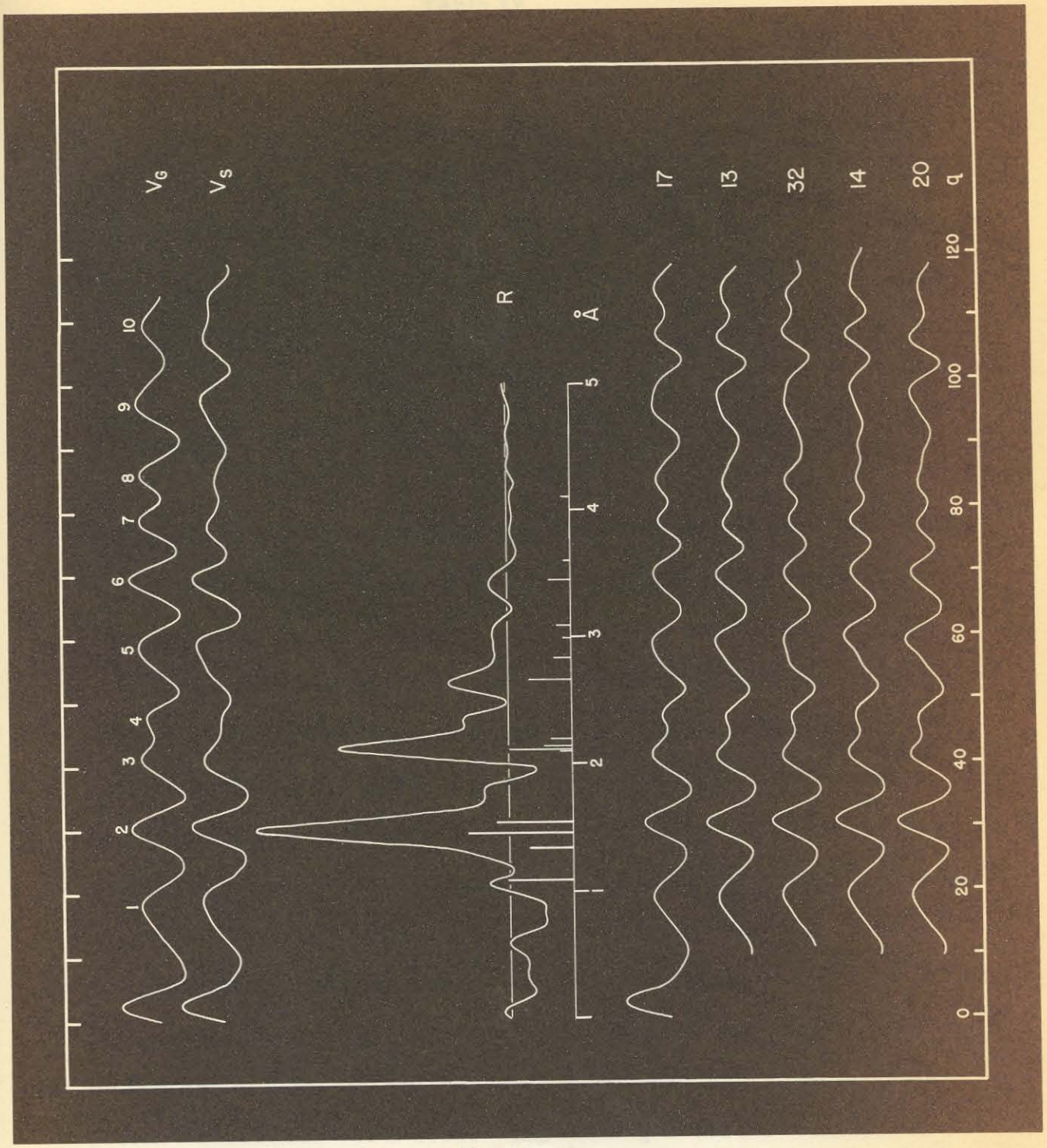

FIG. 5

Table IV

	TMO	MTMO	Difference
C-O	1.45_7	1.45_6	-0.001
C-C	1.55_3	1.53_6	-0.017
C···O	2.12_1	2.12_1	0
C···C	2.13_4	2.10_8	-0.026
$\angle$ C-O-C	94.2°	92.8°	-1.4°
$\angle$ C-C-C	86.8°	86.7°	-0.1°
$\frac{8C\text{-}O+6C\text{-}C}{14}$	1.49_8	1.49_0	-0.008

The limits of error on the determination of parameters for both TMO and MTMO are sufficiently large to make it difficult to say whether any significant change has taken place. If some weight is given the figures in Table IV, then the overall shortening of the bond lengths of MTMO relative to TMO can be attributed to the methylene group and hyperconjugation. Although it is difficult to say just how the cross-ring repulsion energy should compare with that for TMO, the increased strain at C^3 tends to further shorten C-C and stretch C-O. Additional effects (such as delocalization; see discussion of TMO) also enter, but are presumably about the same as for TMO. Until more data for other compounds are available for comparison (methyl allyl ether would be interesting to compare with MTMO), it would be unwise to make any positive assertions about cross-ring bonding in MTMO. Insofar as any confidence may be put into such fine differences, the slight decrease in $\angle$ C-C^3C and the decrease in C···C relative to the unchanged

C···O in going from TMO to MTMO weigh against the possibility of cross-ring C···O bonding.

It should be instructive to compare MTMO to TMO and methylenecyclobutane to cyclobutane at the same time. The parameters reported for methylenecyclobutane[29] are: C-C = 1.55 ± 0.02 Å; C=C = 1.34 ± 0.03 Å; ∠ C-C-C = 92.5° ± 2°. Unfortunately the determination is based on the assumption of equal C-C bond lengths in the ring; since the methylene group is expected to shorten somewhat the adjacent bonds, the value 1.55 Å is an average value. In addition, differential angle strain tends to shorten the two bonds adjacent to the double bond and lengthen the other two. The over-all C-C bond distance is presumably shortened from the cyclobutane value by the methylene group.

The available results for β-propiolactone[24] are inadequate for purposes of comparison, since the investigators assumed equality of the two C-C distances and of the two C-O distances (reported as 1.53 ± 0.03 Å and 1.45 ± 0.03 Å respectively) despite the presence of the carbonyl group. The potent influence of a carbonyl group on C-O and C-C bonds is seen by reference to methyl acetate[14] (C-C = 1.52 ± 0.04 Å; carboxyl C-O = 1.36 ± 0.04 Å; methoxyl C-O = 1.46 ± 0.04 Å) and acetaldehyde[30] (C-C = 1.50 ± 0.02 Å). The only useful quantity from the investigation of β-propiolactone is the weighted average distance in the ring; this is 1.48_4 Å, shorter (as expected) than for TMO by 0.015 Å, and slightly shorter than for MTMO by 0.006 Å. Taken by itself, however, the average C-O distance in β-propiolactone appears much too long relative to the average in, say,

methyl acetate (1.41 Å). A reinvestigation of the lactone might provide an interesting comparison if carefully done.

Trimethylene Sulfide (C_3H_6S)

Previously published work[19] on trimethylene sulfide (TMS) has supplied some useful spectroscopic and calorimetric data. The purpose of the present work is to supply a check on the indirectly derived structural parameters, and to provide further information about distances in four-membered ring molecules.

Experimental. A sample of TMS* of a purity estimated at better than 99 percent was used for this study; it is reported[31] that the material is light-sensitive, so it was kept refrigerated and dark to minimize polymerization. Electron diffraction photographs were taken in an older apparatus (now discarded) on Kodak Process Panchromatic sheet film with sample-bulb temperatures of from -20° C to 15° C, and in a newer apparatus on Kodak 50 plates with a sample-bulb temperature of about 0° C; the camera distance was about 10 cm. and the accelerating potential about 40 kv. in both cases. Visual curves and measurements from the old and new photographs check quite well; data extending out to about q = 110 were observed.

The visual intensity curve (V) is reproduced in Fig. 7. The curve is not very rich in detail, the principal term, C-S, predominating. However, the following features and comparisons were useful in determining a best model and estimating limits of error. Max. 6

*This sample of API-BM certified sulfur compound, purified at the Laramie Station of the U.S. Bureau of Mines, has been made available by the American Petroleum Institute Research Project 48A on the Production, Isolation, and Purification of Sulfur Compounds and the Measurments of their Properties. The gift of a generous sample of TMS is gratefully acknowledged.

and 8 have about the shapes shown in curve V, with max. 6 below the average height of its neighbors; the relative heights of max. 7, 8, 9 is somewhat uncertain, but max. 8 may be slightly above the average of max. 7 and 9. Max. 4 is below the average height of max. 3 and 5, and max. 5 is above the average of max. 4 and 6, and is slightly asymmetric. Max. 7 and min. 8 appear outstanding, and min. 6 is perhaps somewhat deeper than the average of min. 5 and 7.

The radial distribution curve shows clearly separated C-H, C-C, and C-S peaks, and compound peaks with maxima at 2.42 Å (containing C···S, C···S, and three shorter S···H and C···H distances) and 3.24 Å (containing the longer C···H and S···H distances).

The two parameters used in treating TMS were $\frac{C\text{-}C}{C\text{-}S}$ and $\angle$ C-S-C. Two different sets of curves were calculated: one set based on a rigid planar model, the other based on a planar non-rigid model with a large out-of-plane vibration. In addition it was necessary to adjust $\angle$ S-C-H by tilting ;the planes of the lateral methylene groups.

Both rigid and non-rigid models were calculated over the following range of parameters*: C-H = 1.09; C-S = 1.84; $1.52 \leqslant$ C-C $\leqslant 1.58$ (0.02); $76^\circ \leqslant \angle$ C-S-C $\leqslant 82^\circ (2^\circ)$; $\angle$ H-C-H $= 109^\circ 28' + 1/5(109^\circ 28' - \alpha)$, where $\alpha = \angle$ C-C-C or $\angle$ C-C-S.

For the rigid models, $a_{C\text{-}H} = 0.0017$; $a_{C\cdots H} = 0.0056$ for the long cross-ring terms; and $a_{S\cdots H} = a_{C\cdots H} = 0.0036$ for the shorter terms, were used in the temperature factor, $e^{-a_{ij}s^2}$. In the first set of models calculated, the plane of a lateral CH_2 group bisected

*For the non-rigid models, $\angle$ C-S-C is the angle as the molecule passes through the planar configuration.

$\angle$ C-C-S. Curves F_1, G_1, R_1, and S_1 are some of the better curves of this group. The principal points of disagreement are indicated by the critical marks[27]. The best model is probably a compromise between F_1 and G_1, and possibly R_1: curve F_1 is unsatisfactory with regard to max. 8 and 9, while max. 5 and 6 disqualify curves G_1 and R_1. The best model possible is indicated by the open circle in Fig. 8.

Some improvement in the appearance of the calculated curves is obtained by shortening the S···H distance. Such a change has little influence on the features beyond about q = 70, but has a considerable effect on max. 4, 5, 6, 7 and their associated minima. A shortening of about 0.1 Å in the shorter S···H distance was chosen by consideration of how a change in this distance could be made to improve some critical features in a suitable theoretical curve; this corresponds to tilting the lateral CH_2 groups about 15° from the bisector of $\angle$ C-C-S toward the side of the sulfur atom. This change is no doubt too large, but it helps the appearance of several of the curves. No attempt was made to refine the value of this angle, although such a refinement would be highly desirable. The four curves shown in Fig. 6, F_1', G_1', R_1', and S_1', illustrate the changes produced in the four previous curves. A curve based on R_1', but perhaps shifted a bit toward G_1', would probably be in substantial agreement with our observations; the shaded circle indicates this best model in Fig. 8.

From calorimetric and spectroscopic data, it has been inferred[19] that TMS has a planar equilibrium configuration with a very low (unobserved) frequency out-of-plane bending vibration. A frequency of 73 cm^{-1}

is needed for this vibration in order to obtain agreement of the calculated with the observed entropy (assuming point group symmetry C_{2v}; for lower symmetry, 148 cm^{-1} is needed). A number of the observed infra-red and Raman frequencies are explainable as sum-combinations of observed fundamentals with 73 cm^{-1} (148 cm^{-1} leaves these frequencies unexplained).*

If the ring of TMS does indeed have an out-of-plane bending frequency of 73 cm^{-1}, the motion might be expected to have relatively large amplitude; it is probably also anharmonic. An estimate was made of how this vibration affects the cross-ring distances (see below); the result was approximated by a mean shortening of the planar cross-ring C···C and C···S distances of about 0.015 Å, and an effective temperature factor with $a_{C\cdots C} = a_{C\cdots S} = 0.00045$. An arbitrary mean shortening of about 0.020 Å was applied to the cross-ring C···H and S···H distances, using an increased temperature factor with a = 0.0066.

Although the vibration is of fairly large amplitude, it was assumed to be harmonic for the purpose of calculating a distribution function for the cross-ring distances. The following description outlines the method used for calculating approximately the C···S distribution; since C···S and C···C are about equal, the same result was used for C···C as well.

From investigation of the rigid curves C···S was estimated to be about 2.40 Å. The TMS ring was idealized to a square with diagonal

*The preceding argument is a condensed version of that offered in ref. 19.

2.40 Å, and the mode of the vibration was assumed to consist of one pair of opposite masses moving up while the other pair moves down, the bond lengths remaining fixed. To preserve symmetry, it was further assumed that the average mass of the opposed $S\cdots CH_2$ pair was $\frac{32 + 17}{2}$ *; for the pair of opposed CH_2 groups, a combined mass of 34 was used. Under these conditions the square configuration is preserved in projection onto the equilibrium plane, the projected radial shortenings being equal for all four masses. In Fig. 6, looking down onto the equilibrium plane (in the plane of the paper), the solid lines represent the idealized square molecule of TMS in its average planar configuration. The dotted lines represent the molecule at some instant during the vibration, with two masses (+) moving up and two (−) down with respect to the plane of the paper.

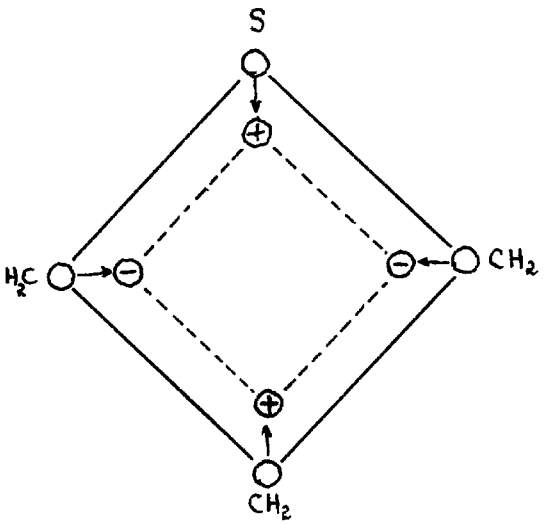

Fig. 6

*See ref. 4, footnote 17.

Treating the two centers of mass as a harmonic oscillator, a mean square vertical displacement between them of 0.05878 $\mathring{A}^2$ is obtained. If x is the vertical separation of the centers of mass and r is the C···S separation, then the relative probability distribution for r is given by

$$P(r) = Ne^{-\left(\frac{1}{2\overline{x^2}}\right)x^2} \frac{dx}{dr}$$

where N is a normalizing factor and the exponential is the distribution function for a harmonic oscillator. Although P(r) is infinite at x = 0 (r = 2.40), a value of P(2.40) was chosen which preserved the computed value for $\overline{r^2}$ (= 4 x $(1.20)^2$ - 2 $\overline{x^2}$) when calculated for r at intervals of 0.01 $\mathring{A}$. By actually computing a curve for this distribution of r, it was found that to a good approximation it can be replaced by a single term of frequency 2.385 and an effective temperature factor with $a_{C\cdots S}$ about 0.00045. Although there are many crude approximations in the calculation as given, the final outcome is probably as good as necessary for the purpose at hand.

The four curves F_2, G_2, R_2 and S_2 are calculated for a non-rigid model, using the approximations for cross-ring terms mentioned above. The planes of the lateral CH_2 groups bisect $\angle$ C-C-S. No curve, or interpolated curve, can be considered satisfactory for this type model.

Finally, four curves (F_2', G_2', R_2', S_2') are shown for which the lateral CH_2 groups were adjusted as for the rigid models. These curves show a definite improvement over the immediately preceding group. Curve R_2' is so well in accord with our observations that it is taken as the best model for this series of curves.

The principal qualitative difference between curve R_1' and curve R_2'

is the slightly higher max. 8 in the latter curve. This is insufficient evidence for discarding the rigid for the non-rigid model, and our decision in favor of the latter is primarily determined by the spectroscopic and calorimetric data mentioned earlier. The situation is further complicated by consideration of several other factors: it is possible (though not, perhaps, probable) that the spectroscopic-calorimetric deviation of 73 cm^{-1} for the out-of-plane bending is in error; an important quantity, $\angle$ S-C-H, was not thoroughly investigated, and should probably be treated as one of the variable parameters; the calculation of the effect of the out-of-plane bending may be in error, either by reason of excessively crude approximations, or anharmonicity; and finally, in the absence of more precise data (sectored electron diffraction photographs) some critical judgements regarding the appearance of the photographs must remain in some doubt.

Listed below are the final parameters and estimated limits of error corresponding to best model R_2':

$$\text{C-S} = 1.85_1 \pm 0.02 \text{ Å}$$

$$\text{C-C} = 1.54_9 \pm 0.03 \text{ Å}$$

$$\angle \text{C-S-C} = \begin{cases} 78.0^\circ \pm 1^\circ & \text{(maximum angle)} \\ 77.3^\circ & \text{(mean angle)} \end{cases}$$

$$\text{C}\cdots\text{S} = \begin{cases} 2.45_9 & \text{(maximum distance)} \\ 2.44_4 & \text{(estimated mean distance)} \end{cases}$$

$$\text{C}\cdots\text{C} = \begin{cases} 2.32_9 & \text{(maximum distance)} \\ 2.31_3 & \text{(estimated mean distance)} \end{cases}$$

$$\frac{\text{C-H}}{\text{C-S}} = \frac{1.09}{1.84} \quad \text{(assumed)}$$

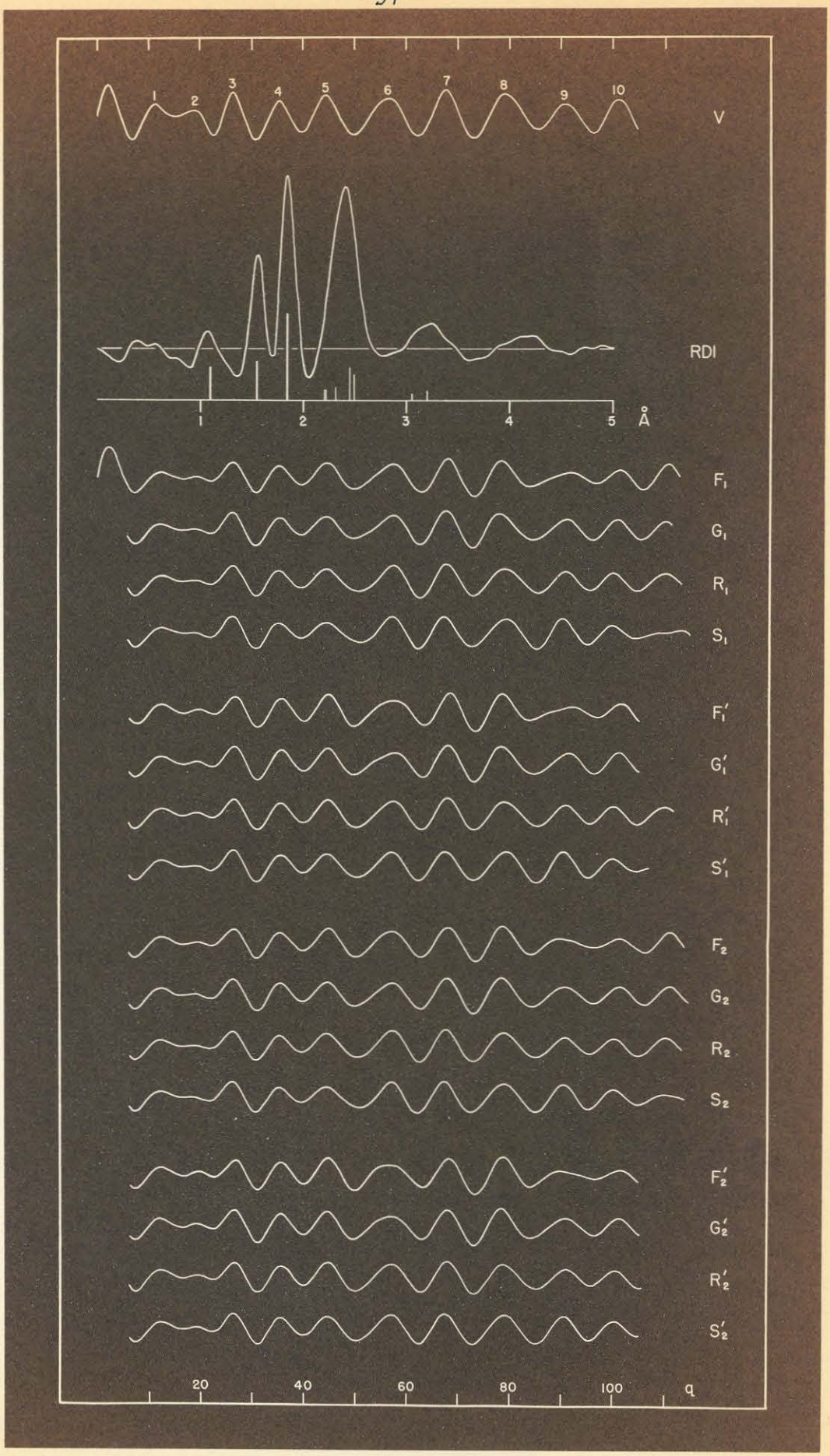
1
2
3
4
5
6
7
8
9
10
V
RDI
1
2
3
4
5
Å
F1
G1
R1
S1
F1′
G1′
R1′
S1′
F2
G2
R2
S2
F2′
G2′
R2′
S2′
20
40
60
80
100
q

Fig. 7

Fig. 3

Parameter Plot for TMS: C-C vs ∠ C-S-C

(C-S = 1.84; C-H = 1.09. See text.)

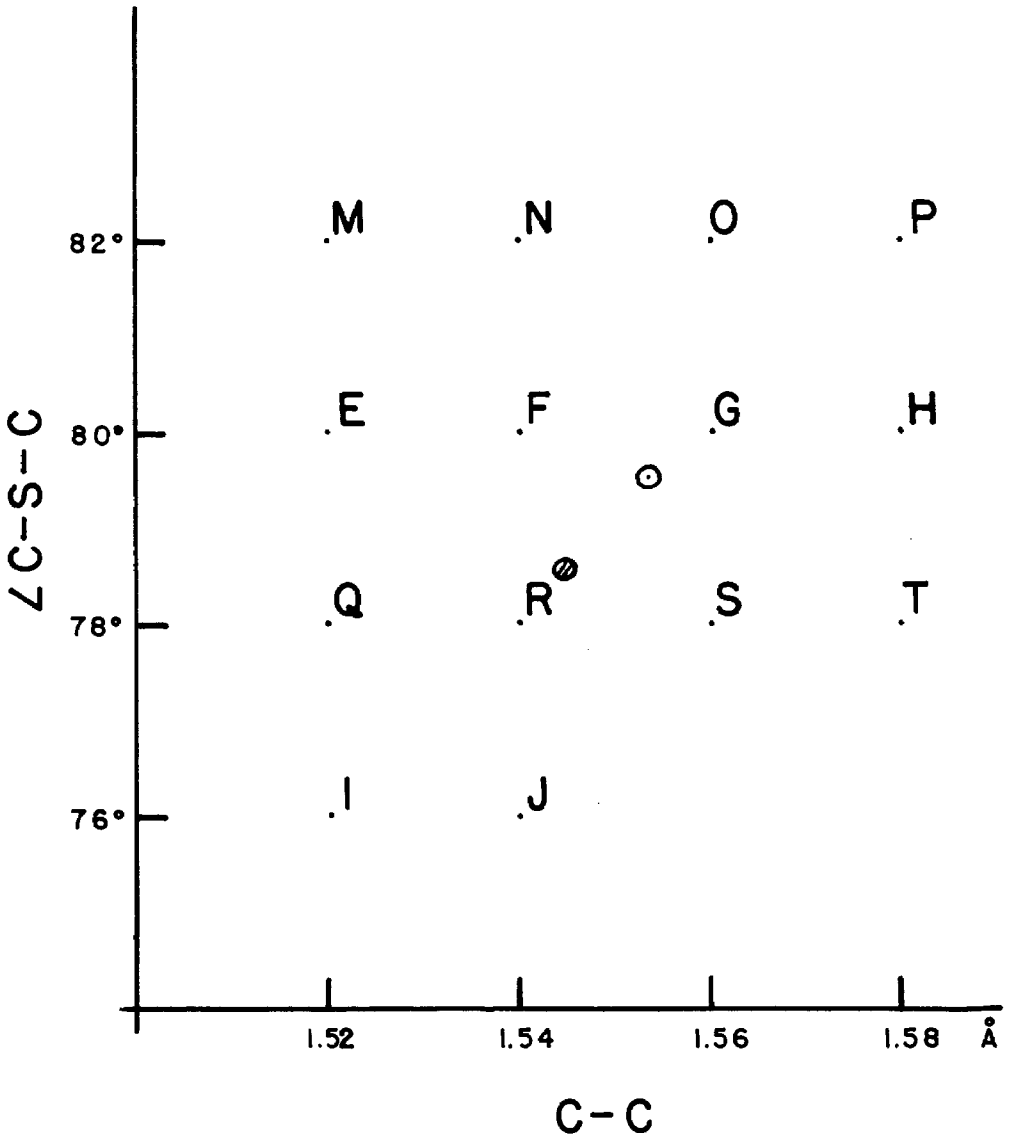

Table IV

Min	Max.	q_o	q_{R_1}	q_{R_1}/q_o	q_{R_2}'	q_{R_2}'/q_o
1		6.87	7.2	(1.048)	7.3	(1.063)
	1	11.05	12.3	(1.113)	12.0	(1.086)
2		15.24	16.5	(1.083)	16.4	(1.076)
	2	19.45	18.8	(.967)	19.3	(.992)
3		22.65	22.1	(.976)	22.5	(.993)
	3	26.29	26.3	1.000	26.6	1.012
4		30.91	30.8	.996	31.1	1.006
	4	35.15	35.3	1.004	35.7	1.016
5		39.76	39.4	.991	40.0	1.006
	5	44.32	44.4	1.002	44.8	1.011
6		49.83	50.4	(1.011)	50.1	(1.005)
	6	56.39	57.3	(1.016)	57.2	(1.014)
7		62.26	62.7	1.007	62.9	1.010
	7	67.62	67.7	1.001	68.1	1.007
8		73.20	73.0	.997	73.2	1.000
	8	78.56	78.8	(1.003)	78.9	(1.004)
9		85.63	85.8	(1.002)	85.1	(.994)
	9	90.73	90.8	1.001	91.0	1.003
10		96.09	95.7	.996	95.9	.998
	10	100.77	99.9	.991	100.3	.995
11		106.38	104.9	(.986)	105.3	(.990)
	11	110.32	109.9	(.996)	110.3	(1.000)
Av. 11 selected features				0.998_7		1.005_8
Av. deviation				0.004_1		0.004_9

$\angle$ C-C-C = 97°30' (maximum)

$\angle$ C-C-S = 92°15' (maximum)

$\angle$ S-C-H = 105°33'

Table IV lists q/q_o for typical curves.

Discussion. The bonded distances in TMS show the characteristic lengthening of four-member rings. The increase from normal is only about 0.01 Å for the C-C bonds, while the C-S bonds have lengthened by at least 0.03 Å *. As for cyclobutane and trimethylene oxide, there is probably an appreciable tendency toward lengthening present in all bonds of the TMS ring. The new result of angle-deformation strain is the application of compressive forces to the C-C bonds and tensile forces to the C-S bonds. (Although $\angle$ C-C-C differs from tetrahedral by about the same amount that $\angle$ C-S-C differs from 90°, it is assumed that the deformation energy for $\angle$ C-S-C is less than for $\angle$ C-C-C. The normal valence angle for sulfur is probably close to 90°, unlike the normal oxygen valence angle discussed in connection with TMO). Since C-S bonds are somewhat weaker** than C-C bonds the relatively greater increment in the C-S bond length is not surprising. Using the

---

* A value of 1.815 Å is here adopted for the reference C-S distance. The following are offered for comparison:

H_3C-SH: C-S = 1.815 Å; S-H = 1.34 Å; $\angle$ C-S-H = 100° (assumed)[32]

H_3C-S-CH_3: C-S = 1.82 ± 0.01 Å [21]; $\angle$ C-S-C = 104° (see legend, Fig. 12)

H_3C-CH_2-SH: C-S = 1.81 ± 0.001 Å; C-C = 1.54 ± 0.02 Å; ($\angle$ C-C-S) = 113° ± 2° [21].

** The ratio of the force constants, k_{C-S} / k_{C-C}, is about 0.70, treating H_3C-SH and H_3C-CH_3 as diatomic molecules, with ν_{C-C} = 993 cm^{-1} (ref. 22, p. 344) and ν_{C-S} = 704 cm^{-1} [33].

heat of formation reported for TMS, 6.20 kcal/mole at 25° C[19], a total strain energy of 15.4 kcal/mole is calculated*, considerably lower than that for cyclobutane (26.0 kcal/mole)[4]. This suggests that the cross-ring repulsions are lower in TMS than in the hydrocarbon, and that the corresponding bond-lengthening effects would also be lower.

Results are also available for ethylene sulfide[25]:

C-S = 1.819

C-C = 1.492

$\angle$ C-S-C = 48°24'

$\angle$ H-C-H = 116°00'

The change in $\angle$ C-S-C from 90° is 41°36' while $\angle$ C-C-S changes from tetrahedral by 43°40'; as for TMO, consideration of the unequal angle strains leads to the conclusion that the C-C bond is being compressed by about twice the stretching force in each C-S bond. "Bent-bond" shortening would be expected to reduce C-S from 1.815 Å to 1.797 Å (i.e., by about 1 percent). The C-C bond is shortened from 1.525 Å by 0.003 Å, so that the expected lengthening for C-S would be $\frac{1}{2}\frac{0.033}{0.70}$ = 0.024 Å, where we have taken the significant difference in stretching force constants into account. The calculated C-S value is thus 1.797 + 0.024 = 1.821 Å, in good agreement with experiment.

Cyclobutene

A considerable amount of structural evidence (see ref. 4) indicates that carbon-carbon single bonds in three-membered rings are shorter, and in four-membered rings longer than the standard distance, 1.54 Å; an explanation of the bond shortenings is suggested by Coulson and Moffitt's[34] treatment of bond angle strain, and Dunitz and Schomaker[4] have related the lengthenings to a plausible repulsion between non-bonded carbon atoms. Cyclobutene, with its four-membered ring, seemed to us to be a worthwhile additional subject for study in connection with these distance effects.

Experimental. Samples of cyclobutene were kindly prepared for us by Drs. E. R. Buchman, J. C. Conly, and W. Neville, by reduction of 1, 2-dibromocyclobutane with zinc dust[35]. Electron diffraction photographs were made both in an older apparatus and in a newly constructed device, and were interpreted by two independent observers. The work had been largely completed using the older data, but the much better newer plates made possible a significant refinement.

Theoretical intensity curves were calculated over the shape parameter ranges $0.837 \leqslant C{=}C/C{-}C \leqslant 0.889$, $0.673 \leqslant C{-}H_{Av.} / C{-}C_{Av.} \leqslant 0.752$, and $-0.08 \leqslant C^1{-}C^4 - C^3{-}C^4 \leqslant +0.08$ Å ($C{=}C$ is $C^1{-}C^2$) for a molecule of C_{2v} symmetry, assuming C_{2v} local symmetry for C^3 and C^4, $\angle C{=}C{-}H = 125^\circ 26' + 1/2\,(125^\circ 16' - \angle C{=}C{-}C)$, and, for most of the calculations, $\angle H{-}C{-}H = 109^\circ 28'$*. In the temperature factor $e^{-a_{ij}s^2}$,

*No doubt $\angle$ H-C-H is somewhat greater than tetrahedral (see ref. 4); however, we have found that variations as large as 10° produce only very small changes in the intensity curves. The assumption on $\angle$ C=C-H is presumably better.

a_{ij} was taken as 0.0016 for C-H, 0.0030 for C···H, zero for C-C and C=C, and, usually, for best agreement beyond q ~120, between 0.0005 and 0.0010 for C···C. All terms except H···H were included and the effective value 1.25 was used for Z_H. As the work proceeded it became clear that a determination of the C-H $_{Av.}$ distance would have error limits of about ± 0.06 Å. We therefore made the additional very reasonable assumption that C-H $_{Av.}$ = 1.093 ± 0.015 Å in order to simplify and make more precise the determination of the remaining parameters.

The effects of small variations of the several parameters are shown by the theoretical intensity curves in Fig. 9, all of which are in acceptable agreement with observation. The usual comparisons (Table V presents some of the quantitative comparisons) led to the following parameter values and limits of error: C=C/ C-C $_{Av.}$ = $0.862 + 0.018 - 0.024$; $|C^1-C^4 - C^3-C^4| \leqslant 0.08$ Å; C-C $_{Av.}$ = $1.53_7 \pm 0.01_0$ Å; C=C = $1.32_5 \pm 0.04_6$ Å; ∠ C=C-C = $94.0^\circ \pm 0.8^\circ$. For any difference $C^1-C^4 - C^3-C^4$ less than 0.06 Å, the curves are about equally satisfactory.

Discussion. Our value 1.53_7 Å for the average carbon-carbon single bond length in cyclobutene is very close to the standard length of 1.54 Å, in contrast to values found for cyclobutane, tetraphenyl cyclobutane, and others, all of which are longer[4]. It is possible that this nearly normal length in cyclobutene merely reflects an ordinary bonding situation; however, it seems rather more likely that the bonding situation is more complicated than in the saturated four-membered ring compounds and that the bond-lengthening and bond-shortening

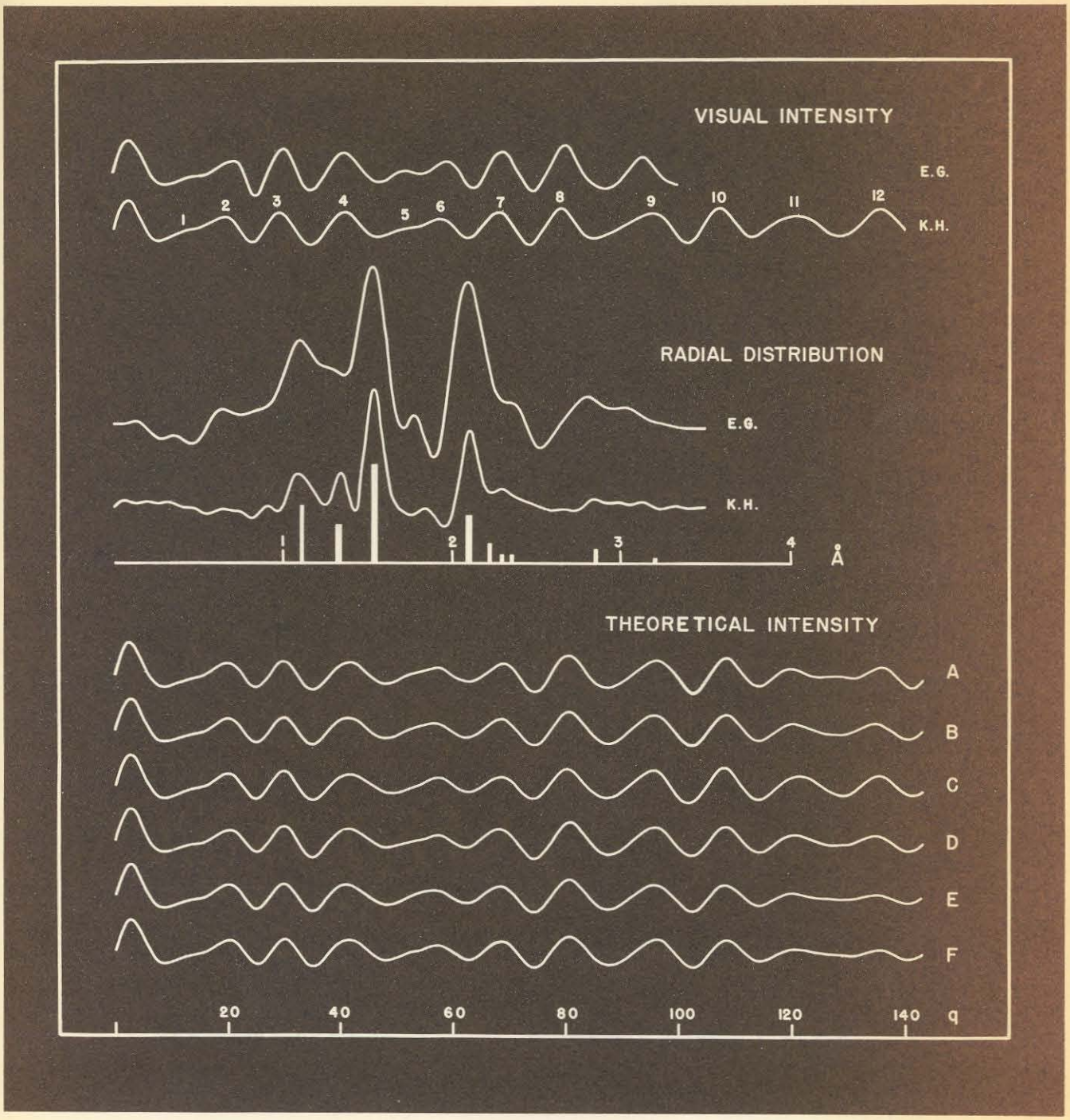
VISUAL INTENSITY
E.G.
K.H.
1
2
3
4
5
6
7
8
9
10
11
12
RADIAL DISTRIBUTION
E.G.
K.H.
1
2
3
4
Å
THEORETICAL INTENSITY
A
B
C
D
E
F
20
40
60
80
100
120
140
q

Fig. 9

Table V

Diffraction Data for Cyclobutene

Model E

Maxima			Minima		
No.	q_{obs}	q/q_{obs}	No.	q_{obs}	q/q_{obs}
1	11.72	(1.126)	1	8.37	(1.039)
2	19.57	(1.022)	2	15.63	(0.985)
3	29.33	1.019	3	24.76	1.010
4	41.26	0.994	4	35.14	0.996
5	50.77	(1.024)	5	46.48	(1.033)
6	57.95	(0.982)	6	54.04	(1.007)
7	68.40	1.011	7	62.92	0.983
8	79.46	1.013	8	73.94	1.009
9	96.54	(0.993)	9	84.97	(1.030)
10	107.84	.996	10	101.91	1.005
11	121.34	(.989)	11	112.87	1.011
12	136.04	(.992)	12	128.20	0.975

ave. 11 features 1.004

ave. deviation 0.007

For best model: $C\text{-}C_{Av.} = 1.53 \times 1.0045 = 1.537$ Å

effects arising from this situation are in near balance. One important bond-lengthening effect may be presumed to be a repulsion between cross-ring carbon atoms such as accounts nicely for the elongated bonds in cyclobutane[4]. Another is a plausible difference in the strains at the tetrahedrally and trigonally coordinated carbon atoms, which, with the simplest guess of greater angle stress at the trigonal atoms (cf. cyclopropene in the introductory section), would shorten the double bond and lengthen the opposite single bond while leaving the adjacent single bonds essentially unaffected (see ref. 5). A shortening effect may be expected from the double bond, which through first order hyperconjugation (and the possibly shorter covalent radius for the trigonally bonded carbon atom[36]) affects principally the adjacent bonds; that this effect may be large is shown by the short single bonds in propylene (1.49 Å), isobutene (1.50 Å), and cis-butene-2 (1.51 Å)[10].

We have considered the effects of these three bond-altering factors, which would seem to be the important ones, and find that bond lengths may be predicted which are in good agreement with observation. This good agreement derives, of course, from rather arbitrary (but in every case reasonable) assumptions, and is fairly sensitive to the balance between cross-ring repulsion and the effect of the double bond.

The single bond lengthening due to cross-ring repulsion we have taken to be 0.028 Å, the observed lengthening in cyclobutane, less 0.007 Å to take account of a presumably greater bent-bond

effect*; for the double bond lengthening we take 0.014 Å, since the bond-stretching force constant is about twice as great as for the single bonds, less about one-half the single-bond value for bent-bond shortening, or 0.004 Å. The estimated shortening effect of the double bond on the adjacent single bonds is 0.035 Å, the average of the isobutene and cis-isobutene-2 values, plus about 0.01 Å to take account of the presumably greater hyperconjugation in cyclobutene due to the presence of the more easily delocalized carbon-carbon single-bond electrons adjacent to the acceptor bond. Hyperconjugation may also be expected to shorten the unique single bond because of this carbon-carbon vs. carbon hydrogen effect; we assume 0.02 Å shortening here since there are two adjacent carbon-carbon single bonds instead of one. The differential angle strain is estimated to shorten the double bond 0.005 Å and to lengthen the opposing single bond 0.010 Å. These values are about one-sixth those computed from the bending force constants 0.33×10^5 and 0.51×10^5 dynes/cm./rad. (from propane and propene[8, 9] for use in the equation $F = kl\,\Delta\theta$; cf. cyclopropene discussion in the introductory section, where the constants are expressed for use in a potential energy function), angle strains of 24° and 31° for $\angle$ C-C-C and $\angle$ C=C-C, and assumed values of 4.7×10^5 and 9.5×10^5

*See ref. 34. A value of 0.012 Å for cyclobutene, corresponding to an average angle strain of 27°, is obtained by interpolation from a curve relating angle strains and bond shortenings for cyclobutane, cyclopropane, and ethylene; the cyclobutane value is 0.005 Å. To a surprisingly good approximation the observed bond lengths in these compounds are related to the standard distance of 1.54 Å as the chord is to the arc of a circle. See C. N. Copley, Chem. and Ind. 663 (1941), and H. J. Bernstein, J. Chem. Phys. 15, 284 (1947).

dynes/cm. for the single-bond and double-bond stretching constants. The factor one-sixth is approximately the ratio between the strain energy per CH_2 group observed in cyclobutane and that calculated using the above / C-C-C bond-bending constant. The results of these considerations are summarized in Table VI:

Table VI

Estimated Effects of Bond-Altering Factors on Bond Lengths in Cyclobutane.

Factor \ Bond	C^3-C^4	C^1-C^4	C^1-C^2
Cross-ring repulsion	+0.021	+0.021	+0.010
Hyperconjugation	-0.020	-0.045	---
Differential angle strain	+0.010	---	-0.005
Resultant bond length	1.551	1.516	1.335
Av. single bond length		1.528	

Conclusion

In discussing the structures of the compounds whose molecular structures have just been presented, we have emphasized the role played by cross-ring repulsive energy and the energy of deformation of valence bonds in four-membered rings. Few calculations of a quantitative nature have been made, but in most places an attempt has been made to demonstrate how consideration of these factors, and others, helps in qualitatively understanding the bond-lengths in such ring compounds. The complexity of attempting more exact calculations is shown in the paper on cyclobutene, but in the simpler case of three-membered rings, it has been possible to demonstrate the effect of differential angle deformation strain by very simple means, avoiding the complete calculation in favor of a check on internal consistency. Some general discussion of the structures of these small-ring compounds is given below.

The problem of evaluating the cross-ring repulsive energy is a difficult one, but no quantitative solution of the problem of bond-lengthenings in four-membered rings can be given without it. The following observations may be of interest in this regard. If Pauling's relationship, $-\Delta R(n) = 0.353 \log n$, is assumed to apply at least roughly to antibonding as well as bonding[4], then the bond numbers n for C•••C in cyclobutane and for the C•••O and C•••S distances in TMO and TMS are very nearly the same, about 0.11, corresponding to very similar increases in cross-ring distances over normal distances of about 0.68 Å, on the average. The following table summarizes

the calculations which can be made on the basis of Pauling's rule for the cross-ring repulsions in three simple ring molecules:

	$C\cdots X$	Reference Distance	$\Delta_{C\cdots X}$	$n_{C\cdots X}$	$E^{a}_{C\cdots X}$	$C\cdots C$	$\Delta_{C\cdots C}$	$n_{C\cdots C}$	$E_{C\cdots C}$	$\widetilde{E_{C\cdots X} + E_{C\cdots C}}$
C_4H_8	2.22	1.54	0.68	0.109	6.4	2.22	0.68	0.109	6.4	12.8
C_3H_6O	2.12	1.43	0.69	0.105	7.4	2.13	0.59	0.146	8.6	16.0
C_3H_6S	2.46	1.81	0.65	0.120	6.5	2.33	0.79	0.076	4.5	11.0

a. $E_{C\cdots X}$ is the cross-ring repulsion energy corresponding to $n_{C\cdots X}$; units are kcal/mole. Single bond energies taken from ref. 23, p. 53.

Unfortunately, three compounds are too few to justify drawing any empirical conclusions. Working with available data, however, we note that (1) the C···X cross-ring lengthening over the single-bond value is very nearly constant (0.68 Å, roughly); (2) the C···C cross-ring distances tend to be larger or smaller than 2.22 Å as C···X is larger or smaller than this amount; (3) the ratios of cross-ring repulsion energies are the inverse of the ratios of the corresponding stretching force constants:

$$\frac{E_{C\cdots O}}{E_{C\cdots C}} = \frac{7.4}{8.6} = 0.86 \text{ and } \frac{k_{C-C}}{k_{C-O}} = 0.86 \text{ (see TMO)}$$

$$\frac{E_{C\cdots C}}{E_{C\cdots S}} = \frac{4.5}{6.5} = 0.69 \text{ and } \frac{k_{C-S}}{k_{C-C}} = 0.70 \text{ (see TMS)}$$

Whether these observations are meaningful or only fortuitous must await the results of further information for compounds such as trimethylenimine and trimethylene selenide.

The results of a microwave investigation of ethylenimine have recently become available[37]: C-C = 1.480 Å, C-N = 1.488 Å are given for the single bond lengths. Assuming, as in previous discussions, that the angle at nitrogen is less strained than the angles at carbon (even if the normal angle for nitrogen is 102°[16]); that the ratio of the stretching force constants $\frac{k_{C-N}}{k_{C-C}}$, is 1.08[22,38]; that the appropriate C-N bond length for use here is 1.480 Å*; and, as before, that the bent-bond shortening is 1 percent of the normal bond length, the usual calculation then is:

$$C\text{-}N = 1.480 - 0.015 + \frac{1/2(1.525 - 1.480)}{1.08} = 1.486$$

Since the normal C-N bond length is uncertain, the calculation is only indicative of the operation of bent-bond shortening and angle deformation effects.

Much remains to be done: more three-membered and four-membered rings should be studied to increase our fund of empirical knowledge of strained rings, and more elaborate calculations than are given here should be made. Sufficient evidence is presented here, though, to indicate the nature and effective magnitude of some of the important factors involved in shortening and lengthening the bonds in small rings.

*Most investigations yield 1.47 Å(found in electron diffraction investigations of methyl-, dimethyl-, and trimethylamine[21]; however, the crystal structure[39] of methylamine has C-N = 1.48 Å, and, lacking more accurate data, we have chosen 1.480 Å as giving a better result. A figure as low as 1.475 Å would still give good agreement.

SOME MISCELLANEOUS ELECTRON DIFFRACTION STUDIES

Decaborane ($B_{10}H_{15}$): A Preliminary Study

Structure determination results are now available for five boron hydrides: B_2H_6, B_4H_{10}, B_5H_9, B_5H_{11}, $B_{10}H_{14}$. All have been studied by electron diffraction[40] and all but the first by X-ray diffraction[41]. We shall be concerned here only with decaborane.

The previous electron diffraction study of decaborane[42] was made with a limited quantity of material of doubtful purity, and nozzle temperatures of 110° - 120° C; the data extended only to about s=17 (q=54), and although many different models were tried, it remained for the X-ray study of crystalline decaborane to discover a satisfactory model for the molecule[43]. A theoretical curve calculated for the crystal structure parameters was claimed to be in good agreement with the available electron diffraction data[44]. The work presented here, however, indicates that the molecule in the gaseous phase may differ somewhat from the molecule reported in the X-ray investigation.

Experimental. A sample of decaborane, probably at least 99 percent pure*, was used for the current work. Electron diffraction photographs were made on Kodak 50 plates in a new apparatus; the accelerating potential was about 40 kv., the camera distance 10 cm., and sample bulb and nozzle temperatures were 70° - 80° C.

*Prepared by Dr. J. R. Ladd and kindly supplied by the General Electric Co. Presumably the 99 percent purity applies only with regard to boron compounds present, since appreciable amounts of volatile hydrocarbon were also present; the sample was sublimed in vacuum to separate out these contaminants.

Diffraction rings were observed to be beyond q=100, almost double the range of the previous study. The rings are sharp and clear, and the pattern is rich in detail. Two visual interpretations are shown in Fig. 10: V_G by the author, V_S more in accord with the observations of Prof. V. Schomaker. The corresponding radial distribution curves (R_G and R_S) are also shown.

In regard to the depth of min. 3 and the shape of max. 2,3, curve V_G matches the interpretation of the previous investigation, but more experienced observers favor the shallow minimum and closer association (possibly even doubling) of the adjacent maxima as shown by V_S. Max. 1 gives the impression of being a small sharp ring. Although V_G and V_S show this feature somewhat differently, both differ markedly from the interpretation of the previous investigators, who showed a distinct separation from the central peak, the maximum having equally deep minima on either side. Since the region out to about q=40 differs in the two curves V_G and V_S, it would be well to establish more confidently the appearance of the photographs to this point.

Discussion. The discussion which follows will be based on the radial distribution curves, R_G and R_S. The numbering system used is that of the crystal structure investigation, and is shown on the topological sketch of Fig. 11 along with a drawing of the molecule. Each boron has at least one hydrogen atom (not shown; each hydrogen has the same number as the boron to which it is attached); in addition there are four bridge hydrogens, H_{VI}, common to B_I and B_{III}, and H_{VII}, common to B_{III} and B_{IV}; a similar arrangement holds for the

primed ring.

The crystal structure parameters for decaborane are given as if the molecule had only a two-fold axis. Since the symmetry of the molecule is asserted to be mm2, however, an adjustment of these parameters was made by the author, and all the interatomic distances for the molecule calculated; the results, separated into boron-boron (skeletal) and boron-hydrogen terms, are shown in Fig. 10. (The height of each bar is proportional to the weight of the term, $\sum_{i,j}{}' \frac{Z_i Z_j}{r_{ij}}$.) Table VII tabulates the results individually.

Following are some of the pertinent results of the crystal structure work: The average normal B-B bond length is 1.76 Å, the average normal B-H bond length 1.25 Å; B_I-B_{IV}' and B_{IV}-B_I' are longer than the normal bonded B-B distances, about 2.0 Å; the dihedral angle between the bases of the two pentagonal pyramids formed by the boron skeleton is about 76°; the bridge hydrogens are located unsymmetrically, H_{VI} being closer to B_I (1.34 Å) than to B_{III} (1.43 Å).

An obvious and immediate result of examining the radial distribution curves is to note an average B-B distance of 1.78_5 Å (or 1.80 Å from R_G; this is probably less reliable than the results obtained from R_S), an increase of 0.025 Å over the average from the crystal structure. The peak at 2.89_5 Å in R_S is composed of non-bonded boron-boron terms, but there is already disagreement between the spectrum of distances calculated from the crystal data and the shape and location of the peak. The bonded B-H terms give rise to peaks on R_S at 1.15 and 1.35 Å, but the exact location of the distances is somewhat obscured by the irregular background (the value 0.97 Å from R_G is obviously wrong). Although

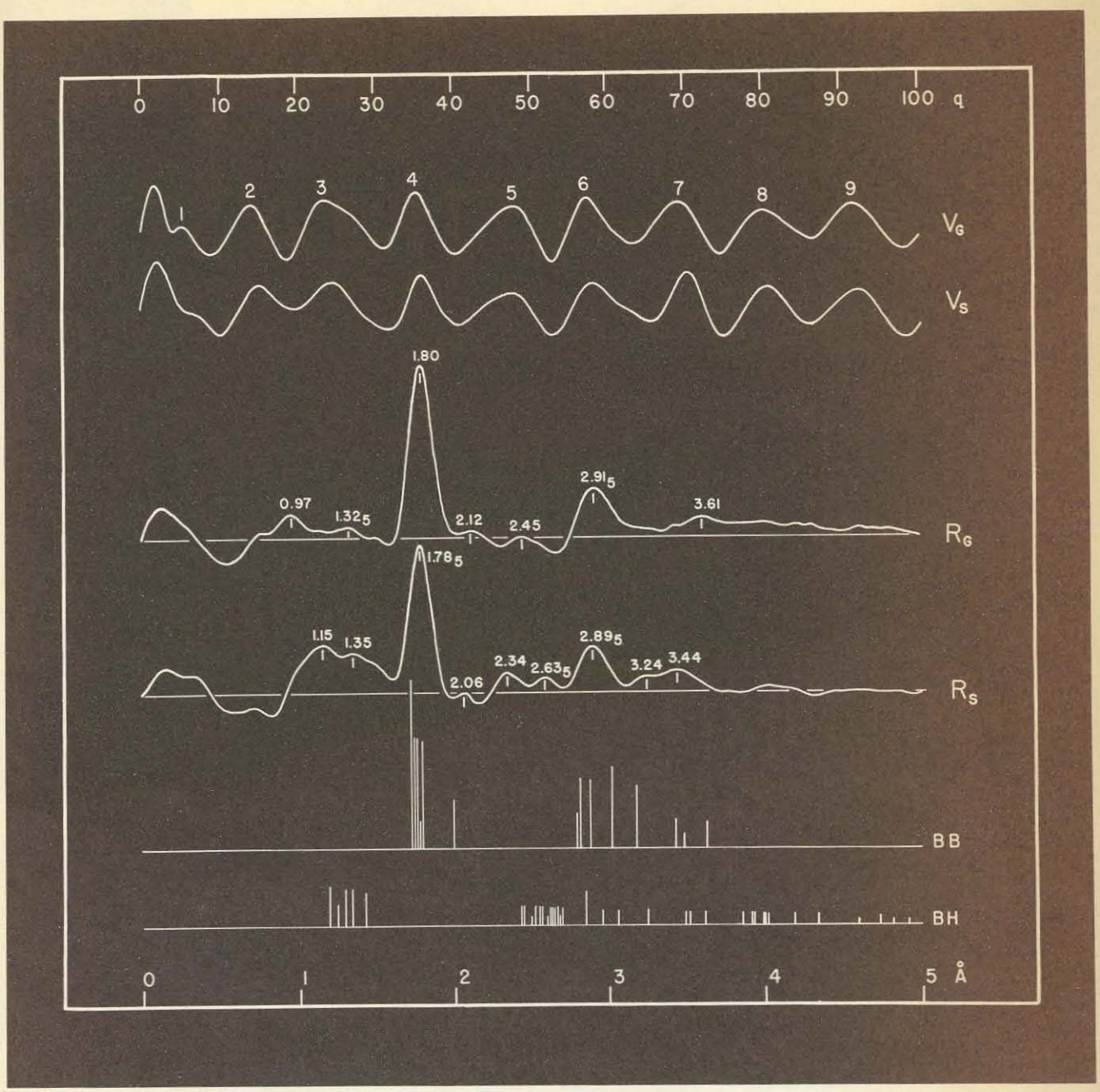
0
10
20
30
40
50
60
70
80
90
100 q
1
2
3
4
5
6
7
8
9
V_G
V_S
1.80
0.97
1.32$_5$
2.12
2.45
2.91$_5$
3.61
R_G
1.78$_5$
1.15
1.35
2.06
2.34
2.63$_5$
2.89$_5$
3.24
3.44
R_S
BB
BH
0
1
2
3
4
5 Å

Fig. 10

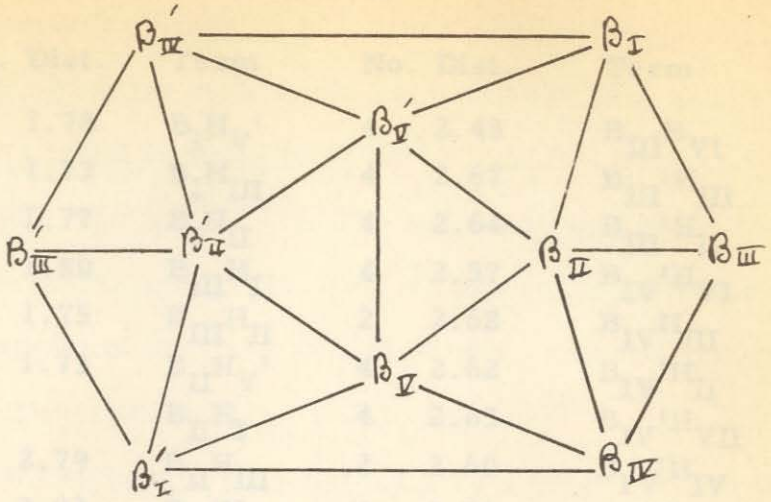

Fig. 11

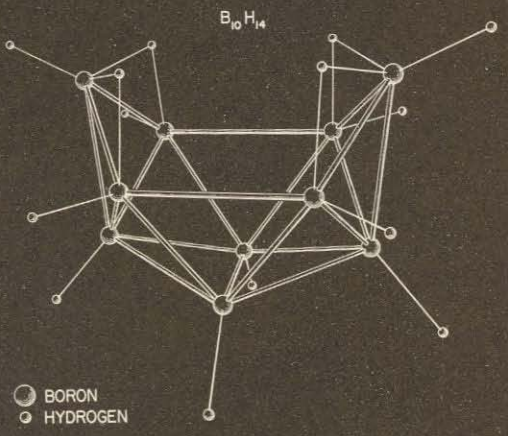

Table VII

Term	No.	Dist.	Term	No.	Dist.	Term	No.	Dist.
B_VB_V'	1	1.78	B_IH_V'	4	2.43	$B_{III}H_{VI}$	4	3.06
B_IB_V'	4	1.73	B_IH_{III}	4	2.67	$B_{III}'H_{III}$	2	4.65
B_IB_{III}	4	1.77	B_IH_{II}	4	2.64	$B_{III}'H_{II}$	2	4.82
$B_{II}B_V'$	4	1.80	$B_{III}H_I$	4	2.57	$B_{IV}'H_{VI}$	4	2.45
$B_{II}B_I$	4	1.75	$B_{III}H_{II}$	2	2.68	$B_{IV}H_{III}$	4	3.62
$B_{II}B_{III}$	2	1.73	$B_{II}H_V'$	4	2.62	$B_{IV}'H_{II}$	4	4.02
			$B_{II}H_I$	4	2.63	$B_{IV}'H_{VII}$	4	3.52
B_IB_{IV}	2	2.79	$B_{II}H_{III}$	2	2.60	$B_{IV}'H_{IV}$	4	4.73
B_IB_V	4	2.82	$B_V'H_I$	4	2.70	$B_{II}'H_I$	4	4.19
$B_{III}B_V$	4	2.88	$B_V'H_{II}$	4	2.52	$B_{II}'H_{VI}$	4	3.25
			$B_V'H_V$	2	2.75	$B_{II}'H_{III}$	2	4.92
B_IB_{IV}'	2	2.00	$B_{IV}'H_I$	4	2.96			
B_IB_{III}'	4	3.18	$B_V'H_{VI}$	4	2.85			
B_IB_I'	2	3.43	$B_{IV}H_{VI}$	4	2.85			
$B_{III}B_{III}'$	1	3.48	$B_{II}H_{VI}$	4	2.55			
$B_{III}B_{II}'$	2	3.68						
$B_{II}B_{IV}'$	4	3.02	$B_V'H_{III}$	4	3.99			
$B_{II}B_{II}'$	1	3.02	$B_V'H_{VII}$	4	3.49			
			$B_V'H_{IV}$	4	4.00			
B_VH_V	2	1.20	B_IH_{IV}	4	3.92			
B_IH_I	4	1.30	B_IH_V	4	3.93			
$B_{III}H_{III}$	2	1.25	$B_{III}H_V'$	4	3.86			
$B_{II}H_{II}$	2	1.20	$B_{III}'H_I$	4	4.34			
B_IH_{VI}	4	1.34						
$B_{III}H_{VI}$	2	1.43						

the distribution of B-H distances from the crystal structure is not incompatible with the peaks on R_S, there is some suggestion that a lower average value for B-H might be desirable; this would be in line with the values found in B_2H_6 (1.19 Å)[45], B_4H_{10} (1.19, 1.11 Å)[46,47], and B_5H_9 (1.20, 1.23 Å)[48,49]. The asymmetrical B-H_b (bridge) bonds found in the crystal (1.30, 1.43 Å) are reasonable ones, both from the viewpoint of the peak at 1.35 Å on R_S and the distances found for a similar situation in B_4H_{10} (1.33, 1.43 Å)[46]*.

The crystal structure parameters give a long distance for B_I-B_{IV}' and B_{IV}-B_I', 2.00 Å. None of the features on either R_G or R_S can be interpreted with certainty as corresponding to this distance; the small peak at 2.06 Å (and at 2.12 on R_S) is probably spurious, a common feature on radial distribution curves. Since the weight of this term is appreciable, it must either be hidden under the B-B peak or moved out to at least the peak at 2.34 Å (or 2.45 Å for R_G). We will return to the former possibility below. The crystal structure distance spectrum also shows a cluster of terms in the range 2.40 - 2.60 Å; these are compatible with either R_G or R_S, although the suggestion is that they should be rather shorter, and possibly, split into two groups to match R_S. Beyond about 3 Å it is difficult to reconcile either R_G or R_S with the non-bonded boron-boron distances found in crystal.

As a starting point for a complete investigation of decaborane by electron diffraction, it might be assumed that all the bonded B-B dis-

*However, the crystal structure gave an asymmetry just opposite that obtained by the electron diffraction result; see ref. 41 and ref. 46. We quote the electron diffraction result.

tances are identical, say 1.785 Å. In view of the symmetrical character of the B-B peak and its relative sharpness, this is not an unreasonable assumption. If we also make the B_I-B_{IV}' distance equal to 1.785 Å, then the boron skeleton becomes a fragment of a regular icosahedron, needing only two atoms to complete the network of vertices. It will be shown that this regularity leads to reasonable agreement with R_S.

For the regular icosahedral skeleton, only two non-bonded boron-boron distances occur, next-nearest neighbors at 2.89 Å and diametrically opposed pairs at 3.40 Å; these distances are easily identified with the peaks on R_S at 2.895 Å and 3.44 Å. Drawing in a reasonable base line, the areas under the peaks at 1.785, 2.895, and 3.44 Å are roughly in the ratio of the calculated weights, 294, 173, and 29 respectively.

Going on to boron-hydrogen distances, we might reasonably take 1.20 Å for B-H (a larger value is tolerable), assuming that the B-H bond makes equal angles with the five adjacent B-B bonds. The spectrum of next-nearest B···H distances clustered about 2.5 Å for the crystal model now becomes a single distance, 2.625 Å, corresponding quite well to the peak at 2.63_5 Å. There are also many distances from a boron to a hydrogen on a next-nearest boron; this distance is 3.96 Å, and is no doubt contributing to the small broad peak at about 4 Å on curve R_S. An easily calculated distance is that from a boron to hydrogen on a boron diametrically opposite; four of these distances occur in the idealized molecule at 4.60 Å, coincident (though possible fortuitously) with a very slight peak in the radial distribution curve.

The problem of the unsymmetrically placed bridge hydrogens presents complications. If, however, we assume 1.33 and 1.43 Å for the B-H_b bonds, and if we assume the hydrogen to lie in the plane of the triangle of associated boron atoms (as for tetraborane), a distance of 2.60 Å separates the hydrogen from opposed boron of the triangle. The B_V-H_{VII} separation is 2.87 Å. Both of these distances can be associated with nearby peaks (2.635 and 2.89_5 Å, respectively), but this still leaves the 2.34 Å peak unexplained. If the triangle B_{III}-B_{IV}-H_{VII} is folded about B_{III}-B_{IV} until the B_{II}-H_{VII} distance becomes 2.34 Å, the dihedral angle, $\angle B_{II}B_{III}B_{IV} - B_{III}B_{IV}H_{VII}$, becomes about 125°, comparable to the dihedral angle of the boron skeleton in tetraborane, 124°32'; crowding of hydrogen atoms makes this arrangement unlikely.

In conclusion, we can say that the model derived from the crystal structure study is in definite disagreement with our observations of the electron diffraction pattern. The overall size of the molecule in the gas phase (expressed as average bonded B-B), is larger than in the solid, with a shorter B-H indicated. A trial structure based on a regular model with equal B-B bonds of 1.78_5 Å and B-H bonds of 1.20 Å (or perhaps 1.22 Å) is suggested as the starting point for a more complete investigation by the correlation procedure; such a model is in somewhat better agreement with the radial distribution curve than the crystal structure model is, but presumably could be made to give even better agreement by making fine adjustments of the B-B distances. A complete correlation procedure, although of necessity laborious, should prove feasible and worthwhile.

[CONTRIBUTION NO. 1967 FROM THE GATES AND CRELLIN LABORATORIES OF CHEMISTRY, CALIFORNIA INSTITUTE OF TECHNOLOGY]

An Electron Diffraction Investigation of Dimethyl Selenide

BY ELIHU GOLDISH, KENNETH HEDBERG, RICHARD E. MARSH AND VERNER SCHOMAKER

RECEIVED JANUARY 17, 1955

The results of an electron diffraction investigation of $(CH_3)_2Se$ are C–H/Se–C, 1.09/1.97 (assumed); Se–C, 1.977 ± 0.012 Å.; Se···H, 2.571 ± 0.034 Å.; C···C, 2.98 ± 0.23 Å.; ∠C–Se–C, 98 ± 10°; and ∠Se–C–H, 110.5 ± 3.5°. The selenium–carbon distance of 1.98 Å. leads to a single-bond radius for selenium of 1.22 Å., which is considerably larger than the value 1.17 Å. chosen by Pauling.

A selenium–carbon distance of 2.01 ± 0.03 Å. has been reported from an X-ray diffraction investigation of 1,4-diselenane.[1] Smaller values have been reported for other molecules, but none of these molecules is comparable to diselenane. In di-*p*-tolylselenium dichloride[2] (Se–C = 1.93 ± 0.03 Å.), di-*p*-tolylselenium dibromide[2] (1.95 ± 0.03), diphenylselenium dibromide[3] (1.91 ± 0.05), and diphenyl diselenide[4] (1.93 ± 0.05) aromatic groups are conjugated with the empty d orbitals and unshared p electrons of selenium and the coördination of selenium, except in diphenyl diselenide, is fourfold rather than twofold. In perfluorodimethyl selenide[5] (1.958 ± 0.022) and perfluorodimethyl diselenide[5] (1.934 ± 0.018) the situation is exceptional because of the perfluoro substitution.[6] We undertook an electron diffraction investigation of dimethyl selenide in order to provide an additional, more precise value for the Se–C distance in a simple compound of bi-covalent selenium. Our result, 1.977 ± 0.012 Å., is in fair agreement with the diselenane value.

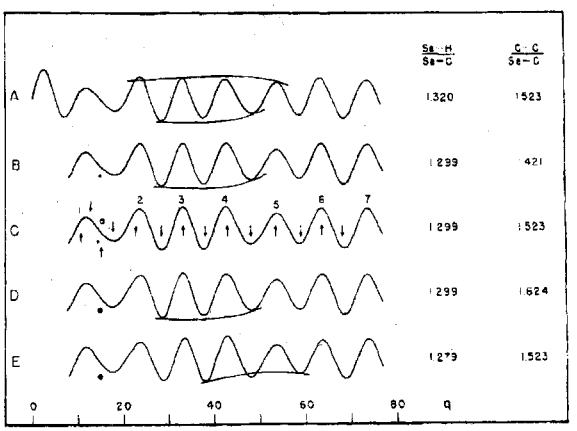

Fig. 1.—Theoretical intensity curves for dimethyl selenide. All curves calculated with Se–C = 1.97, C–H = 1.09, a_{C-H} = 0.0017, $a_{Se\cdots H}$ = $a_{C\cdots C}$ = 0.0041. Best model: Se···H/Se–C = 1.300 and C···C/Se–C = 1.51 (close to curve C). Significant points of comparison with observation are indicated by critical marks. (See W. F. Sheehan, Jr., and V. Schomaker, THIS JOURNAL, **74**, 4468 (1952).)

Experimental

The sample (b.p. 57–59°) was supplied by Mr. Jordan Bloomfield of the Massachusetts Institute of Technology. Electron diffraction photographs were taken on Kodak 50 plates with 40 kv. electrons at 10 cm. distance in a new apparatus recently constructed in these laboratories. The temperature of the sample bulb was about −50°. The photographs were interpreted in the usual way.[7]

Theoretical intensity curves (Fig. 1) were calculated for Se–C = 1.97, C–H = 1.09, 2.52 ≤ Se···H ≤ 2.62, 2.80 ≤ C···C ≤ 3.30, with Z_H^{eff} = 1.25, a_{C-H} = 0.0017 and, for most of the curves, $a_{Se\cdots H}$ = $a_{C\cdots C}$ = 0.0041.[8] Reasonable variations of the *a* values and of the ratio C–H/Se–C were tested and found to have only very small effects on our final results.

The weak, rather sharp feature 1*a* is readily visible on the photographs even though it is shown only very weakly by the best curve, C, and but little more strongly by a corresponding curve with (Z–F)'s rather than *Z*'s as coefficients. This, however, is characteristic of the appearance of such features. All other aspects of C, including even the minor differences in the widths, asymmetries, and amplitudes of the maxima and minima, are in exceptionally good agreement with our observations.

TABLE I

COMPARISONS OF OBSERVED AND CALCULATED POSITIONS OF MAXIMA AND MINIMA (CURVE C)

	Minima		Maxima	
No.	$q_{obsd.}$[a]	$q/q_{obsd.}$	$q_{obsd.}$[a]	$q/q_{obsd.}$
1	7.10	(0.986)	10.64	(1.006)
1a	12.95	(1.081)	15.13	(0.991)
2	17.79	(1.016)	22.79	(1.038)
3	28.42	1.009	33.17	1.004
4	37.99	0.998	42.88	0.996
5	48.01	1.006	53.55	1.009
6	58.92	0.999	63.62	1.002
7	68.10	1.010		
Av. 9 features				1.0037
Av. dev.				0.0044

Se–C = 1.97 × 1.0037 = 1.977 Å.

[a] Measurements of K. H. Check measurements were made by the other authors.

(1) R. E. Marsh and J. D. McCullough, THIS JOURNAL, **73**, 1106 (1951).

(2) J. D. McCullough and R. E. Marsh, *Acta Cryst.*, **3**, 41 (1950).

(3) J. D. McCullough and G. Hamburger, THIS JOURNAL, **63**, 803 (1941).

(4) R. E. Marsh, *Acta Cryst.*, **5**, 458 (1952).

(5) H. J. M. Bowen, *Trans. Faraday Soc.*, **50**, 452 (1954).

(6) An anomalously short C–O distance is found (ref. 5) for perfluorodimethyl ether, an analog of perfluorodimethyl selenide, and progressive substitution of H by F shortens the C–F distance in the series CH_3F ··· CF_4 (L. O. Brockway, *Acta Cryst.*, **7**, 682 (1954)).

(7) K. Hedberg and A. J. Stosick, THIS JOURNAL, **74**, 954 (1952).

(8) We write $a_{ij} = {}^1/_2(\overline{\delta r_{ij}^2} - \overline{\delta r_{Se-C}^2})$. Approximation of the methyl group vibrations as pure bendings and pure stretchings leads to the somewhat larger value 0.0055 for $a_{Se\cdots H}$. Normal coördinate treatment of the molecule, regarded as triatomic with skeletal frequencies assigned by P. Donzelot, *Compt. rend.*, **203**, 1069 (1936), shows that for reasonable values of the potential constants $a_{C\cdots C}$ varies over the approximate range 0.0006–0.0060; the choice of 0.0041 for $a_{C\cdots C}$ is purely arbitrary.

The phase shift expected for the Se–C interaction (J. A. Ibers and J. Hoerni, *Acta Cryst.*, **7**, 405 (1954)) in effect increases $\overline{\delta r_{Se-C}^2}$ by about 0.0016 Å.² and should have been taken into account in estimating the other a_{ij}. The only appreciable change would be the reduction of a_{C-H} to about 0.0009, and its effect on the theoretical curves would be very small.

62

Our final parameters and estimated limits of error, as deduced from qualitative comparisons of calculated curves (Fig. 1) and from ratios of calculated to observed positions of maxima and minima (Table I is an example), are the following: C–H/Se–C = 1.09/1.97 (assumed), Se···H/Se–C = 1.300 ± 0.017, ($\angle$Se–C–H = 110.5 ± 3.5°), C···C/Se–C = 1.51 ± 0.11, ($\angle$C–Se–C = 98 ± 10°), Se–C = 1.977 ± 0.012 Å., Se···H = 2.571 ± 0.034 Å., and C···C = 2.98 ± 0.23 Å.

Discussion

It seems appropriate to regard the selenium–carbon bonds in unconjugated compounds of bivalent selenium as normal and, therefore, to take 1.98 Å. as the normal Se–C single bond length. With a small (and perhaps unjustifiable) correction for electronegativity difference, the selenium radius then becomes 1.22 Å. (1.98 = 0.77 + 1.22 − (0.09 × 0.1)). This is appreciably greater than Pauling's value 1.17 Å.,[9] which is supported by the bond lengths of 2.32 Å. in hexagonal selenium[10] and 2.34 Å. in both α- and β-monoclinic selenium.[11,12] It has been pointed out,[13] however, that nominal single bonds in the heavier elements may actually have appreciable double-bond character; our value for the selenium radius is in agreement with this possibility, which, accordingly, may deserve further consideration.

Acknowledgment.—The support of this work by the Office of Naval Research under Contract N6 onr 24423 is gratefully acknowledged.

(9) L. Pauling, "The Nature of the Chemical Bond," 2nd edition, Cornell University Press, Ithaca, N. Y., 1940, p. 165.

(10) A. J. Bradley, *Phil. Mag.*, **48**, 477 (1924).

(11) R. Burbank, *Acta Cryst.*, **4**, 140 (1951).

(12) R. E. Marsh, L. Pauling and J. D. McCullough, *ibid.*, **6**, 71 (1953).

(13) V. Schomaker and D. P. Stevenson, THIS JOURNAL, **63**, 37 (1941).

PASADENA, CAL.

An Additional Note on Dimethyl Selenide

Since the C-Se-C angle in dimethyl selenide has such large limits of error ($\pm$ 10°), it is somewhat reassuring to note that the angle chosen is compatible with the central angles for the methyl derivatives of neighboring elements. Fig. 12a shows a plot of periodic row (I, II, III) for the fifth and sixth periods versus central bond angle of the hydrides; the parallelism is quite marked. Fig. 12b shows a similar plot for the methyl derivatives of the same elements which supports the choice of 98° made for $\angle$ C-Se-C.

Fig. 12a, b

Central bond angles in certain hydrides and methyl derivatives. The values used and references are:

H_2O : 105°3'	G. Herzberg, "Infrared and Raman Spectra of Polyatomic Molecules", D. Van Nostrand Company, Inc., New York, N.Y., 1945, p. 489
H_2S : 92°16'	
H_2Se: 90°	D. P. Stevenson, J. Chem. Phys. 8, 285 (1940)
	D. M. Cameron, W. C. Sears, and H. H. Nielsen, J. Chem. Phys. 7, 994 (1939)
NH_3 : 107°	M. T. Weiss and M. W. P. Strandberg, Phys. Rev. 83, 567 (1953)
PH_3 : 93.5°	C. C. Loomis and M. W. P. Strandberg, Phys. Rev. 81, 798 (1951)
AsH_3 : 92.0°	Idem.
SbH_3 : 92.5°	Idem.
$(CH_3)_2O$: 111°	V. Schomaker, priv. comm.
$(CH_3)_2S$: 104°	J. H. Gibbs, J. Chem. Phys. 22, 1460 (1954)
	L. O. Brockway and H. O. Jenkins, J. Am. Chem. Soc. 58, 2036 (1936)
	See also H. W. Thompson, Trans. Farad Soc. 37, 38 (1941)
$(CH_3)_2Se$: 98°	This work
$(CH_3)_3N$: 109°	See $(CH_3)_2O$.
$(CH_3)_3P$: 100°	H. D. Springall and L. O. Brockway, J. Am. Chem. Soc. 60, 996 (1938)
$(CH_3)_3As$: 96°	Idem.

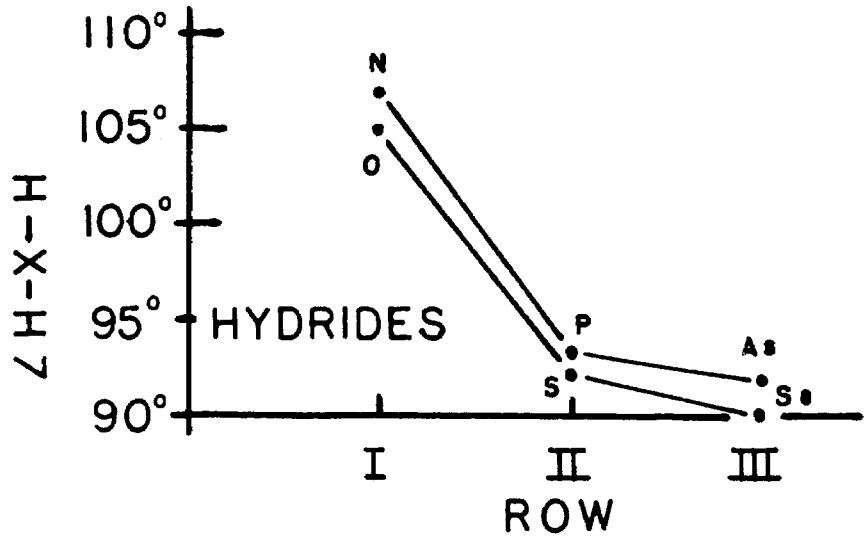
110°
105°
100°
95°
90°
∠H-X-H
HYDRIDES
N
O
P
S
As
Sb
I
II
III
ROW

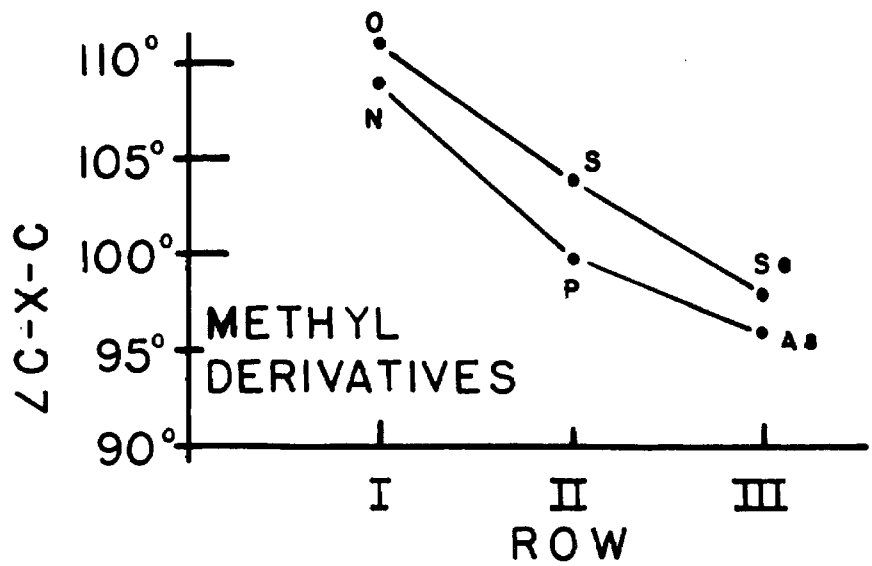
110°
105°
100°
95°
90°
∠C-X-C
METHYL
DERIVATIVES
O
N
S
P
Sb
As
I
II
III
ROW

References, Part I

1. P. W. Allen and L. E. Sutton, Acta Cryst. 3, 46 (1950).

2. W. Gordy, W. V. Smith, and R. F. Trambarulo, "Microwave Spectroscopy", John Wiley and Sons, Inc., New York, N.Y., 1953, p. 371.

3. O. Bastiansen and O. Hassel, Tidsskr. Kemi Bergv. Met. 6, 71 (1946). W. A. Baker and R. C. Lord, J. Chem. Phys. 23, 1636 (1955). See also ref. 4, footnote 19.

4. J. D. Dunitz and V. Schomaker, J. Chem. Phys. 20, 1703 (1952).

5. V. Schomaker, Acta Cryst. 4, 158 (1951).

6. J. D. Dunitz, H. G. Feldman, and V. Schomaker, J. Chem. Phys. 20, 1708 (1952).

7. R. S. Rasmussen and R. R. Brattain, J. Chem. Phys. 15, 120 (1947).

8. E. B. Wilson, Jr. and A. J. Wells, J. Chem. Phys. 9, 319 (1941).

9. D. M. Gates, J. Chem. Phys. 17, 393 (1949).

10. J. P. McHugh, private communication.

11. K. Hedberg and V. Schomaker, J. Am. Chem. Soc. 73, 1482 (1951). G. E. Hansen and D. M. Dennison, J. Chem. Phys. 20, 313 (1952).

12. J. Donohue, G. L. Humphrey, and V. Schomaker, J. Am. Chem. Soc. 67, 332 (1945).

13. W. Shand, Jr., Ph D. Thesis, California Institute of Technology, (1946).

14. J. M. O'Gorman, W. Shand, Jr. and V. Schomaker, J. Am. Chem. Soc. 72, 4222 (1950).

15. J. Fernandez, R. J. Meyers, and W. D. Gwinn, J. Chem. Phys. 23, 758 (1955).

16. V. Schomaker and C.-S. Lu, J. Am. Chem. Soc. 72, 1182 (1950). See also: G. E. Moore and R. M. Badger, J. Am. Chem. Soc. 74, 6076 (1952); J. A. Ibers and V. Schomaker, J. Phys. Chem. 57, 699 (1953)

17. T. P. Wilson, J. Chem. Phys. 11, 369 (1943).

18. G. W. Rathjens, Jr., N. K. Freeman, W. D. Gwinn, and K. S. Pitzer, J. Am. Chem. Soc. 75, 5634 (1953).

19. D. W. Scott, H. L. Finke, W. N. Hubbard, J. P. McCullough, C. Katz, M. E. Gross, J. F. Messerly, R. E. Pennington, and G. Waddington, J. Am. Chem. Soc. 75, 2795 (1953).

20. P. Venkateswarlu and W. Gordy, J. Chem. Phys. 23, 1200 (1955).

21. V. Schomaker, private communication.

22. G. Herzberg, "Infrared and Raman Spectra of Polyatomic Molecules", D. Van Nostrand Company, Inc., New York, N.Y. (1945).

23. L. Pauling, "The Nature of the Chemical Bond", 2nd edition, Cornell University Press, Ithaca, New York, (1940).

24. J. Bregman and S. H. Bauer, J. Am. Chem. Soc. 77, 1955 (1955).

25. G. L. Cunningham, Jr., A. W. Boyd, R. J. Meyers, W. D. Gwinn, and W. I. LeVan, J. Chem. Phys. 19, 676 (1951).

26. D. E. Applequist, Ph. D. Thesis, California Institute of Technology, (1955).

27. W. F. Sheehan, Jr. and V. Schomaker, J. Am. Chem. Soc. 74, 4468 (1952).

28. W. S. Gallaway and E. F. Barker, J. Chem. Phys. 10, 88 (1942).

29. W. Shand, Jr., V. Schomaker, and J. R. Fischer, J. Am. Chem. Soc. 66, 636 (1944).

30. D. P. Stevenson, H. D. Burnham, and V. Schomaker, J. Am. Chem. Soc. 61, 2922 (1939).

31. G. B. Guthrie, Jr., private communication.

32. T. M. Shaw and J. J. Windle, J. Chem. Phys. 19, 1063 (1951).

33. H. W. Thompson and N. P. Skerrett, Trans. Farad. Soc. 36, 812 (1940).

34. C. A. Coulson and W. E. Moffitt, J. Chem. Phys. 15, 151 (1941); Phil. Mag. 40, 7th series, 1 (1949).

35. J. C. Conly, Ph. D. Thesis, California Institute of Technology, (1950).

36. C. A. Coulson, "Contribution a l'Etude de la Structure Moleculaire", Desoer, Liege, 1948, p. 15.

37. T. E. Turner, V. C. Fiora, and W. M. Kendrick, J. Chem. Phys. 23, 1966 (1955).

38. T. L. Cotrell, "The Strengths of Chemical Bonds", Academic Press, Inc., New York, N.Y., (1954).

39. M. Atoji and W. N. Lipscomb, Acta Cryst. 6, 770 (1953).

40. M. E. Jones, Ph. D. Thesis, California Institute of Technology, (1953).

41. W. N. Lipscomb, J. Chem. Phys. 22, 985 (1954).

42. G. Silbiger and S. H. Bauer, J. Am. Chem. Soc. 70, 115 (1948).

43. J. S. Kasper, C. M. Lucht, and D. Harker, Acta Cryst. 3, 436 (1950).

44. C. M. Lucht, J. Am. Chem. Soc., 73, 2373 (1951).

45. K. Hedberg and V. Schomaker, J. Am. Chem. Soc. 73, 1482 (1951).

46. M. E. Jones, K. Hedberg, and V. Schomaker, J. Am. Chem. Soc. 75, 4116 (1953).

47. C. E. Nordman and W. N. Lipscomb, J. Am. Chem. Soc., 75, 4116 (1953); J. Chem. Phys. 21, 1856 (1953).

48. K. Hedberg, M. E. Jones, and V. Schomaker, Proc. Natl. Acad. Sci. U. S. 38, 679 (1952).

49. W. T. Dulmage and W. N. Lipscomb, Acta Cryst. 5, 260 (1952).

PART II

The $BaMg_9$ Structure.

THE $BaMg_9$ STRUCTURE

Introduction

In 1947 Klemm and Dinkelacker [1] (referred to hereafter as K & D) published the complete phase diagram of the barium-magnesium system, completing and correcting a partial investigation of the same system ten years earlier by Grube and Dietrich[2]. The phase diagram of K & D shows two well-defined compounds, assigned the formulas $BaMg_2$ and $BaMg_9$, and an incongruently melting phase of uncertain composition, designated "$BaMg_4$". The structure of $BaMg_2$ has been investigated previously[3] and found to be of the well-characterized $MgZn_2$ type[4]. An investigation of the $BaMg_9$ phase seemed worthwhile since few structures for compounds of formula AB_9 have been reported previously. Our results show a disordered type of structure with interesting groupings of atoms; the true formula for the substance has at least ten magnesiums per barium, rather than nine.

In the following account we attempt to present a logical exposition of the course of the investigation, although the actual order of events was not always as described.

Experimental

The starting materials were cleaned before use but not further purified. Magnesium metal rod (Eimer and Amend; purity unknown)

was turned on a lathe to remove a scaly surface coating; a portion of the rod was then cut off and weighed. The barium metal (also Eimer and Amend) is marked as 99-plus percent pure. It is stored under a protective oil which was removed with turpentine or other solvent before weighing.

Although K & D had prepared melts in iron cruicibles for their study of the barium-magnesium system, our first preparations were made in a long quartz tube sealed at one end. As in all the succeeding preparations the barium and magnesium metals were weighed out in the atomic ratio of one to nine. The metals were placed in the tube and air was flushed out with helium gas which was retained as an inert atmosphere by a rubber stopper. The bottom (sealed) part of the tube with the metals was heated by a gas-oxygen flame to a temperature estimated to be above the melting point for $BaMg_9$ of 707° C given by K & D. The stopper was loosened occasionally during the heating to allow for expansion of the helium.

There are several disadvantages associated with the quartz-tube method: 1) the tube crazed and cracked about the metal slug on cooling, mixing fine quartz dust into the sample; 2) the tube could not be inverted during the heating to improve mixing; 3) the temperature could not be pushed much higher. Subsequent preparations were therefore made in iron containers, as K & D's preparations had been.

One end of a length of seamless "Shelby" iron tubing was hammered and welded shut. The metals were put in and, after displacing the air by helium, the other end was similarly sealed off. The entire system then was heated to white heat by a glass-blowing blast lamp; during the

heating the tube was shaken and turned end over end to ensure adequate mixing. The torch flame was gradually reduced over a period of several minutes and, after cooling to room temperature, the tube was cut open.

A somewhat more elaborate device was also tried. An iron tube, sealed at one end, was threaded at the other end to receive a plug with two holes. While the metals were being heated in the tube helium was passed in continuously through one hole, escaping through the other; the object was to ensure that no air remained or entered during the heating. Since it was not possible to shake the device too sharply or turn it upside down during the heating, and since magnesium vapor escaped through the exit port, this apparatus was abandoned after one preparation.

Fractured surfaces of the slugs of metal have a silvery metallic appearance when fresh, but become dull after exposure to the atmosphere, presumably from oxidation. Crushed samples effervesce in water, the reaction subsiding in a few minutes, and if the sample is not removed from the water, it continues to slowly evolve gas and is completely reacted after several days.*

For most of the succeeding work the method of treatment adopted was to crush a small amount of alloy in an agate mortar and place it in water for fifteen minutes to an hour, depending on how rapidly the reaction proceeded. During this reaction period the water was changed

*As K & D note, "Gepulverte Legierungen, die mehr als 10At.-Proz. Barium enthielten, verpufften beim Einbringen in wasser regelmässig unter Feuererscheinung." One of our samples, very finely powdered, did flash up as it was being poured into water.

several times (to prevent an accumulation of alkaline decomposition products) and finally decanted off as completely as possible. The remaining slurry was spread on filter paper and permitted to dry in the open air. One virtue of this procedure is that it largely disposes of metal "dust", particles too small to be useful in X-ray work but sufficiently numerous to impede the hunt for single crystals under the microscope. In addition, the reaction with water presumably removes any excess barium, and perhaps any $BaMg_2$ (or "$BaMg_4$") which might also have been formed. (See footnote, preceding page.)

When thus prepared the sample has a shiny metallic appearance. The particles are stable in air for prehaps a week or less, and it was necessary to prolong their useful life by mounting them in capillaries.

Under the microscope the powdered samples show shiny metallic fragments ranging in size from about 1/2 mm to 0.1 mm or less. The first X-ray data were taken with crystals judged to be single, using rather crude criteria (metallic appearance, size, regularity, etc.); but further search discovered crystals shaped like hexagonal prisms, and these were used in all subsequent work.

The hexagonal prisms were, usually, about 0.05 - 0.1 mm in diameter, and perhaps 0.1 - 0.3 mm in length. They occurred both singly and in clusters. To show that these crystals were not pure magnesium, several tests were performed under a microscope in which a few of the hexagonal crystals were dissolved in a drop of dilute hydrochloric acid; a drop of dilute sulfuric acid was added and the formation of a white precipitate which followed was taken as

evidence for the presence of barium in the crystals. In a later section X-ray data are presented which identify the hexagonal crystals with some of the individual crystals first used (see preceding paragraph) and then with the gross preparation.

A rough analysis was performed on one early preparation. After reaction with water as described before, the sample was dried, weighed, and dissolved in slightly acid solution. The barium was precipitated as the sulfate, caught on a Gooch filter, dried, and weighed by difference*. The formula calculated from this experiment is $BaMg_{10.4}$.

Despite the probable inaccuracies of this analysis, the formula derived is in agreement with the following observations. If we start with a crude sample of gross composition $BaMg_9$, then the destruction by water of barium or barium-rich phases would leave behind substances of higher magnesium content. Further, the phase diagram of K & D is based on experimental points so widely spaced in the area of interest as to enable a solidus-liquidus curve to be drawn with a maximum falling anywhere from, say, 7 to 13 atomic percent barium (corresponding to composition in the range $BaMg_7$ - $BaMg_{13}$).

Several density determinations were made. The first was with a gross sample which had been crushed and placed in water, as described previously. (Since almost all the sample sinks in water, the density is greater than 1.) A flotation method was used employing two

*Several possible sources of error in this analysis are recognized; co-precipitation, incomplete precipitation, incomplete precipitation recovery, etc. Since no great accuracy was desired, however, no more elaborate scheme was tried. Two runs gave for the atomic ratio of barium to magnesium $1:10.3_1$ and $1:10.4_1$.

organic liquids, propylene dibromide (ρ = 1.9333 gm cm^{-3}) and methylene bromide (ρ = 2.4953 gm cm^{-3}). Randomly chosen crystals from the sample sank in the former and floated in the latter liquid, placing the density between about 2 and 2.5. More precise determinations were carried out on two samples, one containing perhaps several hundreds of crystals, the other a much smaller number chosen for their shiny metallic appearance; a mixture of the two organic liquids was adjusted until the sample particles tended to neither rise nor fall. The density from these two determinations was 2.29-2.30 gm cm^{-3}.

Further determinations were carried out with single hexagonal prisms. To observe the results of the flotation experiment on these diminutive crystals a reflex device for microscopic observation was constructed. This consisted of a mirror supported at 45° from vertical by a block of wood and placed under the microscope objective so as to provide a magnified view of the tip of a vertical 2-ml centrifuge tube. The crystal was placed in the tip of the tube and liquid added; various mixtures were tried until the crystal just floated. Using two individual crystals, a density of 2.23 gm cm^{-3} was obtained, and this is the value used in the next section to determine the unit cell contents.

X-Ray Data

Powder photographs were taken of samples from different melts. The samples were prepared in various ways (e.g., untreated; treated with water; separated by flotation) but all photographs were essentially

identical. In Table VIII are listed, by scattering angle θ (for copper radiation) powder lines for a typical photograph, and, for comparison, data for pure barium and magnesium metals and their oxides, as well as $BaMg_2$. It is seen that most of the lines can be identified with none of these substances.

Laue photographs of the hexagonal prisms were made along and perpendicular to the prism axis*; the latter photographs show horizontal and vertical mirror planes, while the former give a pattern of six-fold symmetry. The Laue symmetry is then D_{6h}, and we assume a hexagonal unit cell, with $\underline{c}$ along the prism axis.

To work with these prismatic crystals for more than a week it was necessary to mount them in sealed capillaries. Several different mounting techniques were tried, of which the following was found most convenient. A flake of shellac was warmed until sticky and a long fine thread drawn out. A length of this thread was placed in a 0.2 mm Lindemann glass capillary tube, one end touching the bottom of the tube, the other end projecting from the mouth. An electrically heated wire was moved along the outside of the tube until a several millimeter portion of the shellac near the tube tip had melted and adhered to the capillary wall; the remaining shellac thread was withdrawn. The crystal was placed in the tube, which was tipped and turned until the

*Some of the latter photographs, showing vertical and horizontal mirror planes, are identical with some Laue photographs made earlier with crystals chosen for their shiny appearance, plane surfaces, etc., and thought to be single crystals. Because of the irregular shape there was no way of identifying any symmetry elements to aid in mounting these crystals, but one, at least, seems to have been mounted with $\underline{c}$ perpendicular to the beam. It therefore seems reasonable to assume the identity of the hexagonal prism crystals with all the other crystals of the sample.

Powder Photo.[a]		Rotation Photograph l = 0	l = 1	l = 2	l = 3	l = 4	Weiss. l = 0	CIT l = 0	Mg[b]	MgO[c]	Ba[d]	BaO[e]	$BaMg_2$[f]
8.38°	s	8.33 s					8.35	8.38					
10.05	w												
10.60	w		10.52 ms				--	10.56					11.3
11.95	vs			11.90 s							12.52 s		
12.41	w												
13.08	w												13.3
13.58	m		13.51 s		13.62 s							13.94 vs	
14.05	w												
14.56	s	14.53 vs					14.58	14.62					14.8
15.01	m								16.12 ms			16.28 s	15.9
16.15	m				16.06 s				16.95				
16.92	vs	16.86 vs		16.92 vs			16.89	16.89		17.19 s			
17.25	m									18.30 vs	18.47 w	17.89 m	
18.30	m				18.20 s								
19.00	vw												
19.30	vw												20.2
19.65	vw												
20.87	vw												
21.08	vw									21.45 vs			
21.52	w										22.09 s		
22.02	w		21.87 ms		21.96 mw								
22.52	w	22.56 ms					22.61	22.67				23.29 m	
22.80	m					22.78 s			23.90 m				
24.25	ms			24.28 s									
24.40	ms					24.43 s							
25.35	w		25.18 ms		25.26 w								
25.78	w	25.81 ms					25.84	25.92			25.78 m		
26.35	vw												
26.78	w		26.72 w										
27.32	m			27.34 ms								27.68 m	
27.78	mw												
28.28	w		28.20 m		28.26 m								
28.92	mw					28.98 vw			28.68 m		29.13 m	29.01 w	
29.70	w				29.68 m								
30.13	m	30.17 ms					30.23	30.32					
30.62	ms									31.15 s			
31.05	w				31.08 mw								
31.65		31.54 m				31.75 w	31.59	31.68	31.53 m				

Notes (Table VIII)

(a) This powder photograph is of an untreated sample. A small fragment of the solidified melt was crushed, powdered, and placed in a Lindemann glass capillary. Thus some quantity of magnesium and barium and their oxides might be present. The angles quoted for this and the other photographs are uncorrected for film shrinkage except for the precision powder camera (CIT) single crystal photograph.

(b) From H. E. Swanson and E. Tatge, "Standard X-ray Diffraction Powder Patterns", National Bureau of Standard Circular 539, Government Printing Office, Washington D. C., 1953, p. 10.

(c) Idem., p. 38.

(d) ASTM File, Card 1363

(e) ASTM File, Card 1801

(f) E. Hellner and F. Laves, Z. Krist. 105, 134 (1943).

crystal rested on the shellac ribbon. By tapping the capillary lightly the crystal could be approximately aligned (with prism axis either parallel or perpendicular to the tube axis). The hot wire was again brought up, and the shellac softened or melted until the crystal was firmly embedded.

If the crystal orientation was not satisfactory the shellac could be completely liquefied and, by judiciously applying the hot wire, convection currents could be induced which would rotate the crystal. When the desired position was attained the hot wire was suddenly withdrawn, freezing the crystal in place.

There are a number of distinct advantages in this method of mounting: (1) the entire process can be observed by microscope; (2) only Lindemann glass and a thin ribbon of shellac are placed in the X-ray beam along with the crystal; (3) if necessary the crystal can be completely immersed in the shellac, giving additional protection from air oxidation; (4) the orientation of the crystal can be changed at any time, without breaking the capillary or even removing it from the mounting pin, by simply melting the shellac from outside with a heated wire and operating with the induced convection currents.

Rotation photographs were taken about $\underline{c}$, the prism axis, using Ni - filtered CuKα radiation. From the layer-line spacing, c_o was calculated to be about 10.5 Å. A striking feature of these photographs is that reflections on the zero, second, and fourth layer-lines are, on the whole, considerably stronger than those on the first, third, and fifth lines. A rotation photograph taken about the unit cell basal diagonal $(11\bar{2}.0)$ gives a repeat distance of 18.3 Å, corresponding to

a_o = 10.6 Å. This photograph shows the zero, third, sixth, and ninth layer-lines appreciably stronger than the others. The implications of these variations of strength are discussed in the next section.

Next, Weissenberg photographs about $\underline{c}$ were made up to and including the fifth layer line, using the equi-inclination technique. Insofar as occurrence of reflections is concerned, the zero, second, and fourth layer-line photographs are identical, as are the first, third, and fifth layer-line photographs. In addition, a reflection occurring on an even layer-line photograph never appears on an odd layer-line photograph, and vice versa; the two groups of occurrences are mutually exclusive, and an even and an odd layer-line photograph can be superimposed to show the complete Weissenberg reciprocal lattice net. (These facts can also be readily observed, with the aid of a Bernal chart, on the rotation photographs.)

After the reflections had been indexed the following two-part rule, embodying the observations of the previous paragraph, was apparent:

If h-k = 3n, then l = 2m;

if h-k = 3n $\pm$ 1, then l = 2m + 1

Or, equivalently:

If h-k = 3n, then l = 2m;

if l = 2m, then h-k = 3n.

The significance of these results is discussed in a later section.

Photographs were also made with the Buerger precession camera, using MoKα radiation; measurement of these photographs gives $\frac{c_o}{a_o} = 0.995_1$. The near equality of a_o and c_o is shown quite strikingly on one photograph which has an almost square array of spots, while

another photograph, with the crystal rotated 30° about $\underline{c}$ from the other, shows graphically the operation of the two-part rule of the previous paragraph.

The cell constant a_o was calculated from a zero layer-line single crystal photograph taken with CuKα radiation in the CIT Powder camera, a high-precision, Straumanis-type apparatus. Using only the ten back-reflections with $\theta > 45°$, we obtained $a_o = 10.581$ Å with an average deviation of 0.002 Å. (Eight front reflections gave $a_o = 10.580$ Å, average deviation = 0.002 Å.) The ratio of c_o/a_o given in the previous paragraph then leads to $c_o = 10.53$ Å. (This latter figure may be in appreciable error if non-uniform expansion or shrinkage occurred on the Buerger precession photograph from which the value of c_o/a_o was obtained; we therefore quote c_o to only two decimal places and give no average deviation.) The unit cell volume is then 1020.8 $Å^3$.

Combining the cell volume with the density (2.23 gm cm^{-3}; see previous section) we obtain 1371.3 atomic mass units for the contents of one unit cell. Table IX gives the number of formula weights per unit cell for a range of possible compositions:

Table IX.

Empirical Formula	Formula Weight (in a.m.u.)	No. of Formula Weights per unit Cell
$BaMg_7$	307.6	4.46
Mg_8	331.9	4.13
Mg_9	356.2	3.85
Mg_{10}	380.6	3.60
Mg_{11}	404.9	3.39
Mg_{12}	429.2	3.20
Mg_{13}	453.5	3.02

Referring back to Table VIII (right hand side) a comparison is presented of the powder photograph data with single crystal data from the rotation photograph about $\underline{c}$, arranged by layer-lines. It is seen that almost every medium or stronger powder line, as well as a good portion of the weaker lines, is accounted for in this way. (Some minor discrepancies in the match arise, no doubt, from film shrinkage, which was not allowed for.) We believe that this correspondence, together with the Laue data mentioned earlier, establishes the crystallographic identity of the single crystals with the crude samples; some elementary magnesium and barium and their oxides may also be present. (Some weak lines otherwise unaccounted for may arise from X-ray tube impurities, residual β radiation, or the presence of $BaMg_4$.)

Data Analysis and Structure Determination

If we consider only the strong, even layer-lines on the c-axis rotation photograph we find that these reflections can be re-indexed on the basis of a subcell which will also be convenient in much of the following discussion. Since l=2m for the strong layer-lines the subcell height will be half the full cell height. For all reflections on these layer-lines, h-k = 3n (see previous section); these indices can be simplified by reference to new a axes at 30° to those of the full cell, but shorter by a factor of $1/\sqrt{3}$. The following equalities establish the relationship between the full cell (unprimed axes) and the subcell (primed axes):

$$c_o' = \frac{1}{2} c_o = 5.26 \text{ Å}$$

$$a_o' = \frac{1}{\sqrt{3}} a_o = 6.11 \text{ Å}$$

$$\underline{a}_2' - \underline{a}_1' = \underline{a}_2$$

$$2\underline{a}_1' + \underline{a}_2' = \underline{a}_1$$

The basal area of the subcell is thus one-third the full cell area, and the subcell volume is one-sixth that of the full cell. (See Fig. 13.)

By studying first these very strong, subcell reflections we can obtain the main features of the structure; the weaker reflections (l=2m + 1) indicate how the subcell structure should be modified to give the complete final structure. (A mere repetition of the subcell structure throughout the full cell cannot, of course, be a solution since otherwise no odd layer-line reflections would occur.)

The general uniformity of intensity of the subcell reflections (i.e., those having l=2m) suggests that the heavily scattering bariums are

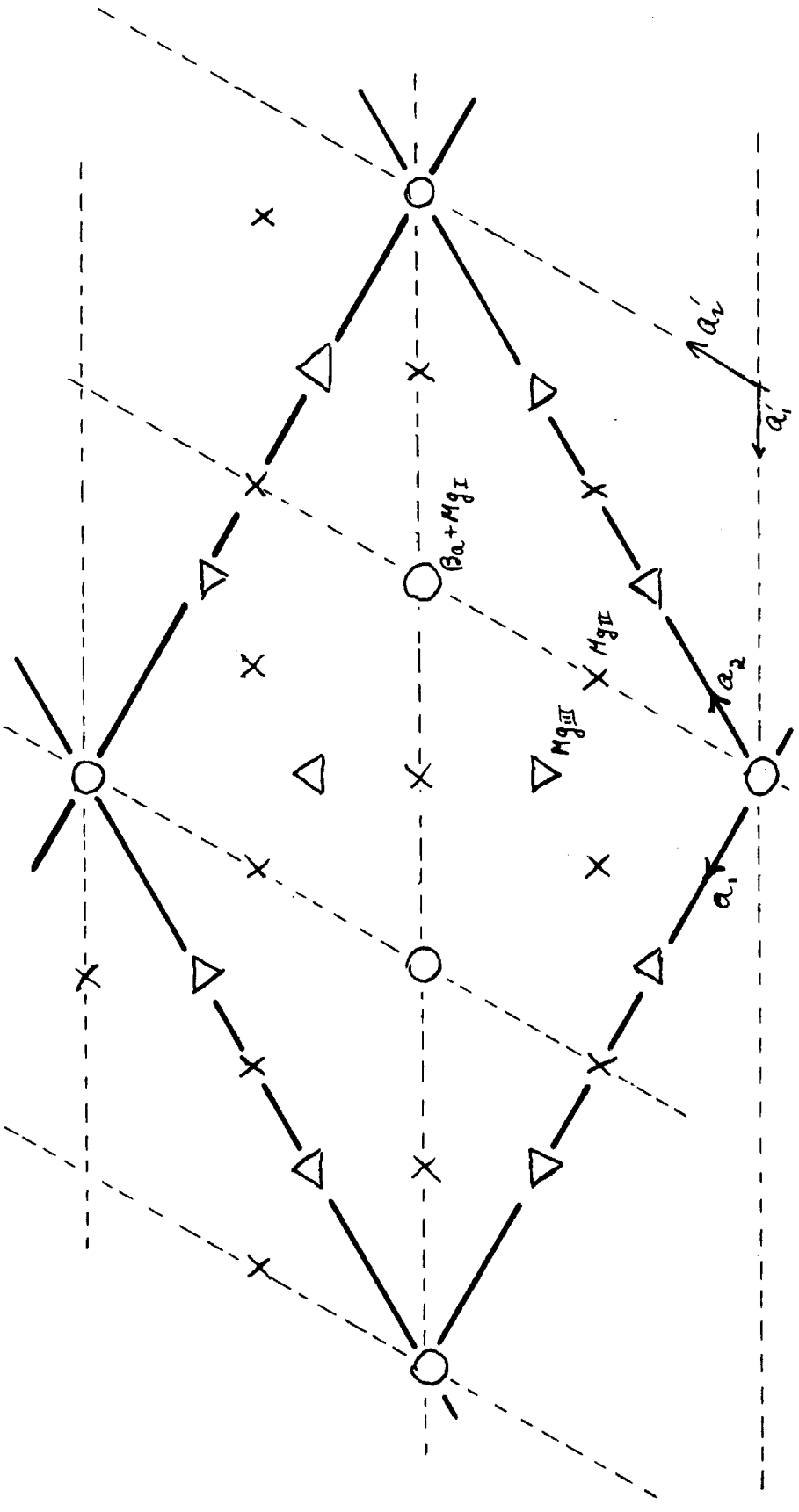

FIG. 13

located at the subcell origin; in the full cell these barium positions are: 000; $\frac{1}{3}\frac{2}{3}0$; $\frac{2}{3}\frac{1}{3}0$; $00\frac{1}{2}$; $\frac{1}{3}\frac{2}{3}\frac{1}{2}$; $\frac{2}{3}\frac{1}{3}\frac{1}{2}$. An electron density projection on the basal plane of the full cell, calculated from hk0 data, could be obtained from the corresponding subcell projection by repetition; thus the projected barium densities at 00, $\frac{1}{3}\frac{2}{3}$, $\frac{2}{3}\frac{1}{3}$ in the full cell basal plane must be identical, i.e. the sum of the electron densities at 000 and $00\frac{1}{2}$ is the same as the sume of densities at $\frac{1}{3}\frac{2}{3}0$ and $\frac{1}{3}\frac{2}{3}\frac{1}{2}$, and the sum of densities at $\frac{2}{3}\frac{1}{3}0$ and $\frac{2}{3}\frac{1}{3}\frac{1}{2}$. (This is a direct result of the observation that if l=2m, then h-k=3n.) By a similar argument (based on the rule that if h-k=3n, then l=2m) it can be shown that the projected sum of the electron densities at 000, $\frac{1}{3}\frac{2}{3}0$, and $\frac{2}{3}\frac{1}{3}0$ must be identical with the projected sum of densities at $00\frac{1}{2}$, $\frac{1}{3}\frac{2}{3}\frac{1}{2}$, and $\frac{2}{3}\frac{1}{3}\frac{1}{2}$. The same considerations apply to the projections of all other atoms in the cell as well, but we will continue to use the bariums as an illustration.

If the structure is an ordered one, a given barium position* must be occupied in all (full) unit cells, or in none of them. However, the conditions of the previous paragraph must also be satisfied: the three vertically projected density sums at 00, $\frac{1}{3}\frac{2}{3}$, and $\frac{2}{3}\frac{1}{3}$ must be identical, and the two horizontal projections for $z=0$ and $z=\frac{1}{2}$ must also be the same. It is impossible to find an ordered structure satisfying these conditions except the trivial one which places a barium at none of the six sites, and the equally unsatisfactory one which places a barium at each of the six sites. The latter solution is discarded because in such

*The phrase "barium position" is used in reference to the location of a barium atom; "barium site" refers to a location where a barium could be present, but may or may not actually occur.

a structure, only the magnesium atoms would contribute to the odd (weak) layer lines, and no reasonable arrangement gives intensities comparable to those observed. It is therefore necessary to consider disordered structures.

The X-ray rotation photographs do not show any heavy streaking, but the stronger spots do show extensions which were considered consistent with the idea of a disordered structure.

The type of disorder to be considered has the following interpretation: In a typical region of the crystal, a given barium site, for example, is occupied by a barium in some of the unit cells, but not in others (in which the site may either remain empty or be occupied by some other atom). Since what is observed is an average of all unit cells in the region, it will be convenient to speak of a fraction of a barium occurring at a certain site, or of a site being occupied by a barium a fraction of the time; the fraction in either case is that fraction of the total number of unit cells in which the site under discussion is occupied by a full barium atom.

Of course, any solution which makes all the subcells identical is incorrect even if the subcell structure is disordered, since no odd layer-lines would be observed. We now proceed to discuss the subcell structure and how it should be modified to produce the true structure.

An electron density projection onto the subcell base, plus packing considerations based on the radii of barium and magnesium, leads directly to the idealized subcell structure. For the electron density projection, hk0 intensity data were obtained from a zero-level Weissenberg photograph; intensities were estimated by comparison with a calibrated

intensity strip (kindly lent by Dr. W. G. Sly), corrected for Lorentz and polarization factors, and reduced to structure factors by taking the square root and multiplying by an empirical constant. The general uniformity of the hk0 intensities suggests that all structure factors signs be taken with positive sign, the principal contribution being from the barium which has previously been assigned to the origin. Using the electron density expression for the two-dimensional plane group p6, and taking all signs positive, the result shown in Fig. 14 was obtained.

The subcell height (5.26 Å) can accommodate only one barium atom (radius 2.0 - 2.2 Å). If we interpret the projection as having one full barium at the origin, then the other densities indicate roughly one magnesium (Mg_{II}) each at $\frac{1}{2}\,0$, $0\,\frac{1}{2}$, and $\frac{1}{2}\,\frac{1}{2}$, and half a magnesium (Mg_{III}) at $\frac{1}{3}\,\frac{2}{3}$ and at $\frac{2}{3}\,\frac{1}{3}$.

The z-parameters can be estimated by considering packing possibilities. With a barium at each corner of the subcell, a magnesium atom (radius 1.5 - 1.6 Å) cannot possibly be put at $\frac{1}{2}\,0\,0$, since the cell edge (6.11 Å) is too short to accept both a barium and a magnesium. We therefore assign $z = \frac{1}{2}$ for all Mg_{II} atoms. Since the cell-face diagonal is 8.06 Å there is considerable space for these magnesiums; later the z-parameters of the Mg_{II} atoms will be changed somewhat to provide better packing in the final structure.

If we were to place the Mg_{III} atoms in the basal plane (z=0) of the subcell at $\frac{1}{3}\,\frac{2}{3}$ and $\frac{2}{3}\,\frac{1}{3}$, the Ba-Mg_{III} and Mg_{II}-Mg_{III} distances would be 3.53 Å and 3.16 Å respectively. Although the latter distance is a reasonable one for a magnesium-magnesium contact, the former dis-

tance may be somewhat too short for a barium-magnesium contact. In addition, examination of the Mg_{III} atoms in projection shows not the simple round shape typical of spherical atoms but a three-lobed appearance, one lobe pointed toward each of the three nearest barium positions. The existence of this symmetrical three-fold splitting is verified by a difference Fourier which shows three distinct maxima. Structure factor calculations show that each lobe is displaced from the central position ($\frac{1}{3}\frac{2}{3}$ or $\frac{2}{3}\frac{1}{3}$) by 0.037 of the (long) diagonal length; of the two new Ba-Mg_{III} distances, 3.13 and 3.74 Å, the first is impossibly short while the second is about right. (The two Mg_{II} - Mg_{III} distances are 3.08 and 3.40 Å.) We therefore postulate that a Mg_{III} atom can occur only when the nearest barium site is not occupied by a barium atom. Subject to this condition we postulate a z-parameter, z = 0, for the Mg_{III} atoms.

The subcell structure described to this point is related to the well-known $CaCu_5$-type structure[5] which has atoms in the following positions (corresponding to a hypothetical $BaMg_5$ structure):

1 Ba: 0 0 0

3 Mg_{II}: $\frac{1}{2}\,0\,\frac{1}{2}$; $0\,\frac{1}{2}\,\frac{1}{2}$; $\frac{1}{2}\,\frac{1}{2}\,\frac{1}{2}$

2 Mg_{III}: $\frac{1}{3}\,\frac{2}{3}\,0$; $\frac{2}{3}\,\frac{1}{3}\,0$

Such a structure still has an undesirably long Ba-Mg_{II} separation of 4.03 Å (noted earlier) and Ba-Ba separation (along c) of 5.26 Å, as well as the short Ba-Mg_{III} distance of 3.53 Å.

The full-cell coordinates corresponding to those so far assumed for the subcell are listed in Table IX.

Fig. 14

hk0 electron density map (subcell base). Barium atoms (heavy lines) drawn for every fifth contour.

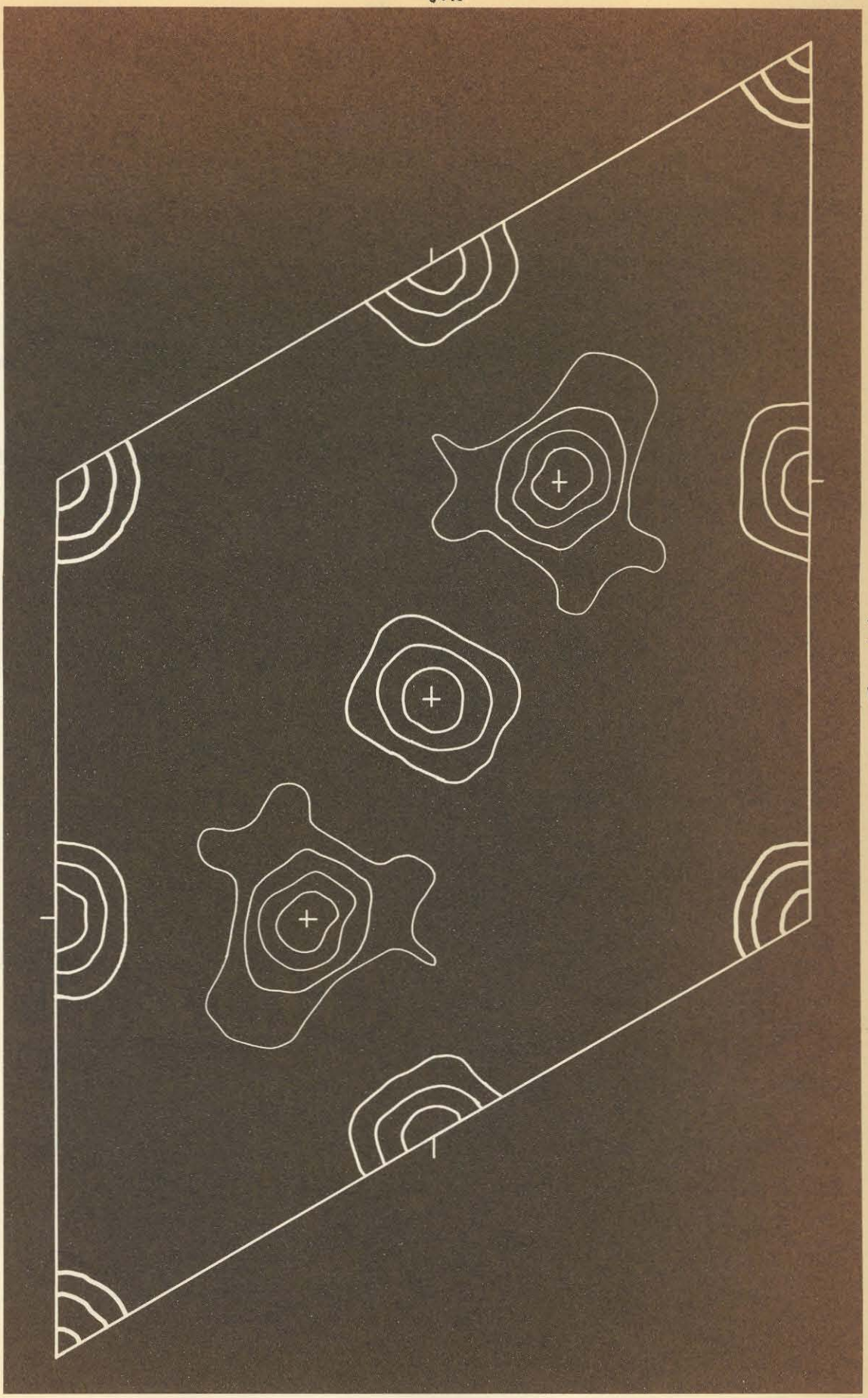

Fig. 14

Table IX.

	Subcell	Full cell
Ba	$0\,0\,0$	$0\,0\,0;\ \frac{1}{3}\frac{2}{3}0;\ \frac{2}{3}\frac{1}{3}0;\ 0\,0\,\frac{1}{2};\ \frac{1}{3}\frac{2}{3}\frac{1}{2};\ \frac{2}{3}\frac{1}{3}\frac{1}{2}$
Mg_{II}	$0\,\frac{1}{2}\frac{1}{2};\ \frac{1}{2}\,0\,\frac{1}{2};\ \frac{1}{2}\frac{1}{2}\frac{1}{2}$	$0\,\frac{1}{2}\frac{1}{4};\ \frac{1}{6}\frac{1}{3}\frac{1}{4};\ \frac{1}{6}\frac{5}{6}\frac{1}{4};\ \frac{1}{3}\frac{1}{6}\frac{1}{4};\ \frac{1}{2}0\,\frac{1}{4};\ \frac{1}{2}\frac{1}{2}\frac{1}{4};$ $\frac{2}{3}\frac{5}{6}\frac{1}{4};\ \frac{5}{6}\frac{1}{6}\frac{1}{4};\ \frac{5}{6}\frac{2}{3}\frac{1}{4};$ the same with $z=\frac{3}{4}$.
Mg_{III}	$\left.\begin{matrix}\Delta & \bar{\Delta} & 0\\ \Delta & 2\Delta & 0\\ 2\bar{\Delta} & \Delta & 0\end{matrix}\right\} + \frac{1}{3}\frac{2}{3}0$	$\left.\begin{matrix}0 & \bar{\Delta} & 0\\ \Delta & \Delta & 0\\ \bar{\Delta} & 0 & 0\end{matrix}\right\} + 0\,\frac{1}{3}0;\ \frac{1}{3}0\,0;\ \frac{2}{3}\frac{2}{3}0$
	$\left.\begin{matrix}\bar{\Delta} & \Delta & 0\\ \bar{\Delta} & 2\Delta & 0\\ 2\bar{\Delta} & \bar{\Delta} & 0\end{matrix}\right\} + \frac{2}{3}\frac{1}{3}0$	$\left.\begin{matrix}\Delta & 0 & 0\\ 0 & \Delta & 0\\ \bar{\Delta} & \bar{\Delta} & 0\end{matrix}\right\} + 0\,\frac{2}{3}0;\ \frac{1}{3}\frac{1}{3}0;\ \frac{2}{3}\,0\,0;$
	$(\Delta = 0.037)$	the same with $z = \frac{1}{2}$
		$(\Delta = 0.037)$

The Mg_{II} atoms form a planar network of interlocking regular hexagons and triangles. The Mg_{III} sites also form regular hexagons, each one slightly shrunk in toward its center away from the others. Within these hexagons the Mg_{II}-Mg_{II} distance is 3.05 Å and the Mg_{III}-Mg_{III} distance is 3.13 Å, both reasonable values for a magnesium-magnesium contact. As postulated previously, the hexagon of Mg_{III} atoms can occur only when the barium site at its center is unoccupied by barium; but the absence of the barium leaves a large gap in the $\underline{c}$ direction, even though the Mg_{II} and Mg_{III} atoms are in contact (3.08 Å, noted earlier). It is therefore postulated (and later verified by the 0 1 0 electron density projection) that the replacement of a barium and the occurrence of a Mg_{III} hexagon is accompanied by the addition of a pair of magnesium atoms (Mg_I) in contact with each other, one on either side of the vacant barium site, and lying on a line parallel to $\underline{c}$ through the site. Thus a barium atom can be replaced by a hexagonal bipyramid of magnesium atoms (2 Mg_I, 6 Mg_{III}). Actually such replacement cannot be carried out rigorously since if two adjacent barium sites were to be vacant there would be insufficient room for two Mg_{III} hexagons side by side. We therefore limit the number of such hexagonal bipyramids to not more than two per full unit cell with the proviso that they not be adjacent. The maximum number of Mg_{III} atoms is thus twelve per full unit cell, or two per subcell. It is assumed, however, that two Mg_I atoms always occur at a vacant barium site. The distance from a Mg_I to a Mg_{III} of an associated hexagon is 3.50 Å, the distance to a Mg_{III} of a neighboring hexagon is 4.06 Å.

Anticipating the results of the h0l projection, we assign $z = \pm 0.149$ for the Mg_I atoms near the basal plane (of the full cell), equivalent to a magnesium radius of 1.57 Å. Of the two barium sites along c in each unit cell, only one can be occupied by a pair of Mg_I atoms; two such pairs total 12.56 Å, and even if the radius of magnesium were as low as 1.50 Å, the total is still too great. Only two bariums, or one barium and two magnesiums (total extension: about 10.7 Å) can occur; the apparent crowding of the latter combination is considered in the discussion.

The following tabulation lists the more important distances between sites in the structure as developed to this point:

Ba-Ba (h)	= 6.11 Å
Ba-Ba (v)	= 5.23 Å
$Ba-Mg_{II}$	= 4.03 Å
$Ba-Mg_{III}$	= 3.74 Å
Mg_I-Mg_I	= 3.14 Å
$Mg_{II}-Mg_{II}$	= 3.05 Å
$Mg_{III}-Mg_{III}$	= 3.13 Å
Mg_I-Mg_{II}	= 3.23 Å
Mg_I-Mg_{III}	= 3.50 Å ; 4.06 Å (to neighboring hexagon)
$Mg_{II}-Mg_{III}$	= 3.08 Å ; 3.41 Å

In calculating hk0 structure factors for comparison with experimental values, the following assumptions were made: 1) the maximum number (3 per subcell) of Mg_{II} atoms is always present; 2) a missing barium is always replaced by two Mg_I atoms, and by a hexagon of Mg_{III} atoms to a maximum of 2 Mg_{III} per subcell (two hexagons per full unit cell). The parameters to be determined were the amount of barium per unit cell, and the displacement, Δ, of the Mg_{III} atoms from

their mean special positions.

Only 18 different h k 0 subcell reflections were observed, and the structure factor calculations involve only four terms. Using approximate values of the compositional and positional from the electron density projection a difference Fourier section along the longer subcell diagonal was calculated, and the results fed back into a second difference Fourier. These results were then used in a trial-and-error procedure to determine the amount of barium and the locations of the Mg_{III} atoms. The results of structure factor calculations using parameters consistent with the results of h 0 l calculations are given in Table X. They are based on 0.55 Ba and 0.90 Mg_I (subcell contents) at 0 0, and $\Delta = 0.037$ for Mg_{III}.

The h k 0 structure factor calculations were useful for determining the Mg_{III} positional parameter, but indicate only roughly the barium compositional parameter; a wide range of values of this latter parameter gave good agreement with experiment (i.e. $\frac{\sum\left||F_o|-|F_c|\right|}{\sum|F_o|} \leqslant$ 10 percent). The poorer agreement for the strong, low-order reflections (about the first six) probably arises from secondary extinction, for which no corrections were made.

The subcell which satisfies our structure factor calculations resembles the previously described $BaMg_5$ structure in which almost half the bariums are absent and have been replaced by pairs of Mg_I atoms. Each of the six Mg_{III} sites in the subcell is occupied, on the average, by $\frac{1}{3}$ of a magnesium atom, corresponding to the two Mg_{III} of the $BaMg_5$ structure.

Table X

h	k	F_o	F_c
0	0	--	--
	1	20.2	17.9
	2	40.0	50.1*
	3	25.7	26.0
	4	35.9	36.2
	5	11.8	9.5
	6	17.9	19.0
1	1	30.9	38.7*
	2	17.3	16.4
	3	13.5	13.0
	4	15.2	14.2
	5	12.7	12.8
	6	6.6	6.6
2	2	39.7	46.2
	3	15.0	13.6
	4	22.0	23.6
	5	8.8	7.8
3	3	11.6	11.3
	4	10.4	10.3

$$R = \frac{\sum\left||F_o| - |F_c|\right|}{\sum|F_o|} = 0.069 \quad (0\,2\,0 \text{ and } 1\,1\,0 \text{ omitted})$$

Intensities of the h0l reflections were obtained from Buerger precession camera photographs. Unfortunately, a precession angle of 24° was used (the maximum attainable for the camera distance used), whereas published tables of the Lorentz and polarization factors for precession camera data are computed only for $\mu = 21^\circ$ and 30° (as well as 5°, 10°, and 15°)[6,7]. Approximate factors were obtained by linear expansion* of the ξ scale of the 21° table by the factor $\frac{\xi_{max(24^\circ)}}{\xi_{max(21^\circ)}} = \frac{2 \times \sin 24^\circ}{2 \times \sin 21^\circ} = 1.134$**. The results appear reasonable compared to those for 21° and 30°.

The observed reflections common to both hk0 and h0l are 300, 600, and 900. The following comparison of the ratios of their structure factors as independently evaluated for the two different zones provides a check, though not a conclusive one, on the extrapolated Lorentz-polarization factors, and on the inner consistency of the intensity estimation:

hkl	F_{hk0}	F_{h0l}	F_{h0l}/F_{hk0}
300	7.92	9.11	1.15
600	10.16	10.63	1.05
900	2.98	3.19	1.07

(Note: The hko and h0l structure factors are on different scales; the nearness of the ratio to unity is accidental. It should also be noted that the hk0 data is from a Weissenberg photograph made with CuKα radiation, the h0l data from a precession photograph made with MoKα; no correction for absorption was made, but see the discussion for an evaluation of the effect of absorption.)

---

*I am indebted to Mrs. Y. C. Leung for this suggestion.

**All values correspond to $\mu = 45^\circ$. The error made in this way is no more than ± 6 percent for $\mu = 21^\circ$[6].

As a check on some of the postulates made about the subcell structure, an h 0 l electron density projection for l even only (strong reflections) was calculated for space group P 6/m. The signs of all structure factors were taken positive for the same reason outlined in connection with the h k 0 projection. One quarter of the resulting projection onto the vertical face of the full cell is shown in Fig. 15 . The Mg_I and Mg_{II} atoms are quite apparent, but the Mg_{III} atoms are covered by the bariums and make themselves felt only as slight horizontal elongations of the barium peaks.

Adding on a constant background correction, we make the following observations: the Mg_{II} peak densities alternate in the ratio of about one to two, as expected, alternate peaks representing two superimposed Mg_{II} atoms; some slight vertical elongation of the single Mg_{II} peaks is observed but could be spurious ("ripple", perhaps, from series termination errors); the Mg_I peak height remains in some doubt, as does its location (between 1.50 and 1.60 Å above z = 0).

Finally, by adding in terms for the odd-layer h 0 l data the complete electron density map shown in Fig.15a is obtained. (Only one-quarter of the projection is shown, since, for space group P 6/m, the rest of the map is generated by reflection through vertical and horizontal mirror planes.) There are several significant differences between this full cell projection and that for the subcell. The origin is almost completely populated by a barium (since no appreciable amount of Mg_I appears above it) while there is almost no barium at $0\,0\,\frac{1}{2}$ (which is consistent with the associated Mg_I peak, near $0\,0\,\frac{3}{8}$, which has a height about equal to that of the single Mg_{II} peak nearby); the peak

Fig. 15

h 0 l electron density map (full cell) for space group C_{6h}^{1},

l even only.

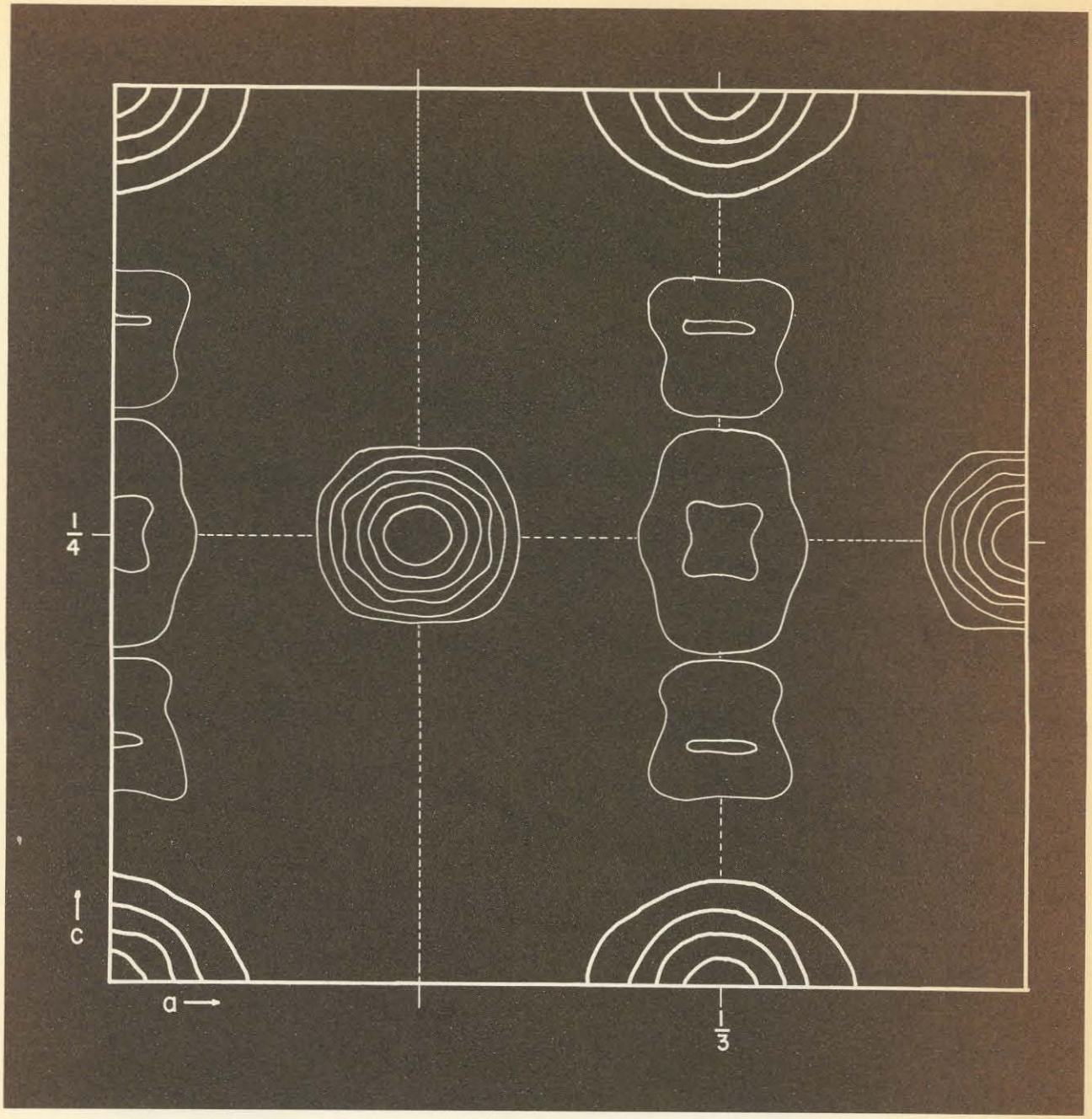

FIG. 15

Fig. 15a

h 0 l electron density map (full cell) for space group C_{6h}^{1},

l odd and even.

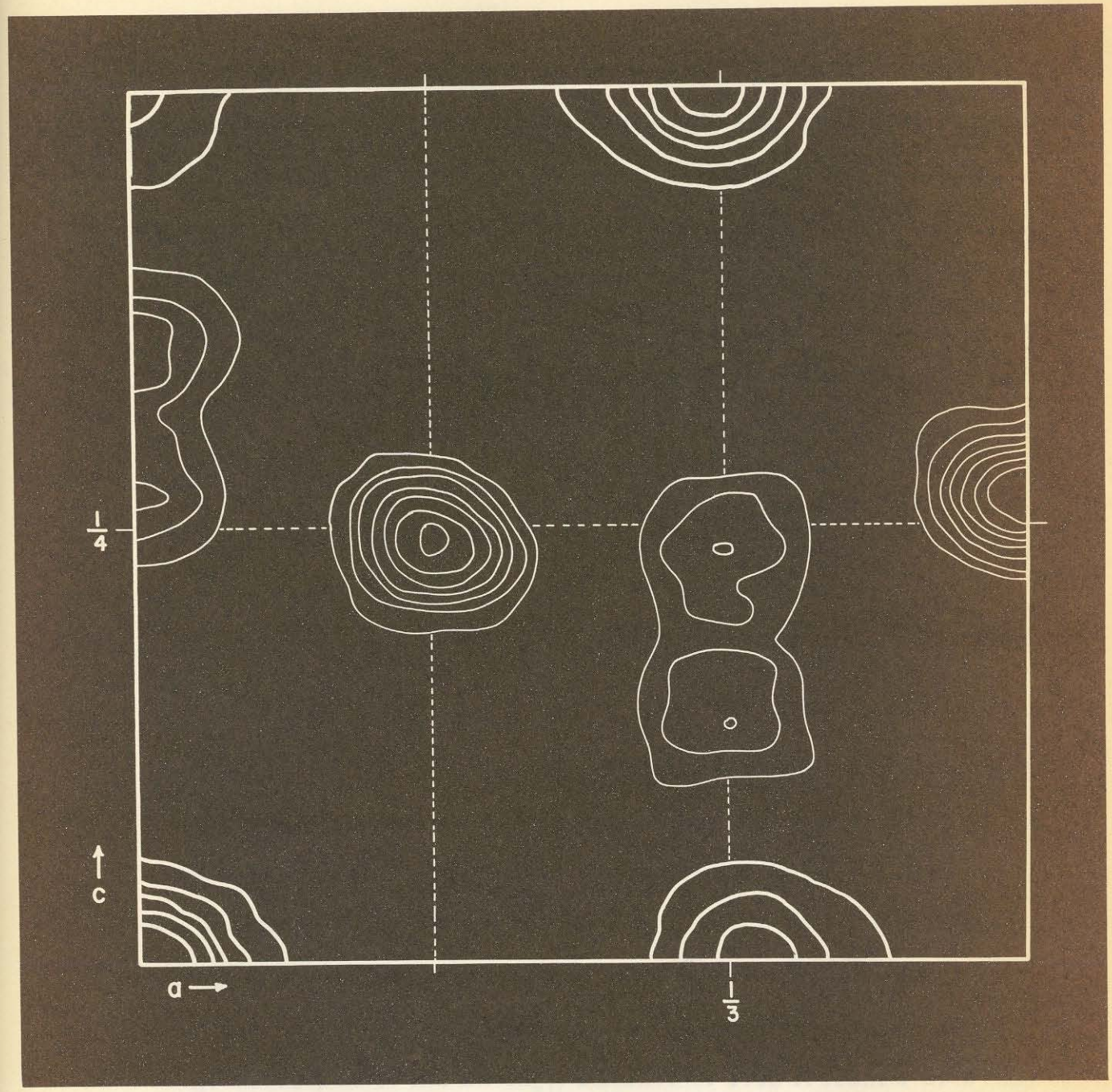

Fig. 15a

which does occur at $00\frac{1}{2}$ must be almost completely the projection of two Mg_{III} atoms. The other barium peaks at $x = \frac{1}{3}$, $z = 0$ and $\frac{1}{2}$, are intermediate between these two extremes.

Another point of interest is the vertical displacement of the Mg_{II} atoms from $z = \frac{1}{4}$. (The Mg_I and the single Mg_{II} peaks unfortunately overlap, somewhat obscuring the exact positions.) The following interpretation can be given to these displacements. Each Mg_{II} is associated with two pairs of barium sites, thus:

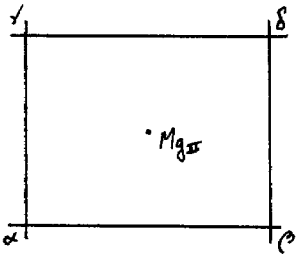

Here α, β, γ, δ are barium populations of their respective sites. Consider two examples. Case A: $\alpha = \delta = 1$; $\beta = \gamma = 0.1$. Here the environment of the Mg_{II} atom is symmetrical, and it remains at $z = \frac{1}{4}$. Case B: $\alpha = \beta = 1$; $\gamma = \delta = 0.1$. Since both α and β are always occupied by barium, these sites have no Mg_{III} rings of their own; the distance from a Mg_{III} atom of an adjoining ring to Mg_{II} is long, 3.41 Å, as is the Ba-Mg_{II} distance of 4.03 Å from α or β to Mg_{II}. On the other hand sites γ and δ can each possess a Mg_{III} hexagon half the time (though not simultaneously). These Mg_{III} atoms

are only 3.08 Å from Mg_{II}, which is tight (but not impossibly so) for a magnesium-magnesium contact. Hence the Mg_{II} atom has plenty of room to move into on side α, β, and is being "pushed" by the close Mg_{II}-Mg_{III} contact on side γ, δ. The net result is the observed displacement from $z = \frac{1}{4}$ toward the side with higher net barium population. A case of interest will be that intermediate between Case A and Case B, with $\alpha = 1$, $\gamma = 0.1$, $\beta = \delta = 0.55$; this is the case which actually occurs, with a net displacement of Mg_{II} from $z = \frac{1}{4}$ toward α, β.

In Fig. 16 is shown a scheme of displacements for the Mg_{II} atoms consistent with the electron density map for this space-group. The signs + and - refer to upward and downward displacements, respectively, from $z = \frac{1}{4}$, without regard to magnitude.

The first set of structure factor calculations was made for space group P 6/m, with a barium distribution of the following type, where A,B,C,D are barium populations:

	A	C		C	A
	B	D	*	D	B
↑ c	A	C		C	A

with A + B = C + D and A + 2C = B + 2D, in accordance with earlier statements. Using reasonable values of the z parameters for Mg_I and Mg_{II} as obtained from the h 0 l projection, it was found to be impossible to obtain good agreement of calculated with observed structure factors without going to impossible values of A greater than 1.

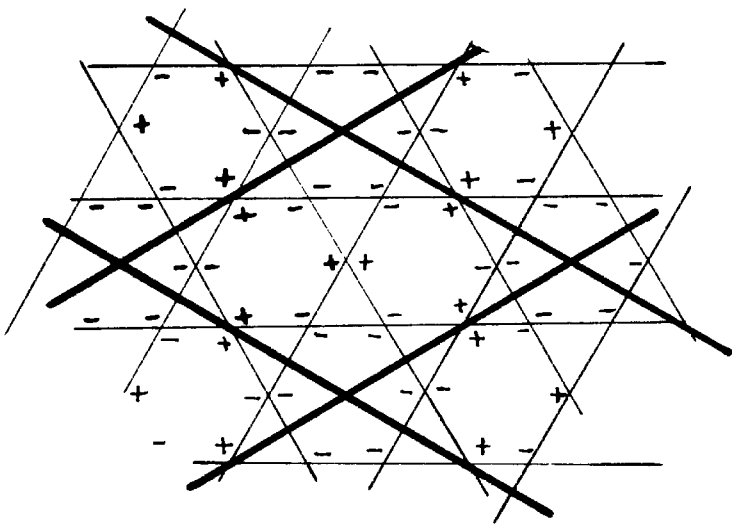

Fig. 16

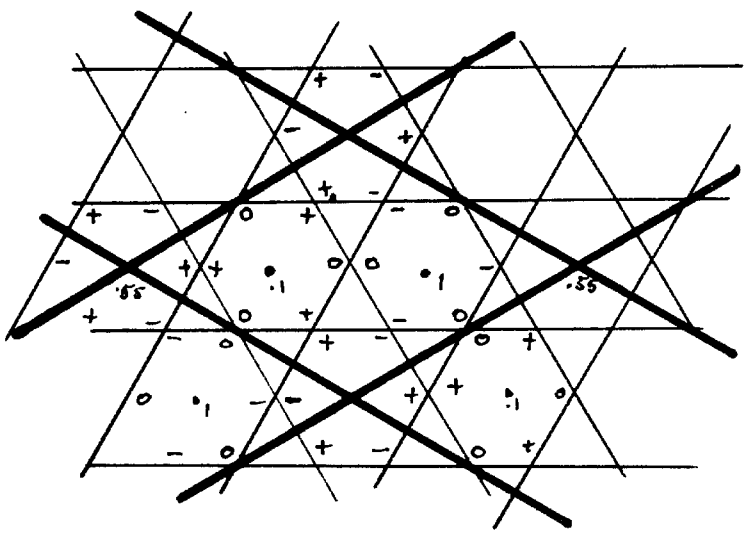

Fig. 18

The poor agreement of the structure factors arises from the excessive weakness of the calculated structure factors for l odd relative to the calculated factors for l even, i.e., the ratio $\frac{F_c}{F_o}$ was too small for the lines with l odd by an amount which could be overcome only by introducing population figures greater than one. In this respect, the relative strengths of the strong and weak layer lines are a direct measure of the population distribution and of the disorder.

Combinations of different symmetry elements were then tried, with the final choice being the following:

	A	B	C	A
	B	A	C	B
	*		*	
↑ c	A	B	C	A

with A + B = 2C. (The starred points are centers of symmetry.)

This arrangement is conveniently referred to space-group D_{6h}^4 (P 6/mmc) with origin at one of the centers of symmetry. Work with the previous space-group had suggested a barium content of 3.3 Ba per full unit cell; taking A = l, the other values are B = 0.l, C = 0.55. In h 0 l electron density map was again calculated; the sign associated with each structure factor was that calculated for the bariums only. (This assumption is justified by the final structure factor calculations, where the sign of the total factor is almost always the sign of the barium contribution alone.) The result is shown in Fig. 17.

Fig. 17

h 0 l electron density map (full cell) for space group D_{6h}^{4}.
(The origin is at a different atom than in Fig. 15, 15a.)

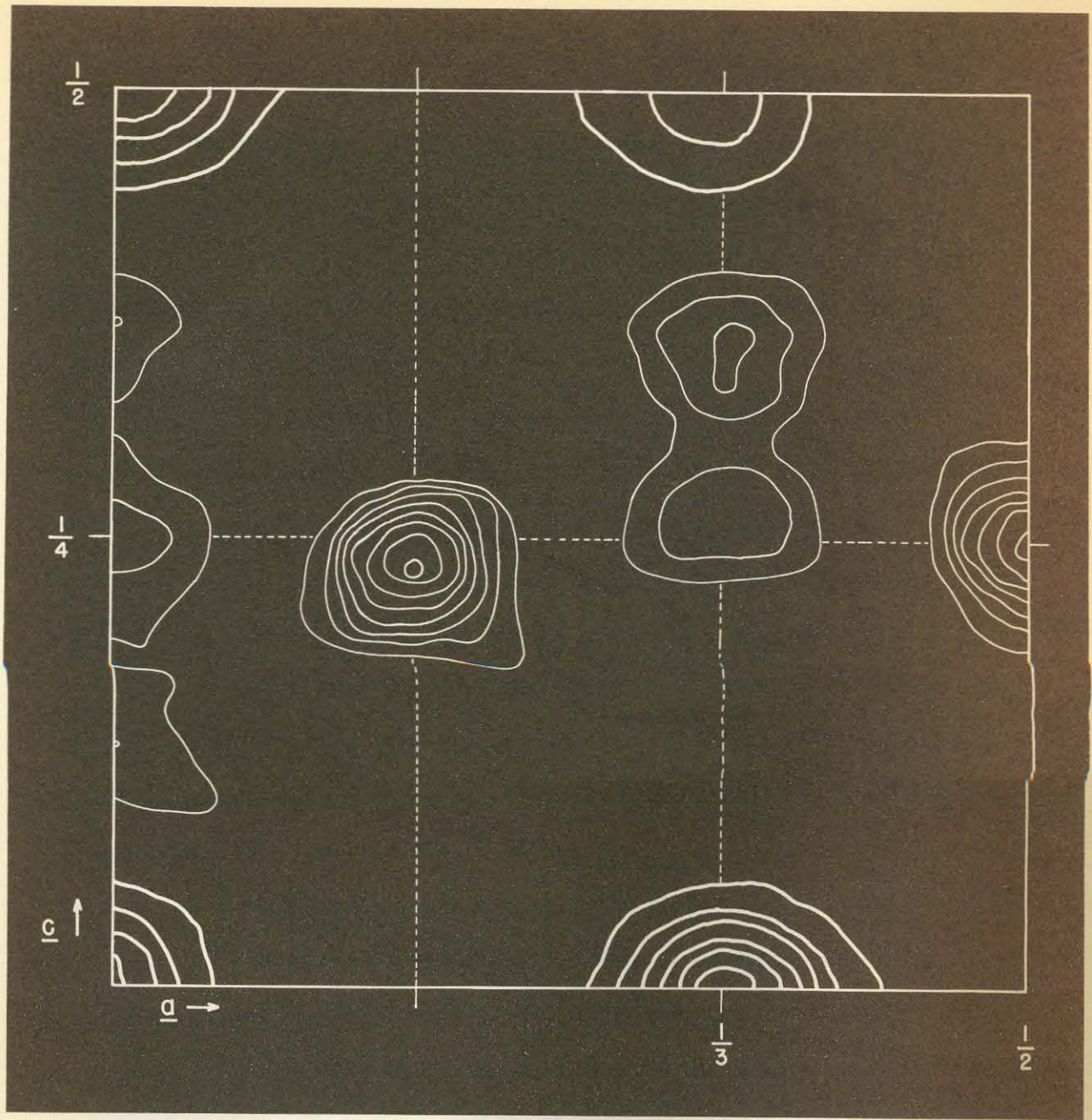

Fig. 17

In all its essential structural details, the new h0l map bears out all the interpretations made thus far. The barium peaks are lopsided because of the Mg_{III} atoms behind them, displaced off to one side; if these Mg_{III} atoms are subtracted out, the residual barium peak heights are in a ratio very close to 1:0.1:0.55. The Mg_I peaks complement the associated bariums, and the Mg_{II} peaks are displaced up or down from $z = \frac{1}{4}$ in a way consistent with the ideas proposed previously.

The coordinates in Table XI were used in a new structure factor calculation, the results of which are given in Table XII. The composition corresponding to the population figures given is $Ba_{3.3}Mg_{34.8}$, or $BaMg_{10.54}$. This is believed to represent to a fair degree of accuracy the average structure of the crystal.

Some of the features of the complete structure can be easily interpreted. If we consider the barium sites, for example, to be arranged in chains parallel to $\underline{c}$, we note two types: ABABA..., and CCCCC.., where A = 1 Ba, B = 0.1 Ba, and C = 0.55 Ba. Each unit cell has three chains running through it, two of the first type and one of the second. It is reasonable that, for reasons of packing efficiency, adjacent chains of the first type prefer staggered relative alignments, i.e., an A site prefers to be horizontally adjacent to a B site. If two chains of the first type satisfy this requirement, the third cannot also be of this type and meet this requirement simultaneously with respect to its neighbors; the third chain is therefore a compromise, satisfying one neighbor half the time, the other neighbor the other half. The net result is that a C site in the third chain is really an average of

Table XI

.55	Ba	each at	$00\frac{1}{4}$, $00\frac{3}{4}$
.10	Ba	" "	$\frac{1}{3}\frac{1}{3}\frac{1}{4}$, $\frac{1}{3}\frac{1}{3}\frac{3}{4}$
1.00	Ba	" "	$\frac{1}{3}\frac{1}{3}\frac{1}{4}$, $\frac{1}{3}\frac{1}{3}\frac{3}{4}$

.45	Mg_I	each at	$00\frac{1}{4} + .149$	$00\frac{3}{4} + .149$
			$00\frac{1}{4} - .149$	$00\frac{3}{4} - .149$
.90	Mg_I	" "	$\frac{1}{3}\frac{2}{3}\frac{1}{4} + .149$	$\frac{2}{3}\frac{1}{3}\frac{3}{4} + .149$
			$\frac{1}{3}\frac{2}{3}\frac{1}{4} - .149$	$\frac{2}{3}\frac{1}{3}\frac{3}{4} - .149$

1	Mg_{II}	each at	$0\frac{1}{2}0$ $\quad$ $0\frac{1}{2}\frac{1}{2}$
			$\frac{1}{2}00$ $\quad$ $\frac{1}{2}0\frac{1}{2}$
			$\frac{1}{2}\frac{1}{2}0$ $\quad$ $\frac{1}{2}\frac{1}{2}\frac{1}{2}$

$\frac{1}{2}$ Mg_{II} " " :

$\frac{1}{6}\frac{1}{3}$	$0; -.020; \frac{1}{2}; \frac{1}{2} + .020$
$\frac{1}{6}\frac{1}{6}$	"
$\frac{1}{3}\frac{1}{6}$	"
$\frac{1}{3}\frac{1}{6}$	$0; .020; \frac{1}{2}; \frac{1}{2} - .020$
$\frac{1}{6}\frac{1}{6}$	"
$\frac{1}{6}\frac{1}{3}$	"

Table XI
(Continued)

.25 Mg_{III} each at:

0	$\frac{1}{3}$ - .037	
0	$\frac{1}{3}$ - .037	
$\frac{1}{3}$ - .037	0	$\frac{1}{4}$; $\frac{3}{4}$
$\frac{1}{3}$ - .037	0	
$\frac{1}{3}$ - .037	$\frac{1}{3}$ - .037	
$\frac{1}{3}$ - .037	$\frac{1}{3}$ - .037	

.70 Mg_{III} each at:

.037	$\frac{1}{3}$ + .037		.037	$\frac{1}{3}$ + .037
.037	$\frac{1}{3}$		.037	$\frac{1}{3}$
$\frac{1}{3}$	.037	$\frac{1}{4}$	$\frac{1}{3}$	.037 $\frac{3}{4}$
$\frac{1}{3}$	$\frac{1}{3}$ + .037		$\frac{1}{3}$	$\frac{1}{3}$ + .037
$\frac{1}{3}$ + .037	.037		$\frac{1}{3}$ + .037	.037
$\frac{1}{3}$ + .037	$\frac{1}{3}$		$\frac{1}{3}$ + .037	$\frac{1}{3}$

Table XII

h	l	F_o	F_c	h	l	F_o	F_c
0	0	--	--	0	3		0
1			-1.9	1		72.8	-82.5
2			2.8	2		138.2	119.7
3		220.7	226.0	3			0
4			-6.0	4		65.5	-61.6
5			3.0	5		94.6	83.5
6		257.1	284.1	6			0
7			-6.9	7		--	-21.8
8			.8	8		75.2	67.0
9		77.6	80.2	9			0
0	1		0	0	4	288.6	339.8
1		58.2	52.6	1			-2.5
2		77.6	-63.9	2			5.3
3			0	3		131.0	120.6
4		--	9.5	4			-2.6
5		77.6	-61.2	5			1.9
6			0	6		174.6	197.7
7		--	8.5	7			-6.9
8		41.2	34.7	8			2.7
9			0	9		41.2	40.3
0	2	89.7	-83.5	0	5		0
1			1.4	1		70.3	60.2
2			-1.7	2		46.1	-46.2
3		264.4	-255.8	3			0
4			6.5	4		--	6.0
5			-3.2	5		84.9	-68.2
6		31.5	-15.3	6			0
7			6.6	7		--	15.4
8			-.3	8		31.5	-30.3
9		92.2	-99.4	9			0

Table XII
(Continued)

h	l	F_o	F_c
0	6	123.7	-112.1
1			-.7
2			3.9
3		206.2	-226.9
4			9.9
5			-4.0
6		63.1	-56.9
7			4.3
8			3.0
0	7		0
1		--	-18.3
2		--	62.8
3			0
4		--	-27.7
5		41.2	33.7
6			0
7		--	6.7
8		43.7	42.5
0	8	215.9	252.7
1			-3.5
2			9.0
3		128.5	124.9
4			3.0
5			-.3

h	l	F_o	F_c
0	9		0
1		58.2	53.0
2		--	-34.0
3			0
4		--	8.4
5		60.6	60.0
6			0
0	10	84.9	-50.6
1			-2.6
2			8.8
3		97.0	-116.7
4			12.6
5			-4.7
0	11		0
1		38.8	-34.3
2		72.8	67.5
3			0

R = 0.101

(Unobserved reflections and reflections on edge of photograph omitted, as well as 602, 209, 0 0 10)

an A site and a B site, and the population figure relation is $C = \frac{1}{2}(A+B)$.

The displacements of Mg_{II} atoms from z = 0 and z = $\frac{1}{2}$ are controlled by the factors cited before, but it should be noted that all that is finally observed as an average displacement. If the environment is this:

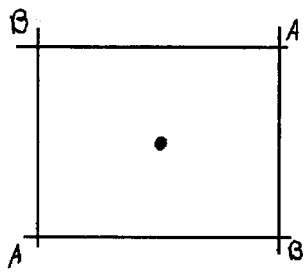

the Mg_{II} tends to move neither up nor down. If however, it is located thus:

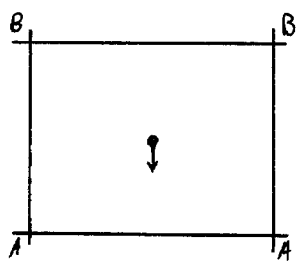

it tends to move down, by a certain amount, toward the side with higher net barium content. Since the following case:

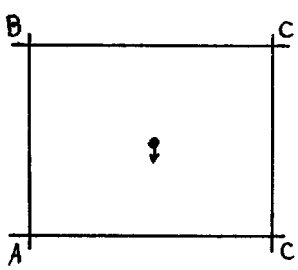

is an average of the preceding two, the net observed displacement should be one-half that for the second case. The scheme of Fig. 18 shows the resultant arrangement, with 0 indicating no displacement, + an upward displacement and - a downward one.

The Mg_{III} arrangement can be viewed in two different ways. On the one hand, in each group of three, one Mg_{III} is closest to an A site, one to a B site, and one to a C site; the total content of the group of three Mg_{III} must not exceed one magnesium. On the other hand, each barium site is surrounded by a hexagon of Mg_{III} atoms, each hexagon slightly shrunk in to provide good magnesium-magnesium contact; each point of a hexagon can be occupied by no more than (1-A), (1-B), or (1-C) magnesium, as the case may be. Symbolizing the group of three associated Mg_{III} as:

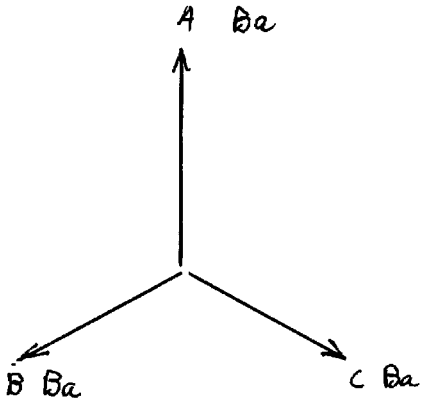

and remembering that C is an average of A and B, we derive the Mg_{III} population figures as follows:

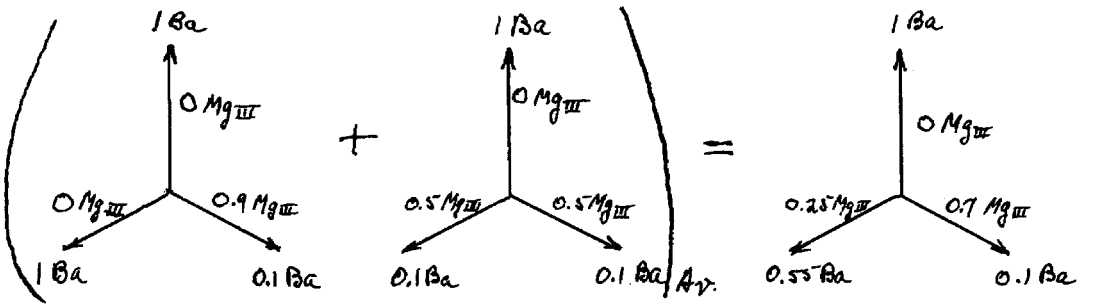

Because B=0.1 rather than 0, the sum of the three associated Mg_{III} sites is only 0.95 magnesium, rather than 1.0, assumed in the earlier discussion; the present figure corresponds to 11.40 Mg_{III} per full cell, instead of 12 as previously.

The following revision of the earlier list gives the inter-atomic distances for the average structure:

Ba-Ba (h) = 6.11 Å
Ba-Ba (v) = 5.23 Å

Ba-Mg_I = 3.66 Å
Ba-Mg_{II} = 4.03 Å; 3.89 Å
Ba-Mg_{III} = 3.74 Å

Mg_I-Mg_I = 3.14 Å
Mg_{II}-Mg_{II} = 3.06 Å; 3.05 Å
Mg_{III}-Mg_{III} = 3.13 Å
Mg_I-Mg_{II} = 3.23 Å; 3.30 Å
Mg_I-Mg_{III} = 3.50 Å; 4.06 Å
Mg_{II}-Mg_{III} = 3.08 Å; 3.26 Å; 3.25 Å

All of these distances are quite reasonable ones except the Mg_I-Mg_{III}, which is rather long; however, we may say with Goethe*: "Half ihm doch kein Weh und Ach/Musst' es eben leiden".

*Goethe, J. W. v., "Heidenroslein".

Discussion of Structure and Determination

The formula of the structure just described, $BaMg_{10.54}$, is in good agreement with the results of chemical analysis mentioned earlier (which gave $BaMg_{10.4}$), but the calculated density, 2.11 gm cm^{-3}, is lower than the experimentally determined value by about 5 percent. Since, however, the density was determined with different crystals than were used in gathering the X-ray data, it is possible that the compositions of the crystals were not identical. It is also possible that the experimental density determination is in error by an appreciable amount.

The disorder which gives rise to the C chains has already been mentioned. Each chain of type ABABA$\cdots$ can be considered the average result of a disorder in which barium atoms regularly alternate with pairs of magnesiums (Mg_I) for a distance of about nine unit cells along the chain, but in the tenth cell the two magnesiums are replaced by a barium. Thus the A sites are always occupied by bariums, while the B sites are occupied by barium only 10 percent of the time. A structural interpretation of this disorder is suggested in the following argument. Take for the radius of barium (coordination number 12) 2.215 Å [8], and for the effective magnesium radius 1.57 Å, as found in this investigation from the Mg_I-Mg_I distance. The sum of the diameters of a barium and two (Mg_I) magnesiums is then 10.71 Å, about 0.2 Å greater than c_o, whereas two consecutive bariums add up to 8.86 Å, more than 1.5 Å shorter than c_o. The "strain" of compressing a barium and two magnesiums into a unit cell, accumulated

over nine unit cells, is relieved in the tenth cell by the substitution of a barium for the magnesium pair. A possible extension of this argument is to regard c_o as being equal to the weighted average of diameter sums for the two different combinations, i.e.,

$$c_o = \langle c_o \rangle_{Av.} = \frac{9 \times 10.71 + 1 \times 8.86}{10} = 10.52_7 \text{ Å}$$

in good agreement with the experimental value.

Of the several possible statistical interpretations which might be given, the following one is offered. It is based on the type of chain described in the preceding paragraph, regularly alternating barium with two magnesiums; presumably, such an arrangement is preferred from the viewpoints of packing and coordination, although, as noted, a counter-tendency demands the random substitution of a barium for 10 percent of the magnesium pairs in each chain. Consider first an "ideal" unit cell, in which it happens that the chain segments are of the strictly alternating type, with, say, a barium at the origin and a magnesium pair at $\frac{1}{3}\frac{2}{3}0$; through $\frac{2}{3}\frac{1}{3}0$ runs a chain which might start off equally well with either a barium or a magnesium pair, and can be regarded as an average of the other two chains. The formula of this cell is Ba_3Mg_{36} (i.e., 3 $BaMg_{12}$). If, as happens with about $\frac{1}{10}$ probability, a cell occurs which is like the ideal but has, in one chain, a barium substituted for a magnesium pair ("monosubstitution") the formula becomes Ba_4Mg_{32} (i.e., 4 $BaMg_8$).

The ratio in which these two types of cell occur is about seven to three. (Since the probability for "monosubstitution" is only $\frac{1}{10}$, the pro-

babilities of occurrence of "bi-" and "trisubstituted" cells -- cells in which two or three magnesium pairs are substituted by barium -- are negligibly small.) The overall composition is then

$$\frac{7 \times Ba_3Mg_{36} + 3 \times Ba_4Mg_{32}}{10} = Ba_{3.3}Mg_{34.8} .$$

(Taking into account "bi-" and "trisubstitution" lowers the magnesium content by 0.06 magnesium per cell.)

The structure is, on the whole, quite well packed. Each barium has associated with it at least twelve magnesiums (Mg_{II}) at contact or slightly larger distances; the presence of Mg_I and Mg_{III} atoms may give even larger coordination numbers. Each of the magnesiums also has associated with it at least twelve magnesiums (Mg_{II}) at contact or slightly larger distances; the presence of Mg_I and Mg_{III} atoms may give even larger coordination numbers. Each of the magnesiums also has about coordination number twelve.

It is possible that there is a range of composition over which crystals of this phase form, the local composition of the melt determining the formula of each crystal. One end of this range may be $BaMg_{12}$ (Ba_3Mg_{36}), in crystals of which there is a strict alternation in the vertical chains of barium and pairs of magnesium; a composition close to $BaMg_{10.5}$ may mark the other end of the range, for although the overall composition of our crude samples was intended to be $BaMg_9$, the actual substance formed is probably close to the $BaMg_{10.54}$ of the present investigation and $BaMg_{10.4}$ of the chemical analysis. On the basis of structural considerations it would be expected that

crystals near the barium-rich end of the phase would have smaller c_o and longer a_o than crystals from magnesium-rich phases. A plot of cell-constants versus composition would provide valuable information on this point*. Interesting information could also be obtained from the structure of $SrMg_9$ (reported by K & D, ref. 1), since the radius of strontium is about 0.07 Å less than that of barium**.

Few compounds with formula XY_9 have been reported, and the crystal structures of only one or two are of interest. Perhaps the most closely related to the present work is $ThZn_9$[9]. It is based on the $CaCu_5$ type structure with space group D_{6h}^1 (P 6/mmm), and has a substitutional disorder which is indicated by writing the formula Zn_5 ($Zn_{0.4}$, $Th_{0.6}$); the cell constants are a_o = 5.237 Å, c_o = 4.442 Å.

More closely related to the $BaMg_9$ structure are the structures of $TiBe_{12}$[10] and $CeMg_{12}$[11]. All three structures have hexagonal unit cells, and each is conveniently referred to a subcell of the same type. Although the types of disorder are quite similar, the $BaMg_9$ disorder is more complex than that in $TiBe_{12}$ and $CeMg_{12}$; $TiBe_{12}$, for example, is based on chains parallel to c in which there is strict alternation of titanium atoms with pairs of beryllium atoms. In the

---

*In a private communication from Prof. A. J. King of Syracuse University, the cell constants of a substance described as $BaMg_9$ are given as a_o = 10.396 Å and c_o = 10.652 Å, all ± 0.005 Å; these are based on Laue, Weissenberg, and powder photographs. The space group is given as $D_6^6(C6_32)$ with four $BaMg_9$ per unit cell; no density is given, but is calculated from the data as 2.37 gm cm^{-3}. Until further information is received from Prof. King, however, it is thought best not to attempt a reconciliation of his data with that presented in this paper.

**Prof. King reports for $SrMg_9$ cell constants similar to those he gives for $BaMg_9$: a_o = 10.322, c_o = 10.506.

h k 0 subcell projection, $TiBe_{12}$ shows Be atoms split into three lobes just as the Mg_{III} atoms in $BaMg_9$ are. Many other structural features are common to these three alloys, but $TiBe_{12}$ and $CeMg_{12}$ have 48 subcells per full unit cell whereas $BaMg_9$ has only six.

The linear absorption coefficient for the structure presented in this paper is 312 cm^{-1} for CuKα radiation, and only 39 cm^{-1} for MoKα *. The estimated h 0 l intensities should therefore be more reliable than the h k 0 intensities, but the h 0 l precession photograph from which the h 0 l data was obtained was not of the best quality, and the Lorentz-polarization factors may be in error from the extrapolation process used. The situation regarding absorption is less favorable for the strontium compound (with MoKα radiation) despite the smaller atomic number:

	CuKα	MoKα
$BaMg_{10.54}$	312	39
$SrMg_{10.54}$	165	79

(Note: It was assumed that the cell dimensions would not be greatly different for the two compounds, as indicated by Prof. King's results.)

In correcting for thermal vibrations, the same isotropic temperature factor was assumed to apply to both barium and magnesium; visual estimation was used to draw a best line through the points of a plot of $\log \frac{F_c}{F_o}$ vs. $\sin^2\theta$. For the h 0 l structure factor calculation,

*Mass absorption coefficients taken from Internationale Tabellen zur Bestimmung von Kristallstrukturen, Zweiter Band, p. 577-8.

for example, a value for B estimated in this way was 0.76 $\mathring{A}^2$. Because barium and magnesium differ greatly in mass, a more realistic approximation would have been to assign different factors to the two kinds of atoms, using a small value of B for barium and an appropriately larger one for magnesium.

No attempt has been made to assign limits of error or standard deviations to either the positional or compositional parameters, since most of these were estimated from electron density maps or by trial-and-error. The structure derived appears to be correct in all its essentials, but could be refined further by the use of the three-dimensional data and least-squares or equivalent procedures.

A subjective statement regarding the reliability of the results presented may, however, be in order. It is felt that the atomic ratio of magnesium to barium should not be in error by more than about 5 percent; the z-parameters for Mg_I and Mg_{II} are probably good to about 0.1 $\mathring{A}$, the positional parameter Δ for Mg_{III} should be within 0.05 $\mathring{A}$ of the true value.

References

1. W. Klemm and F. Dinkelacker, Z. anorg. Chem. 255, 2 (1947).
2. G. Grube and A. Dietrich, Z. Elektrochem. 44, 755 (1938).
3. E. Hellner and F. Laves, Z. Krist. 105, 134 (1943).
4. F. Laves, Metallwirtschaft 15, 631 (1936).
   See also J. B. Friauf, Phys. Rev. 29, 34 (1927).
5. W. Haucke, Z. anorg. allgem. Chem. 244, 17 (1940).
6. J. Waser, Rev. Sci. Instrum. 22, 563 (1951).
7. M. Atoji and W. N. Lipscomb, Acta Cryst. 7, 595 (1954).
8. L. Pauling, J. Am. Chem. Soc. 69, 542 (1947).
9. H. Nowotny, Metallforschung 1, 31 (1946).
10. R. F. Rauechle and R. E. Rundle, Acta Cryst. 5, 85 (1952).
11. A. Miller, private communication.

PROPOSITIONS

1. It is sometimes necessary to determine the density of a fragment of crystalline material too small to be viewed by the unaided eye. A device for measuring, in favorable cases, the density of such objects is proposed; it is based on the use of a suitable liquid above its critical point, confined with the crystal in a glass capillary by a mercury column. By adjusting the mercury column, the density can be continuously varied. Unfortunately, the method has severe limitations.

2. Although it has not been possible to observe any definite sign of the presence or absence of 1, 3-π-bonding in 3-methylenetrimethylene oxide, it may be possible to observe it in methylenecyclobutene, another compound prepared by Dr. Applequist[1]. Since cyclobutene and methylenecyclobutane are already available for comparison, and since MO calculations are already made for this substance, an electron diffraction study might be more fruitful than the 3-oxacyclobutanone study proposed by Dr. Applequist.

3. On the basis of electron diffraction data it appears that the molecule of decaborane is not quite the same in the gas phase as it is reported from the crystal study[2]; specifically, a boron skeleton based on a regular icosahedron provides a better match with the radial distribution curve. Such a model has the advantage of removing the

two rather long boron-boron bonds of 2.01 Å, and replacing them by bonds of more nearly normal length. A thorough correlation study, though difficult, is recommended.

4. The effect of differential angle strain on the length of bonds in three-membered and four-membered ring compounds has in the past usually remained unevaluated. A simple procedure is outlined, with examples, which demonstrates the operation and magnitude of this factor in simple three-membered rings. A feature of the calculation is the non-necessity of actually evaluating true bond-bending potential energy constants.

5. It is hoped that magic-number enthusiasts will welcome the identification of the "surprising"[3] ratio of valence electrons to atoms in γ-alloys, 21/13, as the ratio of two successive terms of the well-known Fibonacci series. Other alloy types may also have electron to atom ratios which are exactly, or almost exactly, the ratio of two successive terms of the series, e.g., the β-alloys (3/2).

6. Accurate and reliable microwave and electron diffraction data are now available for a considerable number of halogen derivatives of methane. Examination of these data verifies the long-known fact that a C-X bond length is directly affected by the attached atoms[4]. It is proposed that a simple correlation is possible between the length of a given C-X bond and the sum of the electronegativities of the other attached atoms; the electronegativity difference also enters,

aside from the Schomaker-Stevenson correction. This second-order correction fits the available data quite well.

7. The study of dimethyl selenide presented here demonstrates the danger in taking for the covalent radius of an atom one-half the separation found in the element; the radius thus derived may, as in this case, be too short by virtue of double-bond character[5]. It is suggested that a thorough revision of the Schomaker-Stevenson radii be undertaken in which the radii would be derived from observed distances in simple molecules and would be suitably corrected for electronegativity differences; a special case should be made for bonds between identical atoms.

8. It does not appear at all certain that $NOBr_3$ exists in the gas phase, or even in the solid phase[6]. It would be of considerable interest to know whether the solid compound is analogous to $POBr_3$, $POCl_3$, etc., or is an equimolal mixture of NOBr and Br_2.

9. A proof of the following theorem may or may not be obvious to the reader:

> If two prime numbers (greater than five) differ by two, then their average is always divisible by six.

If it is not, a proof is offered.

References

(1). D. E. Applequist, Ph. D. Thesis, California Institute of Technology, 1955.

(2). J. S. Kasper, C. M. Lucht, and D. Harker, Acta Cryst 3, 436 (1950).

(3). L. Pauling, "The Nature of the Chemical Bond", 2nd edition, Cornell University Press, Ithaca, New York, 1940, p. 418.

(4). Ibid., p. 235.

(5). V. Schomaker and D. P. Stevenson, J. Am. Chem. Soc., 63, 37 (1941).

(6). M. Trautz and V. P. Dalal, Z. anorg. allgem. Chem. 110, 1 (1920). R. L. Datta and N. R. Chatterjee, J. Am. Chem. Soc. 45, 480 (1923).